CARDIAC SODIUM CHANNEL PALMITOYLATION REGULATES CHANNEL FUNCTION AND CARDIAC EXCITABILITY WITH IMPLICATIONS FOR ARRHYTHMIA GENERATION

Zifan Pei

Submitted to the faculty of the University Graduate School
in partial fulfillment of the requirements
for the degree
Doctor of Philosophy
in the Department of Pharmacology and Toxicology
Indiana University

May 2017

Accepted by the Graduate Faculty, Indiana University, in partial fulfillment of the requirements for the degree of Doctor of Philosophy.

Theodore R. Cummins, Ph.D., Chair

Doctoral Committee

Gerry S. Oxford, Ph.D.

Andy Hudmon, Ph.D.

December 09, 2016

Michael Rubart-von der Lohe, MD.

Patrick L. Sheets, Ph.D.

Dedication

This work is dedicated to my thesis advisor, Dr. Theodore R. Cummins, my parents, Lin Pei and Jieping Miao and my fiancé Baichuan Zhang.

Acknowledgements

With all the challenges, joy and hardship along the way, the journey through Ph.D. program has become one of the most important experience in my life. Upon finishing my dissertation, I would like to take the time to thank all of the individuals that have inspired, guided and supported me during my research. I am truly grateful that they have influenced me in all aspects and have empowered my scientific and personal growth. My dissertation work would not have been completed without their tremendous help.

First and foremost, I would like to express my deepest appreciation to Dr. Thedore Cummins, for providing me the great opportunity to explore the current thesis project. Dr. Cummins taught me fundamentals of conducting scientific research. Under his guidance, I learned how to address research problems, design experiments and find solutions to it. He also inspired me by his hardworking and his passion towards scientific research. On a personal level, I deeply appreciate his willingness to support his students to pursue their career goals. Without his professional guidance and persistent help this dissertation would not have been possible.

I am also indebted to my committee members: Dr. Gerry S. Oxford, Dr. Andy Hudmon, Dr. Michael Rubart-von der Lohe and Dr. Patrick L. Sheets. They have provided precious insights and assistance for my dissertation project. Specifically, I would like to thank Dr. Gerry S. Oxford for providing me with significant and constructive suggestions during my research and defense. And I would like to thank Dr. Michael Rubart-von der Lohe for numerous helpful

advices and inspiring discussions on cardiac electrophysiology. Also, I would like to thank Dr. patrick sheets for reading the dissertation and giving me insightful advice during my writing of thesis. Special thanks goes to Dr. Andy Hudmon, who helped me develop many biochemistry assays, especially for his generous help during the tritium labeling experiments. I would not be able to accomplish this project without his professional assistance.

Aside from my committee, I would like to thank all faculties and staffs from the department of Pharmacology and Toxicology and the members of the Stark Neurosciences Research Institute for all the guidance and support. I would like to acknowledge Dr. Jianting Zhang, Dr.Jill C. Fehrenbacher, Dr.Rajesh Khanna, Dr.Tao Lu for their advices and assistance in all aspects of my graduate study. Additionally, I would like to express my gratitude to all the colleagues in Cummins lab. I would like to recognize Dr.Yucheng Xiao, Dr.Zhiyong Tan, Dr.Cindy Barbosa, Dr.Reesha Patel, James Jackson, Yanling Pan, Agnes Zybura and Emily Mason, for all their help during my graduate studies. Special thanks goes to Dr. Yucheng Xiao for his endless help during my first two years in the lab. He is always willing to take time to teach me experimental techniques and lab practices. I deeply appreciate his patience and help.

I would also like to thank members from hudmon lab, for the continuous help for my biochemistry experiments. Especially Dr. Jingwei Meng, he has spent a lot of time helping me develop the biochemistry assays and trouble shotting. Apart from my academic life, I would also extend my deep appreciation to my family for their unconditional love, care and support. I would like to thank my

parents for their continuous encouragement and support. It is because of the passion, diligence and dedication learned from them that motived and empowered me to achieve the current accomplishments. I would also like to thank my fiancé Baichuan Zhang, for this accompany and endless support, which encouraged and strengthened me and helped me get through all the difficulties in life.

Zifan Pei

Cardiac sodium channel palmitoylation regulates channel function and cardiac excitability with implications for arrhythmia generation

The cardiac voltage-gated sodium channels (Nav1.5) play a specific and critical role in regulating cardiac electrical activity by initiating and propagating action potentials in the heart. The association between Nav1.5 dysfunctions and generation of various types of cardiac arrhythmia disease, including long-QT3 and Brugada syndrome, is well established. Many types of post-translational modifications have been shown to regulate Nav1.5 biophysical properties, including phosphorylation, glycosylation and ubiquitination. However, our understanding about how post-translational lipid modification affects sodium channel function and cellular excitability, is still lacking. The goal of this dissertation is to characterize Nav1.5 palmitoylation, one of the most common post-translational lipid modification and its role in regulating Nav1.5 function and cardiac excitability.

In our studies, three lines of biochemistry evidence were shown to confirm Nav1.5 palmitoylation in both native expression background and heterologous expression system. Moreover, palmitoylation of Nav1.5 can be bidirectionally regulated using 2-Br-palmitate and palmitic acid. Our results also demonstrated that enhanced palmitoylation in both cardiomyocytes and HEK293 cells increases sodium channel availability and late sodium current activity, leading to enhanced cardiac excitability and prolonged action potential duration. In contrast, blocking palmitoylation by 2-Br-palmitiate increases closed-state channel

inactivation and reduces myocyte excitability. Our computer simulation results confirmed that the observed modification in Nav1.5 gating properties by protein palmitoylation are adequate for the alterations in cardiac excitability. Mutations of potential palmitoylation sites predicted by CSS-Palm bioinformatics tool were introduced into wild-type Nav1.5 constructs using site-directed mutagenesis. Further studies revealed four cysteines (C981, C1176, C1178, C1179) as possible Nav1.5 palmitoylation sites. In particular, a mutation of one of these sites(C981) is associated with cardiac arrhythmia disease. Cysteine to phenylalanine mutation at this site largely enhances of channel closed-state inactivation and ablates sensitivity to depalmitoylation. Therefore, C981 might be the most important site that regulates Nav1.5 palmitoylation. In summary, this dissertation research identified novel post-translational modification on Nav1.5 and revealed important details behind this process. Our data provides new insights on how post-translational lipid modification alters cardiomyocyte excitability and its potential role in arrhythmogenesis.

Theodore R. Cummins, Ph.D., Chair

Table of contents

List of tables

List of figures

List of abbreviations

Nav1.5	cardiac voltage-gated sodium channel
TTX	tetrodotoxin
VGSC	voltage-gated sodium channel
ECG	electrocardiogram
SA	sinoatrial
AV	atrioventricular
APD	action potential duration
LQT	long QT syndrome
BrS	Brugada syndrome
CAMK	Ca2+/Calmodulin-dependent serine/theronine protein kinase
PKA	protein kinase A
PKC	protein kinase A
PI3K	phosphatidylinositol 3- Kinase
PAT	palmitoyltransferase
DHHC	aspartate-histidine-histidine-cysteine
APT	acyl protein thioesterase
ABE	acyl-biotin exchange assay
HEK	human embryonic kidney
NEM	N-ethylmaleimide
2BP	2-Br-palmitate
PA	palmitic acid

EAD	early after-depolarization
17-ODYA	17-octadecynoic acid
LC	Liquid chromatography

I. INTRODUCTION

A. Overview of the thesis project

Cardiac voltage-gated sodium channels (Nav1.5), a voltage-gate sodium channel subtype that is mainly expressed in cardiac tissues, play an essential role in regulating cardiac electric activity by initiating and propagating action potentials in the heart. Altered Nav1.5 function is associated with multiple cardiac diseases including LQT3 and Brugada syndrome. Many studies have investigated the underlying mechanism of how Nav1.5 dysfunction leads to cardiac arrhythmia diseases.

Mechanistically, LQT3 disease is associated with Nav1.5 gain-of-function mutation with a constant and enhanced entry of Na^+, while most clinical cases of Brugada syndrome reflect a loss of function of Nav1.5, associated with decreased expression level or enhanced channel inactivation (Moric, Herbert et al. 2003). Previous studies indicate that Nav1.5 polymorphisms can induce direct changes to the channel biophysical properties and lead to LQT3 or Brugada syndrome. It is clear that genetic background plays a critical role in regulating Nav1.5 protein expression and function; many studies have also revealed that post-translational modifications of Nav1.5 contribute to altered channel function under physiological and pathological conditions. Nav1.5 is subject to various post-translational modifications. Among them, Nav1.5 phosphorylation, ubiquitination and glycosylation have been extensively studied. Their roles in cardiac diseases and specific sites of post-translational modification have been

revealed. However, our understanding of Nav1.5 regulation by lipid modifications is still lacking.

In this project, we demonstrate that Nav1.5 is subject to palmitoylation, a reversible post-translational lipid modification. Nav1.5 palmitoylation was found in both a heterologous expression system and cardiac tissues. In cardiomyocytes, palmitoylation increases channel availability and late sodium current activity, leading to enhanced cardiac excitability and prolonged action potential duration. In contrast, blocking palmitoylation substantially hyperpolarized voltage-dependence of inactivation and abolished cardiomyocyte excitability. Our computer simulations suggest that these alterations of Nav1.5 function alone are sufficient to induce the changes found in cardiac action potentials, such as the shifted voltage-dependence of inactivation and altered persistent current. Clinically, these changes could potentially lead to Long QT syndrome or Brugada syndrome.

We also identify four cysteines as possible Nav1.5 palmitoylation substrates and mutagenesis of all four cysteines mimics the effect of palmitoylation inhibition. Moreover, a mutation of one of these cysteines associated with cardiac arrhythmia (C981F), induces a significant enhancement of channel closed-state inactivation and ablates sensitivity to depalmitoylation. Our data indicate that alterations in palmitoylation can substantially control Nav1.5 function and cardiac excitability and this form of post-translational modification is likely an important contributor to acquired and congenital arrhythmias.

In summary, our experimental data and computer simulations suggest that palmitoylation not only has profound impact on Nav1.5 activity and cardiac excitability, but is also likely to play a previously unrecognized role in both inherited and acquired cardiac channelopathies. This project presents novel mechanism underlying cardiac arrhythmias and may represent a new target in treating cardiac diseases.

B. Brief overview of ion channels and history of discovering membrane excitation

Cell membrane forms the boundary of the cell and separates cells from exterior environment. The lipid bilayer of biological membranes has selected permeability to different molecules (ions and polar molecules), controlling the flow of substance across the membrane. There are different types of membrane transport proteins that determine the permeability of the membrane. Among them, active transporters facilitate an 'active' transport of molecules (usually against their concentration gradient) using cellular energy. Passive transporters, (e.g. ion channels), on the other hand, allow the 'passive' diffusion of molecules (usually in the same direction as the concentration or electrochemical gradient) without energy assumption.

Ion channels, pore-forming integral membrane proteins gate the flow of ions across the cell membrane and therefore, contribute to control the cell resting membrane potential and regulate cell excitability. Two Nobel prize winning physiologists, Sir Alan L. Hodgkin and Sir Andrew F. Huxley, first discovered the ionic mechanism underlying action potential generation using the squid giant axon(Hodgkin and Huxley 1952). These landmark experiments demonstrated that the transmembrane sodium and potassium currents were responsible for the generation of the action potential. Moreover, they were able to identify the influence of membrane potential on sodium current kinetics and quantitatively describe the sodium conductance and gating mechanism. This work provides the

foundation of understanding action potential generation and propagation and paves the way for later ion channel studies.

After Hodgkin and Huxley identified the voltage dependent gating of ion channels using the voltage clamp technique, this technique became widely used to study voltage gated ion channels. In 1964, a paralytic neurotoxin called tetrodotoxin (TTX) was discovered by Toshio Narahashi and John W. Moore (Mosher, Fuhrman et al. 1964, Narahashi, Moore et al. 1964, Scheuer 1970). TTX was found in the liver of the puffer fish and was revealed to have selective blockage for sodium ion flow across the membrane, indicating the existence of a specific pathway for sodium ion conductance (Narahashi, Moore et al. 1964). Several years later, Hille discovered that saxitoxin, a shellfish toxin, was another distinct blocker of sodium current while studying the voltage-gated ion channels from frog neuron (Hille 1968). By comparing the mobility of different cations, he was also able to obtain more insight into sodium channel structure and ion selectivity. He described the pore region of the sodium channel as a filter that controls the ion selectivity. Besides, he also suggested that the non-covalent bond (hydrogen bond) between ions and channels must be present to allow the flow of ions through the putative selectivity pore (Hille 1971). These findings led to the identification and understanding of sodium channel protein. Now, our knowledge of sodium channel proteins and mechanisms underlying membrane excitability have progressed significantly since those days. As the result of the rapid development of patch clamp and other advanced techniques, we now have a clearer understanding of sodium channel structure, kinetics, function and

modulation. As this dissertation focuses primarily on voltage-gated sodium channel post translational modification, it is important to briefly introduce the structure and function voltage-gated sodium channels.

C. Voltage-gated sodium channels

Voltage-gated sodium channels (VGSCs) are integral membrane protein complexes that allow sodium ion flow across the membrane and conduct transmembrane sodium currents(Goldin 2001). VGSCs consist of the pore forming α subunit and one or more β auxiliary subunits that regulate functions of channels (Catterall, Goldin et al. 2005). The sodium channel α subunit consists of four transmembrane domains (DI-DIV), with each containing six transmembrane segments (S1-S6, Figure 1). Segments 1, 2, 3 and 4 serve as voltage sensor and change confirmations in response to membrane potential change. Segments 5 and 6 form the pore of the channel and this is responsible for ion conduction through the channel(Yellen 1998). Altogether, 12 transmembrane segments in the α subunit form a complex pore like structure in the plasma membrane (Figure 2) and this subunit has a molecular weight of about 220-260 kD(Levinson and Ellory 1973, Catterall, Goldin et al. 2005, Payandeh, Scheuer et al. 2011).

VGSCs have three basic configurations: resting(closed), activated (open), and inactivated (Figure 3a). Under resting membrane potential, the cell membrane potential is at negative hyperpolarized voltages and the VGSCs activate(open) in response to the membrane potential depolarization. When membrane depolarization begins, several positively charged residues on the S4 segments are able to sense the membrane potential change, and this leads to outward movement of S4 segments, initiating the conformational change of VGSCs (Figure 3b) (Catterall 2000). The channel is then in transition to activated(open) configuration, providing a conduction pathway for the sodium

currents through the channel pore(Stuhmer, Conti et al. 1989). Very soon after channel activation (usually within milliseconds), the inactivation gate that tethered to the sodium channel protein will block the channel and prevent sodium conductance(Goldin 2003). VGSCs transition to a non-conducting, inactivated conformation. This process is often referred to as ‘fast inactivation’. Structure function studies revealed that the IFM motif (located in the intracellular linker of DIII and DIV) with three hydrophobic amino acids Isoleucine, Phenylalanine, and Methionine are largely responsible for the channel fast inactivation(West, Patton et al. 1992). There is also another type of inactivation that develops in response to longer depolarization time periods (usually hundreds of milliseconds) called ‘slow inactivation’(Silva 2014). Slow inactivation will sustain for a few seconds or even tens of seconds and is associated with altered excitability in neurons and myocytes, leading to various disease phenotypes such as hyperkalemic periodic paralysis and long-QT syndrome(Vilin and Ruben 2001). However, the detailed molecular mechanism of slow inactivation is still unknown(Ulbricht 2005). Once VGSCs enter an inactivated configuration, the channels are refractory to future stimuli and will not be able to open again until the membrane potential has repolarized to negative potentials. This process is called ‘recovery from inactivation’. It prevents the cells from premature re-excitation and is critical in regulating action potential firing in excitable cells. Altered recovery rate may contribute to a disrupted action potential generation pattern. Previous study on skeletal muscle sodium channel reveals that defective recovery from fast inactivation may lead to disease phenotype producing myotonic

discharges(Richmond, VanDeCarr et al. 1997). Once sodium channel is fully recovered from inactivation, it will restore to the original state and regain their ability to open upon the next stimulus.

The voltage-gated sodium channel family consists of 9 members and they share more than 50% common amino acid sequence in transmembrane segments and extracellular domains(Yu and Catterall 2003). However, they are found to be expressed in a variety of tissues and have distinct biophysical properties. For example, Nav1.4 is predominantly expressed in skeletal muscle cells and its mutation is associated with myotonia and periodic paralysis(Loussouarn, Sternberg et al. 2015). Nav1.8 and Nav1.9 show a much slower rate of inactivation compared to other subtypes of VGSCs(Cummins and Waxman 1997). Based on the sensitivity to tetrodotoxin(TTX), VGSCs can be divided into two groups: TTX sensitive VGSCs(Nav1.1, Nav1.2, Nav1.3, Nav1.4, Nav1.6, Nav1.7) and TTX resistant VGSCs(Nav1.5, Nav1.8, Nav1.9). Table 1 summarizes the properties of 9 subtypes of sodium channels and their disease associations.

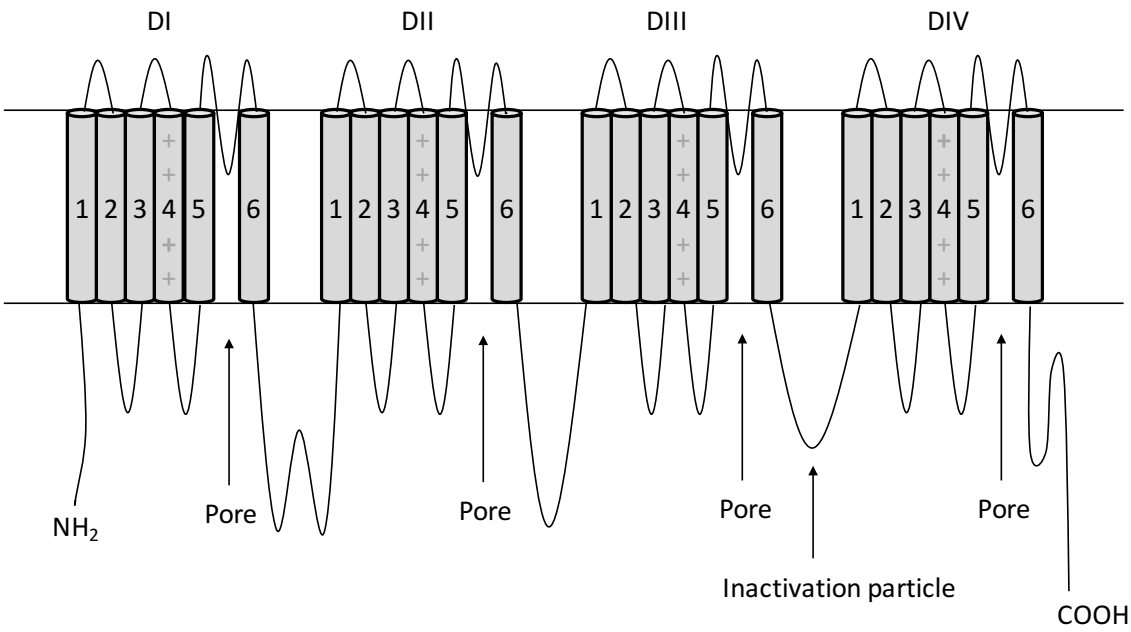

Figure 1. Schematic representation of the linear structure of α subunit for voltage-gated sodium channels (VGSCs). The α subunit consists of four homologous transmembrane domains(DI-DIV). Each domain contains six transmembrane segments (S1-S6). Among all, S1-S4 serve as the voltage sensor of the channel and S5-S6 segments form the pore. The IFM inactivation particle is located in DIII to DIV linker.

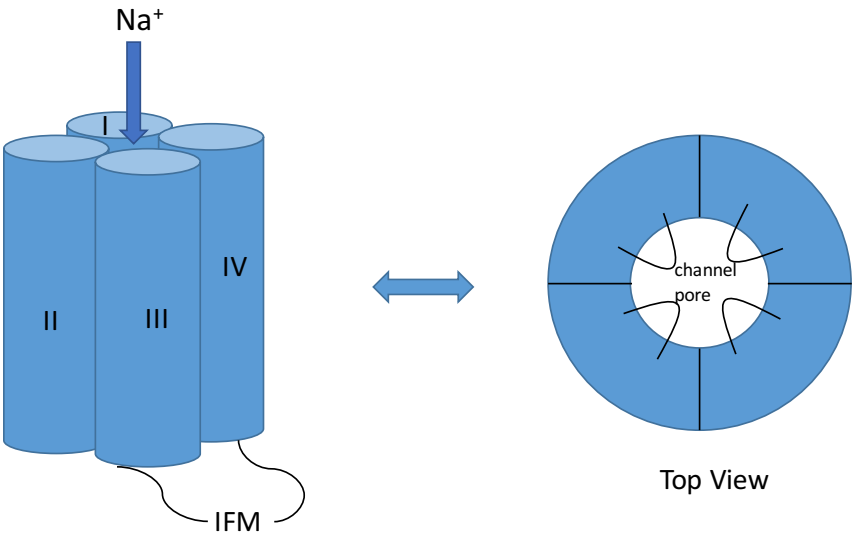

Figure 2. Simplified scheme of three-dimensional arrangement of sodium channel α subunit. Four homologous domains (DI - DIV) are folded together and they form a pore like structure. Each domain contains six transmembrane segments (S1-S6). IFM motif locates in the DIII to DIV intracellular linker and forms the inactivation gate. In the top view, the P-loops connecting the S5 and S6 segments in each domain are shown, and they together form the channel pore.

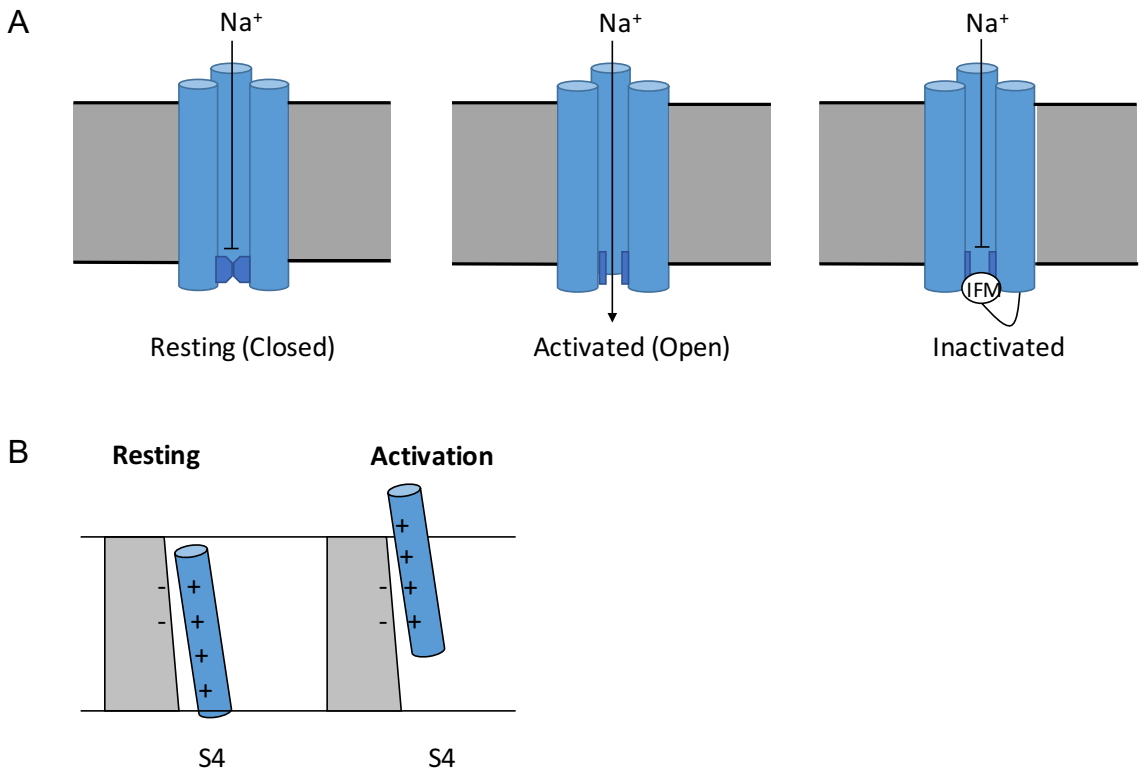

Figure 3. Schematic representation of three states of voltage-gated sodium channels. A. Diagram showing the proposed scheme for voltage-gated sodium channels transitions from resting state to activated and inactivated state. Sodium channels are closed at resting state and change open configuration open activation. IFM inactivation gate blocks the channel during inactivation state, preventing Na^+ flow into the cell. B. A simplified scheme showing the movement of S4 segment during activation.

Table 1. Sodium channel subtypes and associated disease phenotypes

Isoform	Gene	Chromosomal location	TTX IC50 (nM)	Expression	Channelopathies
Nav1.1	SCN1A	2q24	5-10	CNS,PNS	Epilepsy, Pain
Nav1.2	SCN2A	2q24.3	10	CNS,PNS	Epilepsy
Nav1.3	SCN3A	2q24	2-15	CNS,PNS	Epilepsy, Pain
Nav1.4	SCN4A	17q23.3	5	Skeletal muscle	Myotonia, Periodic paralysis
Nav1.5	SCN5A	3p21	1000-2000	Heart	Cardiac Arrhythmia
Nav1.6	SCN8A	12q13	1	CNS,PNS	Epilepsy, Pain
Nav1.7	SCN9A	2q24	4	PNS	Pain
Nav1.8	SCN10A	3p22.2	>50,000	PNS	Pain
Nav1.9	SCN11A	3p22.2	40000	PNS	Pain

D. Cardiac sodium channels and its role in cardiac excitability

Voltage-gated sodium channels (VGSCs) are responsible for initiation and propagation of action potentials in excitable cells (e.g., neurons, muscles, myocytes) (Hodgkin and Huxley 1952, Agnew 1984, Catterall 2000). The cardiac subtype Nav1.5 is predominantly expressed in the heart and plays an essential role in regulating cardiac electric activity(Rogart, Cribbs et al. 1989).

The resting membrane potential of cardiomyocytes is usually maintained at -80 to -90mV(Grant 2009). This potential is determined by the selective permeability of the cell membrane to different ions and the activities of ion pumps like Na^+-K^+-ATPase. This resting stage is also referred to as phase '4' in a cardiac action potential (Figure 4). The VGSCs remain closed at resting membrane potential. Once changes in transmembrane potential are detected by voltage sensor domain, the outward movement of voltage sensor will be triggered. VGSCs will then change conformation to an activated conducting configuration. Sodium ions then flow (down their concentration gradient) into the cell, leading to further membrane depolarization. VGSCs activation lasts for a few milliseconds and is responsible for the rapid depolarization phase of an action potential (phase '0' of the action potential)(Carmeliet 2002, Ulbricht 2005). The buildup of positive charges inside of the membrane causes VGSCs to inactivate and then transition to a closed conformation. At the same time, the change in membrane potential leads to the opening of voltage-gated potassium channels. The rapid outflow of positively charged K^+ ions slightly lower the membrane potential and constitute the repolarization phase (phase '1') of the action

potential. Then, the activation of voltage-gated calcium channels and delayed rectifier potassium channels maintain a plateau phase (phase ‘2’) of the action potential(Kenyon and Sutko 1987). Then L-type Ca2+ channels inactivate and many potassium channels remain open (primarily the rapid delayed rectifier K^+ channels (I_{Kr}) and the inwardly rectifying K^+ current, I_{K1}), resulting in a rapid repolarization phase (phase ‘3’) of the action potential.

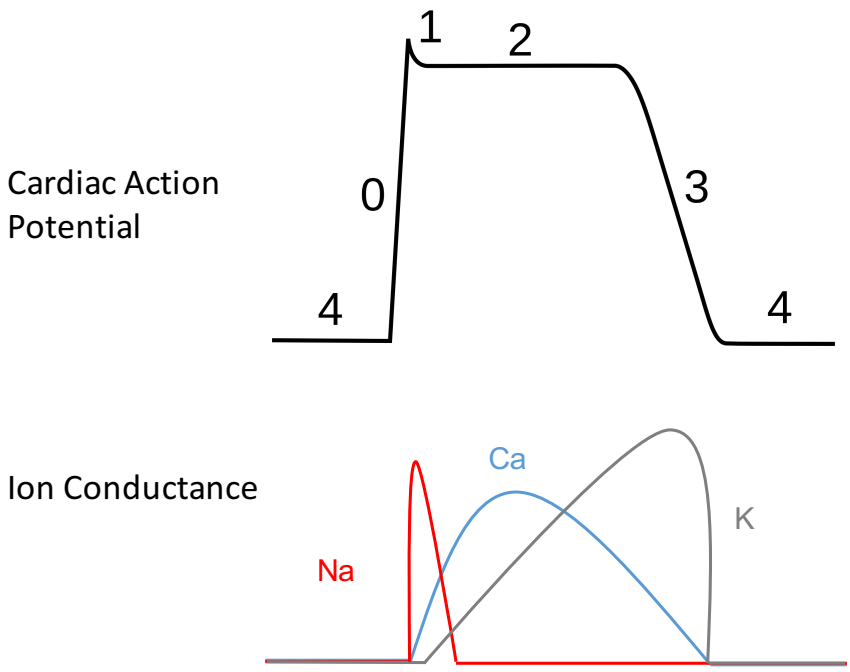

Figure 4. Illustration of single cardiac action potential and its corresponding ion conductance in different phases. Top panel depicts standard cardiac action potential waveform and 1-4 indicate four phases in cardiac action potential. Lower panel indicates the corresponding ion conductance participating in each phase of the action potential. Sodium current is primarily involved in phase 0 of the action potential in the ventricular cardiomyocyte. Potassium currents participates in phase 1,2 and 3 in cardiac action potential. Calcium current is primarily involved in phase 2 of the action potential.

E. ECG and cardiac action potential

Electrocardiogram (ECG) is a measurement of the electrical activity of the beating heart (Kligfield, Gettes et al. 2007). Clinically, ECG is widely used to determine the risk factors of cardiac arrhythmia. Figure 5 summarizes the cardiac action potential and corresponding ECG. The P wave indicates the atrial depolarization, which spreads from the sinoatrial (SA) node towards the atrioventricular (AV) node, and from the right atrium to the left atrium. P wave has a duration around 80ms. The QRS complex represents the rapid depolarization of the ventricles and has a duration between 80 to 100ms. Following the QRS complex, there is a ST segment connecting QRS complex and the T wave. The ST segment indicates the period when the ventricles are depolarized and the length of the ST segment is associated with the plateau phase of the action potential. The following T wave indicates the ventricular repolarization and normally has a longer duration compared with the depolarization phase. Therefore, the total QT interval, measured from the beginning of the QRS complex to the end of the T wave, represents ventricular depolarization and repolarization and can be used to estimate the average action potential duration(Rautaharju, Surawicz et al. 2009). QT interval ranges can vary with heart rate, therefore, a corrected QT interval (QT interval dividing by the square root of the RR interval, refered to as ‘QTc’) is often used to study the range of QT interval (Jackman, Friday et al. 1988, Funck-Brentano and Jaillon 1993). The QT interval is usually within the range from 350 ms to 440 ms(Levine, Rosero et al. 2008). However, it can be longer under pathological conditions (Morita, Wu et al.

2008). In clinical cases, a prolonged QT interval (> 440 ms) is often used as an important parameter to diagnose or predict potential risk of cardiac arrhythmia generation(Schwartz 1985).

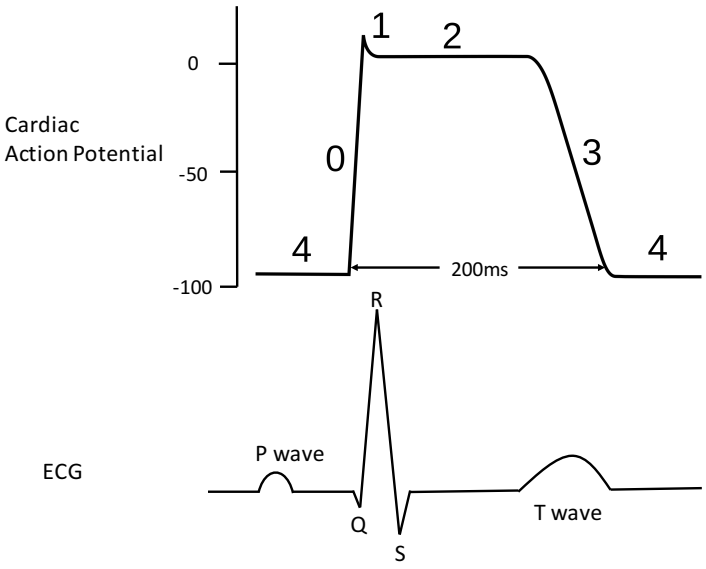

Figure 5. Ventricular action potential and its relationship with the ECG study. The top panel shows a standard single cardiac ventricular action potential wave form. The lower panel depicts a corresponding ECG trace. The QRS complex represents the rapid depolarization phase (phase ‘0’) of the action potential, and the T-wave represents the repolarization phase (phase ‘3’) of the action potential. The QT-interval (from the starting point of the Q wave to the end point of the T-wave) is an indicator of the length of the action potential duration (APD).

F. The role of cardiac sodium channels in the genesis of cardiac arrhythmias

As described previously, cardiac sodium channels regulate the sodium conductance during the rapid upstroke phase (phase 0) of the cardiac action potential and rapidly inactivate after opening. Alterations of Nav1.5 functions may contribute significantly to various kinds of cardiac arrhythmia diseases. Nav1.5 abnormalities are typically caused by mutations in genes encoding cardiac sodium channels (SCN5A) or its accessory proteins (Song and Shou 2012).

A large number of studies focus on the effects of SCN5A mutations on the normal molecular structure and function activities of Nav1.5, and how that leads to arrhymogenic diseases. Previous studies demonstrate that altered Nav1.5 function may induce many different types of cardiac arrhythmia diseases, including long QT syndrome type 3 (LQT-3), Brugada syndrome, cardiac conduction defect, atrial fibrillation, dilated cardiomyopathy or overlapping syndromes (Ruan, Liu et al. 2009). Among them, LQT-3 and Brugada syndrome are most common arrhythmia phenotypes that connect with Nav1.5 malfunctions.

Long QT syndrome is an inherited or acquired cardiac abnormality with delayed repolarization of the heart, which increases the risk of sudden death due to ventricular arrhythmia. It is often characterized by prolonged QT interval on electrocardiogram (Schwartz 2012). Prolonged QT interval is generated by increased action potential duration and delayed ventricular repolarization (Figure 7). Long-QT syndrome (LQTS) can be generated from mutation of several genes encoding a protein that is involved in ventricular repolarization. Based on which

gene mutation leads to LQT phenotype, LQTS is classified into different subtypes (Table 2). LQT-3 is specifically associated with mutations in SCN5A, the gene encoding cardiac sodium channels.

Many SCN5A mutations have been identified and characterized in patients with LQT-3 phenotype. Most mutations are sodium channel gain-of-function mutations(Wang, Shen et al. 1995). The most commonly studied mechanism is the sodium channel fast inactivation defect, which leads to a non-inactivating persistent (late) sodium channel current (Figure 8). Even though persistent current amplitude is rather small compared to peak current (usually less than 1%), it significantly contributes to delayed repolarization of cardiac action potential and further leads to a prolonged action potential duration and QT interval (Bennett, Yazawa et al. 1995).

Another commonly occurring mechanism of SCN5A mutation to cause LQT-3 is the increased window current (Wang, Yazawa et al. 1996). In general, more than 99% of Nav1.5 are inactivated by the end of action potential phase 1 and are in a refractory period until fully recovered from inactivation during phase 4. Only a small portion of sodium channels (usually less than 1%) can activate during phase 3, when cells are at voltages depolarized enough to activate a small fraction of channels but not enough to fully inactivate all the channels. The overlap between voltage dependence of activation and inactivation curves reflects this window (overlap) of membrane potential under which a small fraction of sodium channel can be activated but not inactivated. Therefore, these small fraction of sodium currents are often referred to as ‘window currents’ (Figure 6).

The voltage range of the window current is generally very small under physiological condition and hence will not affect action potential generation significantly. However, under pathological condition, i.e. delayed inactivation (inactivation shifted to more depolarized potentials), the voltage range will become wider, leading to an increased window current during action potential phase 3 and contribute to cardiac arrhythmia generation (Wedekind, Smits et al. 2001). Apart from the above mentioned two mechanisms, other less common mechanisms have also been revealed, including an enhanced peak sodium current density (Rivolta, Abriel et al. 2001), slower inactivation (Ruan, Liu et al. 2007), and faster recovery from inactivation (Clancy, Tateyama et al. 2003).

Brugada syndrome is another arrhythmia phenotype that can be caused by SCN5A mutation. There are 6 common types of Brugada syndromes and type I is associated with Nav1.5 malfunction (Table 3). Unlike LQT-3, Brugada syndrome patients generally have a SCN5A loss-of-function mutation. One of the common molecular mechanisms of Brugada syndrome is the decreased sodium peak current, which can result from a decreased surface expression of sodium channels(Mohler, Rivolta et al. 2004), trafficking defect or defect of interaction with accessory subunits (Valdivia, Tester et al. 2004). Another mechanism involves the alteration in sodium channel gating properties, including delayed activation (Smits, Koopmann et al. 2005) or enhanced inactivation(Bezzina, Veldkamp et al. 1999, Dumaine, Towbin et al. 1999). Therefore, loss-of-function mutations in SCN5A of will reduce the probability of channel opening and significantly decrease the sodium inflow, which further leads to a shortened

action potential duration and the loss of action potential dome (caused by transmural repolarization gradients, Figure 9A). This is often reflected in patients ECG as ST segment elevation and occurrence of arrhythmias (Figure 9B).

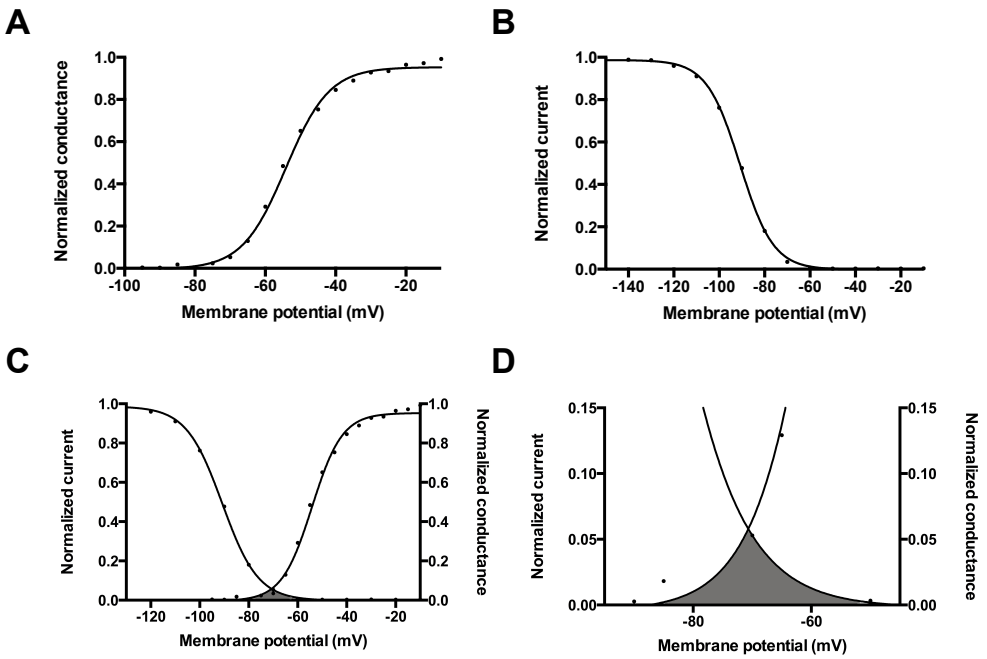

Figure 6. Voltage dependence of activation and inactivation of cardiac sodium channel. A. Representative curve of cardiac sodium channel voltage dependence of activation. 50ms depolarizing voltage steps was applied from a holding potential of -100 mV. The activation curve was plotted by normalized conductance versus membrane potential, indicating fraction of channels activated under different voltage. B. Representative curve of sodium channel voltage dependence of inactivation. 500ms prepulse was applied from -170 to -20 to inactivate the channels. Then, the fraction of channels remain active was measured by a test pulse at -10mV. The inactivation curve was plotted by normalized current versus membrane potential, indicating the fraction of channels inactivated. C, D. Representative window current (grey area). The window current was generated under the voltage that depolarized enough to activate sodium channels but not sufficient to fully inactivate all sodium channels.

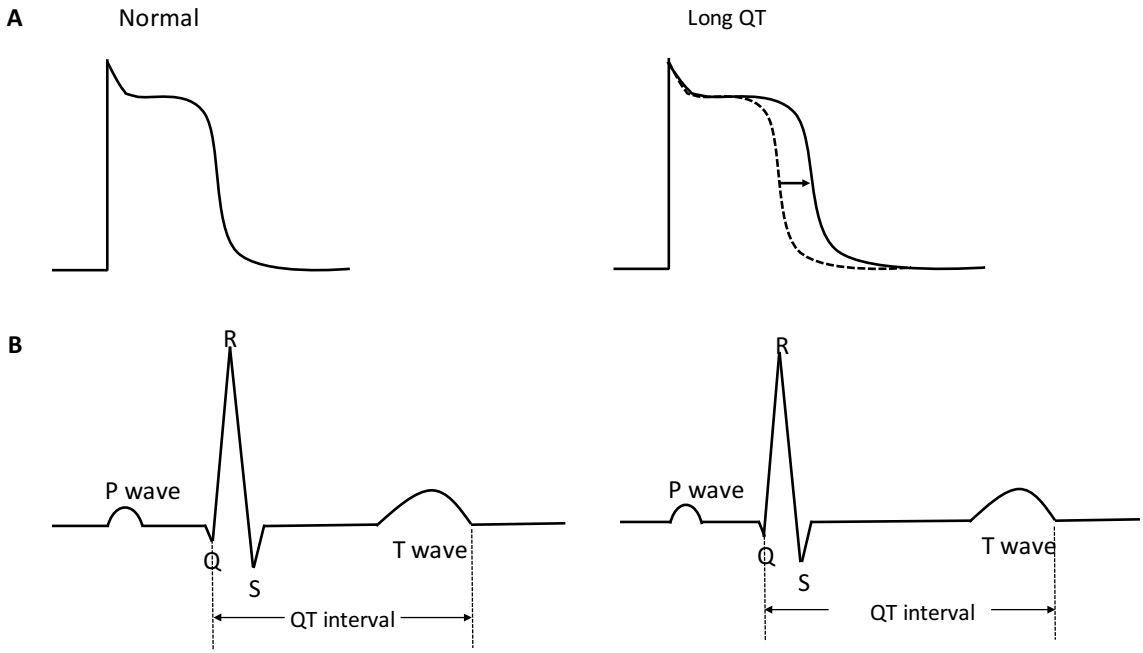

Figure 7. ECG and action potential waveform under normal and LQT condition. A. Action potential waveform under normal (left) and LQT disease (Koval, Snyder et al.) condition. There is an increase in action potential duration and delay of ventricular repolarization. B. Prolonged QT intervals on the ECG(Koval, Snyder et al.) compared to the normal ECG (left).

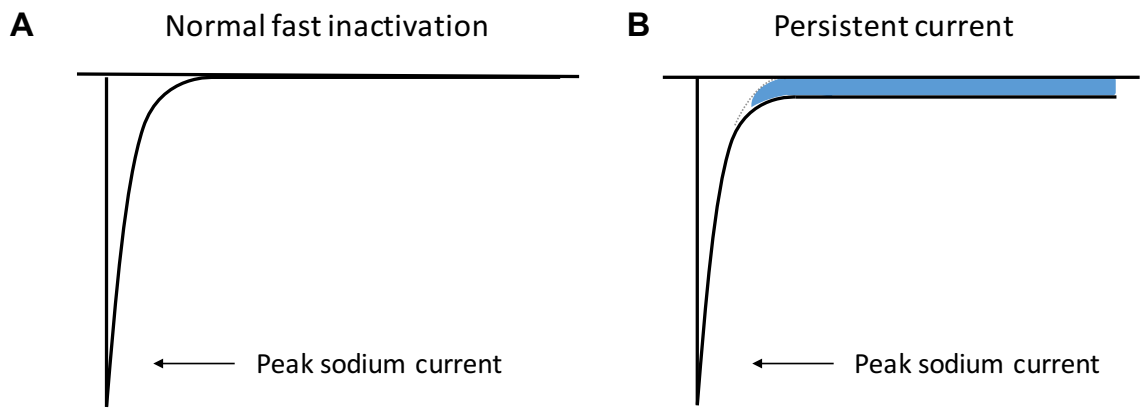

Figure 8. Impaired fast inactivation leads to the generation of persistent (late) sodium current. A shows the representative current trace of normal fast inactivation. Sodium channel opens and inactivates quickly after opening. B indicates the persistent current generation when sodium channel fast inactivation is impaired. Blue color indicating the non-inactivating persistent current.

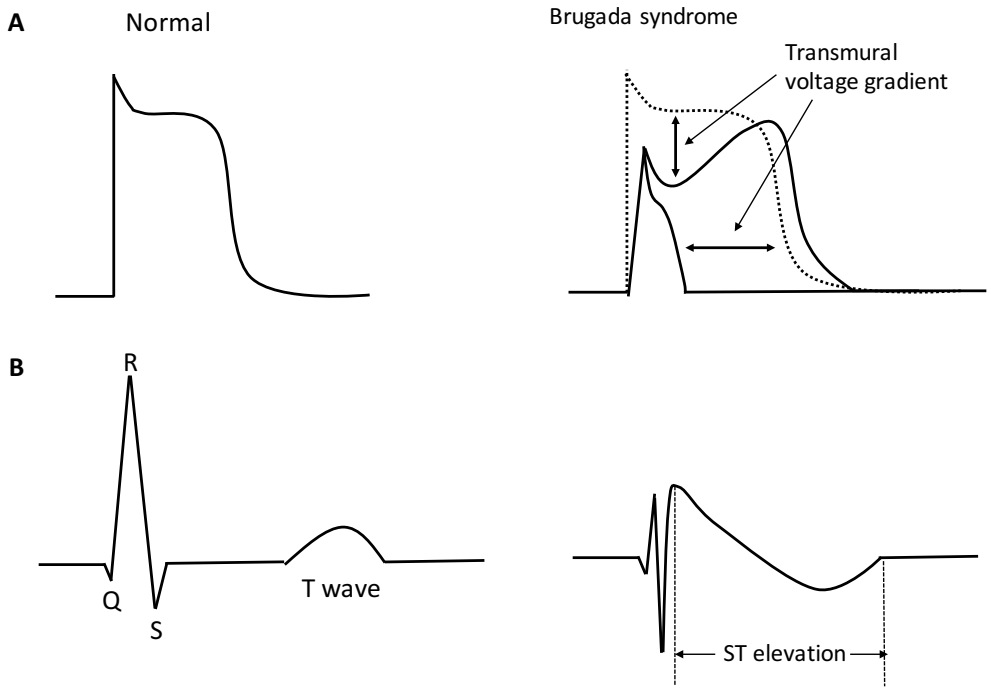

Figure 9 Action potential waveform and ECG of normal (left) and Brugada syndrome condition(right, solid line). Under Brugada syndrome, there is a loss of action potential dome due to transmural voltage gradient and an elevated ST segment.

Table 2. Long-QT syndrome (LQTS) subtypes and involved genes(Issa, Miller et al.).

Syndrome	Gene	Locus	Prevalence
LQTS1	KCNQ1	11p15.5	42%-45%
LQTS2	KCNH2	7q35	35%-45%
LQTS3	SCN5A	3p21	8%-10%
LQTS4	ANK2	4q25	<1%
LQTS5	KCNE1	21q22.1	<1%
LQTS6	KCNE2	21q22.1	<1%
LQTS7	KCNJ2	17q23	<1%
LQTS8	CACNA1C	12p13.3	<1%
LQTS9	CAV3	3p25	<1%
LQTS10	SCN4B	11q23	<1%
LQTS11	AKAP9	7q21	<1%

Table 3 Brugada syndrome (BrS) subtypes and involved genes(Nielsen, Holst et al. 2013).

Syndrome	Gene	Locus	Prevalence
BrS1	SCN5A	3p21	11%-24%
BrS2	GPD1-L	3p22.3	<1%
BrS3	CACNA1C	12p13.3	6%-7%
BrS4	CACNB2	10p12.33	4%-5%
BrS5	SCN1B	19q13.11	1%-2%
BrS6	KCNE3	11q13.4	<1%

G. Post-translational modifications of cardiac sodium channels

VGSC function is determined by their intrinsic biophysical properties (i.e., rapid activation and inactivation), but it can also be regulated by post-translational modifications. Nav1.5 is the target of many post-translational modifications, including glycosylation, phosphorylation, methylation, acetylation, redox modifications, and ubiquitination (Marionneau and Abriel 2015). Because of the modern protein analysis technologies like mass spectrometry, we are able to study the precise location of post-translational modification sites and consensus sequence among different channel subtypes, leading to a better understanding of the mechanistic details of these regulations.

Phosphorylation is the most extensively studied post-translational modification of Nav1.5. Various protein kinases have been identified to modulate different aspects of sodium channel function through diverse pathways including Ca^{2+}/Calmodulin-dependent serine/theronine protein kinase (CAMK)(Aiba, Hesketh et al. 2010, Ashpole, Herren et al. 2012, Koval, Snyder et al. 2012), protein kinase A and C (PKA and PKC)(Qu, Rogers et al. 1994, Murray, Hu et al. 1997, Shin and Murray 2001, Hallaq, Wang et al. 2012), Phosphatidylinositol 3-Kinase (PI3K)(Park, Leong et al. 1999, Lu, Wu et al. 2012, Lu, Jiang et al. 2013), Adenosine Monophosphate-activated Protein Kinase (APMK)(Light, Wallace et al. 2003). Many of the phosphorylation sites that have been identified were located in the first intracellular linker loop (DI to DII linker, Figure 10) and a number of them was found to be conserved among different species and subtypes(Marionneau, Lichti et al. 2012).

Glycosylation, another common post-translational modification of ion channels, is the enzymatic process that attaches glycans to ion channel proteins. Glycosylation of Nav1.5 was determined 20 years ago by Cohen and Levitt(Cohen and Levitt 1993). N-linked glycans (attached to a nitrogen of asparagine) and O-linked glycans (attached to the hydroxyl oxygen of serine, threonine) are often terminated by sialic acids which can alter voltage-gated sodium channel function through their negative charges. It has been shown that sialylation shifts the voltage-dependence of activation and inactivation towards hyperpolarized potentials, enhances the rate of fast inactivation and reduces the rate of recovery from fast inactivation (Bennett 2002, Johnson, Montpetit et al. 2004). Pathophysiologically, reduced cardiac sodium channel sialylation has been shown to shorten the cardiomyocyte refractory time and enhance susceptibility to ventricular arrhythmias by slowing fast inactivation and increasing the rate of recovery from inactivation (Ednie, Horton et al. 2013).

Ubiquitination, another well studied post-translational modification of Nav1.5, refers to the enzymatic process in which an ubiquitin protein is attached to the sodium channel protein. This process is closely associated with sodium channel internalization. Ubiquitination of Nav1.5 has been demonstrated from both in vitro and in vivo studies(van Bemmelen, Rougier et al. 2004, Rougier, Albesa et al. 2010, Laedermann, Decosterd et al. 2014). While many studies have suggested that regulation of ubiquitination of Nav1.5 could lead to an altered surface expression level of Nav1.5 in cardiac cells(Kang, Zheng et al. 2009, Laedermann, Cachemaille et al. 2013, Rougier, Gavillet et al. 2013), the

detailed mechanism involved in this process and the study of its clinical relevance, is still lacking.

Arginine methylation of Nav1.5 in stable cell lines and human ventricles was determined recently using mass spectrometry(Beltran-Alvarez, Pagans et al. 2011, Beltran-Alvarez, Tarradas et al. 2014). Studies revealed that arginine R513, R526, and R680, located in the DI and DII intracellular linker of cardiac sodium channel, are subject to arginine methylation. Nav1.5 methylation also enhances cell surface expression of Nav1.5 and sodium current density (Beltran-Alvarez, Espejo et al. 2013).

Although many post-translational modifications of Nav1.5 have been extensively studied, the regulation of VGSCs by lipid modifications is poorly understood. Our research is of great importance that it provides new insights into how post-translational lipid modification regulates Nav1.5 activities and influences cardiac excitability.

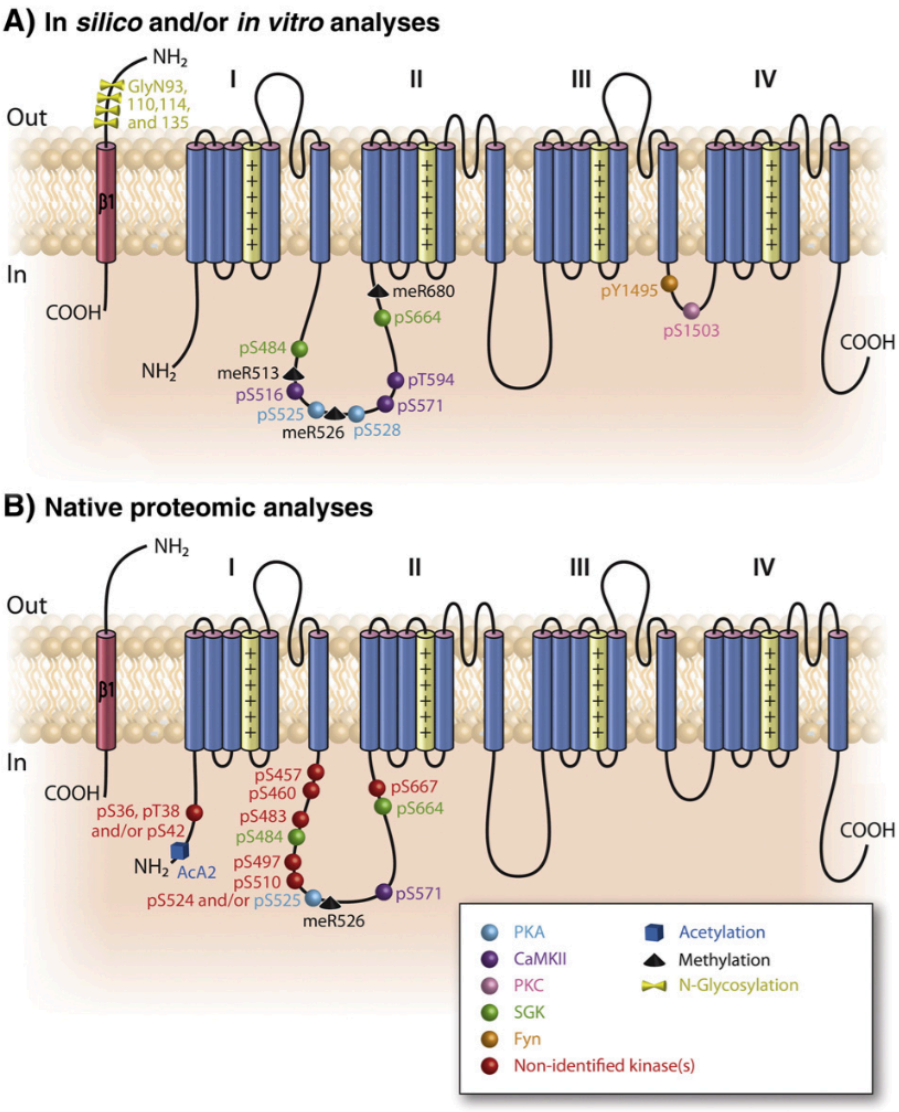

Figure 10. Localization of post-translational modification sites on the human cardiac NaV1.5 using in silico and/or in vitro analyses (A) and native proteomic analyses from cardiac tissues (B) 16 sites were identified using *in silico*/*in vitro* analyses, and thirteen were identified using native proteomics. Five sites (pS484, pS525, meR526, pS571 and pS664) have been confirmed by MS. This figure is from the review paper 'Regulation of the cardiac Na+ channel NaV1.5 by post-translational modifications' (Marionneau and Abriel 2015).

H. Palmitoylation of ion channel proteins

Palmitoylation has been recognized as an important post-translational mechanism for the regulation of various membrane proteins, but our knowledge of how palmitoylation regulates ion channels is limited(Shipston 2011). Protein S-Palmitoylation involves the addition of a 16-carbon palmitic acid chain to an intracellular cysteine residue through a thioester linkage(Figure 11).

S-Palmitoylation is a reversible process that can dynamically regulate protein life cycle and function(Shipston 2011). Multiple enzymes that facilitate the palmitoylation process have been identified in recent years (Lobo, Greentree et al. 2002, Roth, Feng et al. 2002). Palmitoyltransferases (PATs), the catalytic enzymes for protein palmitoylation, form a diverse family of proteins (23 members in mammals)(Fukata, Fukata et al. 2004, Greaves and Chamberlain 2011, Korycka, Lach et al. 2012). PATs are characterized by the presence of a aspartate-histidine-histidine-cysteine (DHHC) motif within a cysteine-rich domain (Salaun, Greaves et al. 2010). The reverse process, depalmitoylation, is mediated by acyl protein thioesterases (APTs)(Zeidman, Jackson et al. 2009). According to previous studies, non-enzymatic palmitoylation could be possible but is very rare and only reported in vitro(O'Brien, St Jules et al. 1987, Ross and Braun 1988, Mollner, Ferreira et al. 1998).

Palmitoylation is involved in various phases of ion channel life cycle, including synthesis, maturation, trafficking, membrane localization, internalization and recycling. Palmitoylation plays an important role in the biosynthesis of brain voltage-gated sodium channels (Nav1.2) and potassium channels to regulate channel maturation and quality control (Schmidt and Catterall 1987, Zhang,

Foster et al. 2007). The formation of ligand-binding sites in nicotinic acetylcholine receptors is also regulated by palmitoylation (Drisdel, Manzana et al. 2004, Alexander, Govind et al. 2010). Palmitoylation regulates trafficking of glutamate channels(Hayashi, Rumbaugh et al. 2005, Hayashi, Thomas et al. 2009) and the spatial organization of aquaporin channels(Suzuki, Nishikawa et al. 2008). The addition of palmitic acid also regulates protein hydrophobicity and facilitates association to the membrane. However, few studies have focused on how palmitoylation directly alters channel biophysical activity at the membrane. Palmitoylation of the intracellular linker between domain II and III in Kv1.1 has been shown to increase the intrinsic voltage sensitivity of the channel(Gubitosi-Klug, Mancuso et al. 2005). In 1987, brain sodium channel palmitoylation was identified to occur in the early stages of biosynthesis(Schmidt and Catterall 1987). Electrophysiological data indicates that two putative palmitoylation sites in a Nav1.2 channel likely regulate brain sodium channel activity as well as modulating channel affinity to PaurTx3 and ProTx-II toxin (Bosmans, Milescu et al. 2011).

The functional effect of ion channel palmitoylation is dependent on both the channel type and the location of the palmitoylation sites. Palmitate lipid may attach to different locations including C-terminus, N-terminus, juxta-transmembrane region or intracellular loop, leading to the distinct alteration in various aspects of ion channel protein function (Shipston 2014). It is still unclear how palmitoylation alter the functional activity of ion channel protein. One hypothesized mechanism is that the palmitate molecules interact with the

membrane lipids (Figure 12), changing the lipid membrane environment surrounding the targeted channel as well as impacting protein configuration, thus potentially modulating channel activity.

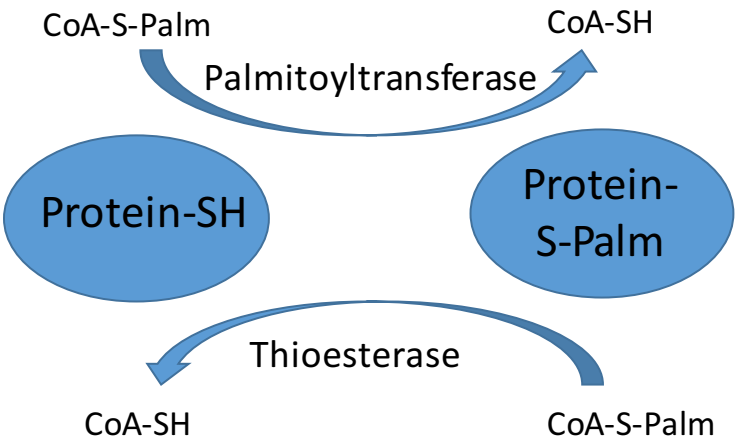

Figure 11. A schematic illustration of the dynamic regulation of protein palmitoylation. Palmitoylation is a reversible process due to the labile thioester bond. Palmitoyltransferase mediates the palmitoylation process with the presence of palmitoyl-CoA. Depalmitoylation is mediated by thioesterase.

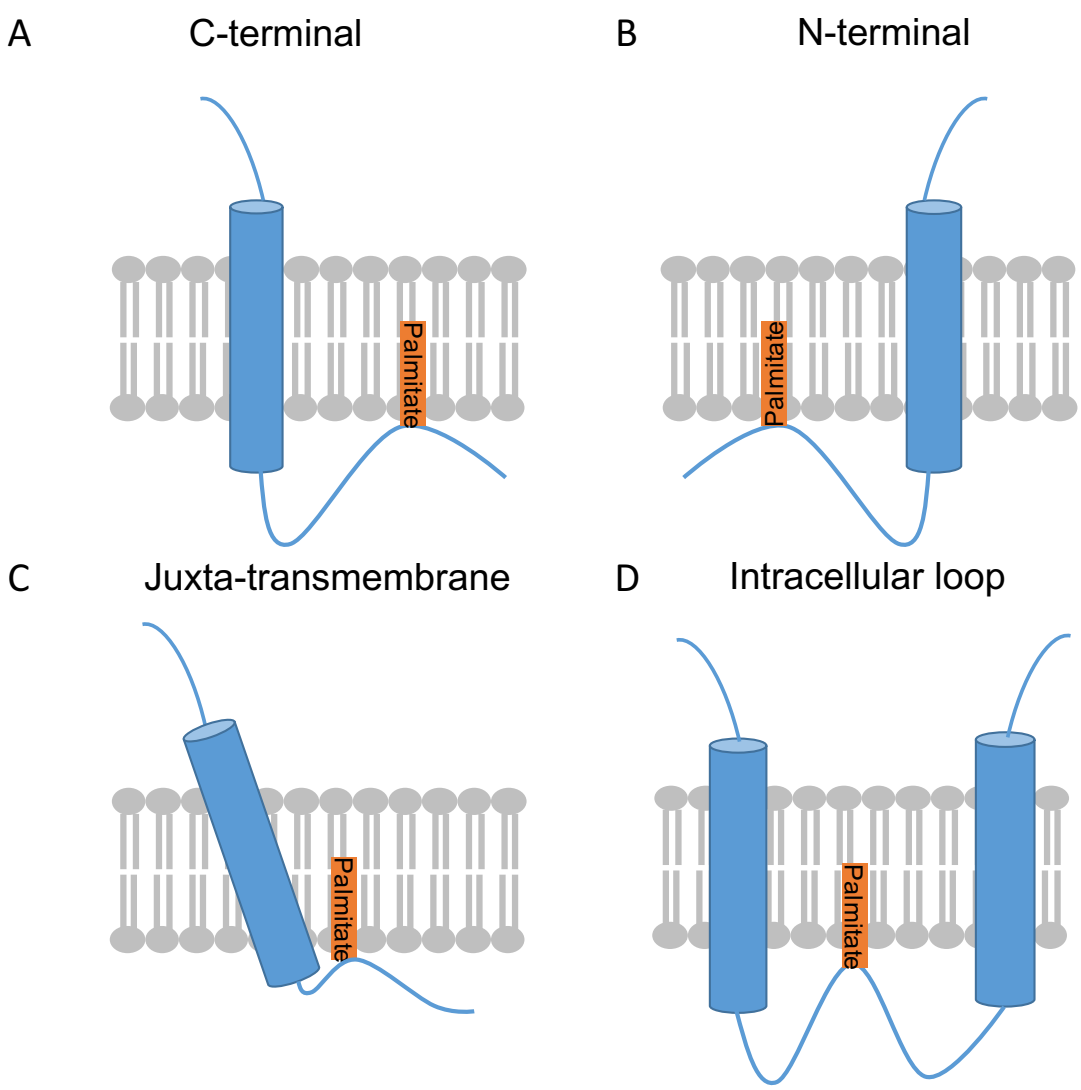

Figure 12. Schematic representation of palmitoylation on different locations of ion channel proteins. Cysteine palmitoylation can occur on C-terminal (A), N-terminal (B), juxta-transmembrane region (C) or intracellular loop of ion channel proteins. This figure is adapted and slightly modified from 'Ion channel regulation by protein S-acylation' (Shipston 2014).

I. Hypothesis and specific aims

Previous research has demonstrated that palmitoylation plays an essential role in regulating ion channel function. However, very few studies demonstrate how palmitoylation directly alters ion channel biophysical activity at the membrane and its physiological and pathological consequences. One previous study shows two putative palmitoylation sites in a Nav1.2 channel modulates brain sodium channel activity by regulating channel inactivation and channel pharmacology (Bosmans, Milescu et al. 2011). However, the direct biochemical evidence of sodium channel palmitoylation is lacking in this study and the physiological consequence of the sodium channel palmitoylation is still unknown. It raises several questions for us: 1. is it possible to have direct biochemical determination of sodium channel palmitoylation; 2. whether palmitoylation of other sodium channel subtypes would also occur and would that occur in conserved sites; 3. what is the physiological consequence of voltage-gated sodium channel palmitoylation and could palmitoylation be associated with any disease phenotype under specific pathological conditions.

Overall, the central hypothesis of this dissertation project is that palmitoylation can regulate cardiac sodium channel activity and cardiac excitability, and can be a novel pathomechanism underlying cardiac arrhythmias. The hypothesis consists of three specific aims.

The first specific aim is to show the direct biochemical evidence of cardiac sodium channel palmitoylation. Few studies have demonstrated ion channel palmitoylation with biochemical results. Brain sodium channel palmitoylation has been shown with metabolic labelling of palmitate (Schmidt and Catterall 1987).

However, these experiments usually require exposure time from one month to half a year. In recent years, development of the acyl-biotin exchange assay (ABE) enables much faster detection of protein palmitoylation. Hence, this method was applied in most of our biochemistry experiments. We also performed experiments using the click chemistry method and detailed comparison of three methods were discussed in Section IV B. Bioinformatics tools and ABE assay were used to determine the potential palmitoylation sites.

My second specific aim focuses on the alteration of cardiac sodium channel functions by palmitoylation. Sodium channel biophysical properties, including fast inactivation, voltage-dependent activation and inactivation, recovery from inactivation, slow inactivation and recovery from slow inactivation were assessed to investigate palmitoylation effect on sodium channel function.

Although palmitoylation is likely an important regulator of ion channel activity, evidence for the direct influence of palmitoylation on cellular excitability, and its potential involvement in cardiac sodium channelopathies, is lacking. Therefore, in our final specific aim, we investigated palmitoylation effect on cardiac myocyte excitability. Cardiac sodium channel biophysical properties and action potential parameters were studied under non-treatment, depalmitoylated and enhanced palmitoylation condition.

Overall, the objective of this project is to understand palmitoylation of cardiac sodium channel protein and its physiological relevance. This dissertation addresses the following questions of this project: 1) whether Nav1.5 is palmitoylated in heterologous expression system and cardiac tissues; 2) how

does palmitoylation alter Nav1.5 functions; 3) where are the palmitoylation sites on Nav1.5; 4), how does palmitoylation regulate cardiac excitability and its relevance with cardiac arrhythmia disease. This study adds important insights to the study of cardiac sodium channel post-translational modifications and provides previously unrevealed cellular and ionic mechanisms underlying arrhythmogenesis.

II. MATERIALS AND METHODS

A. Ethical information and animal protocols

Human embryonic kidney (HEK293) cells were obtained from ATCC (Manassas, USA). Use of HEK293 cells was approved by the Institutional Biosafety Committee and conformed to the ethical guidelines for the National Institutes of Health for the use of human derived cell lines.

The use of animals was in compliance with the Guide for the Care and Use of Laboratory Animals published by the US National Institutes of Health and was approved by the Indiana University School of Medicine Animal Care and Use Committee.

B. Animals.

Postnatal Day 1 Sprague Dawley rats were obtained from Harlan-Sprague Dawley, Inc. (Indianapolis, IN, USA). Animals were kept in the Laboratory of Animal Source Center and used on the day of arrival.

C. Chemicals

2-Br-palmitate, Palmitic acid, Lidocaine and Mexiletine hydrochloride were obtained from Sigma-Aldrich. Flecainide and Ranolazine were purchased from Abcam.

D. Experimental cDNA constructs

hNav1.5 constructs were introduced into pcDNA3.1(+) with the CMV promoter using HindIII and XbaI restriction enzyme sites.

E. Mutagenesis of voltage-gated sodium channels

Specific mutation sites were introduced using the QuikChange II XL site-directed mutagenesis kit according to the manufacturer's instruction.Mutagenesis primers were designed to introduce the specific base pair change into wild type hNav1.5 channel cDNA. All the constructs were sequenced (ACGT Inc. Wheeling, IL, USA) to confirm the specific mutation at target sites. Primers that were used to generate human Nav1.5 cDNA mutation constructs are included in Table 4.

Table 4. Primers used for site-directed mutagenesis in hNav1.5

Mutagenesis Site	Sequence
C981F forward	CCACCTGGGATTTCTTCTGTGGTCTCCTGC
C981F reverse	GCAGGAGACCACAGAAGAAATCCCAGGTGG
C981A forward	CCACCTGGGATTTCGCCTGTGGTCTCCTGC
C981A reverse	GCAGGAGACCACAGGCGAAATCCCAGGTGG
C1178A forward	GCGCTGTCCCGCCTGTGCGGTGGACACCACA
C1178A reverse	TGTGGTGTCCACCGCACAGGCGGGACAGCGC
C1176A, C1178A, C1179A forward	GGACTGCTTCACTGAAGGCTGTGTCCGGCGC GCTCCCGCCGCTGCGGTGGACACC
C1176A, C1178A, C1179A reverse	GGTGTCCACCGCAGCGGCGGGAGCGCGCCG GACACAGCCTTCAGTGAAGCAGTCC

F. HEK293 cell culture

HEK293 and HEK293T cells (ATCC CRL-1573 and CRL-3216, respectively, Manassas, VA, USA) were cultured in Dulbecco's Modified Eagle Medium (Life Technologies, Grand ISLAND, NY, USA) supplemented with 10% fetal bovine serum (Atlanta Biologicals, Laurenceville, GA, USA) and 1% penicillin/streptomycin (Invitrogen, Grand Island, NY, USA). Cells were kept at 37°C incubator with 5% CO_2.

G. Harvest, isolation and culture of neonatal rat cardiomyocytes

Sprague Dawley rat pups of postnatal day 1 were used in the harvest, isolation and culture of rat cardiomyocytes. After pups were sacrificed, hearts were collected and placed in calcium and magnesium-free ice-cold PBS. Hearts were gently squeezed using flat tip forceps to remove the remaining blood. The ventricles were cut and transferred into 1.5ml eppendorf tubes and pre-warmed PBS containing 0.5mg/ml collagenase (Worthington, Lakewood, NJ, USA) was added as the digestion solution. The ventricle tissues were cut into small pieces and transferred into a new 15ml conical tube containing the same digestion solution. The cardiac tissues were further digested in the 37°C water bath for 45 minutes with a gentle mix every 5 minutes. The cell suspension was collected every 15 minutes and fresh digestion solution was added each time. After collecting cell suspension, 1 ml of horse serum was added to terminate the digestion. Cell suspension was centrifuged at 900 rpm for 10 minutes. The supernatant was discarded and the palette was resuspended with 10ml cell culture media (DMEM+10%FBS). The tube was centrifuged second time at the

same speed for 10 minutes. The supernatant was discarded again and the cells were mixed into suspension with 10ml cell culture media. Collected cells were plated in 10cm cell culture dishes for 2hrs to allow fibroblast cells attach and then transferred to 24 wells plates with 0.2% gelatin pre-coated coverslips. Cells were incubated under normal cell culture conditions (37°C, 5% CO_2) in Dulbecco's Modified Eagle Medium supplemented with 10% fetal bovine serum. After 24 hours incubation, the culture medium was replaced with a low serum medium (0.5% horse serum, 0.5% fetal bovine serum) to prevent hypertrophy(Simpson, McGrath et al. 1982). Cardiomyocytes were cultured for up to 72 hours.

H. Solutions

1. Standard extracellular bathing solution for HEK293 cell voltage clamp recordings

The standard external bathing solution for sodium current recording contained (in mM) 140 NaCl, 1 $MgCl_2$, 1 $CaCl_2$, 3 KCl, and 10 HEPES, pH 7.3 adjusted with 1N NaOH. The osmolarity was adjusted to 276 Osm.

2. Standard intracellular electrode solution for HEK293 cell voltage clamp recordings

The standard pipette solution contained (in mM) 140 CsF, 10 NaCl, 1.1 EGTA, and 10 HEPES, pH 7.3 (adjusted with CsOH) and the osmolarity was adjusted to 293 Osm.

3. Standard extracellular bathing solution for cardiomyocytes voltage clamp recordings

The external bathing solution of cardiomyocyte whole cell voltage clamp

recordings contains (mM): 120 NaCl, 1.2 MgCl2, 1.5 CaCl2, 10 Hepes, 10 tetraethylammonium-chloride, 5.0 sucrose, 5.0 glucose and 0.05 $CdCl_2$, pH was adjusted to 7.4 with NaOH. Osmolarity of the solution was adjusted to 283 Osm. Tetraethylammonium-chloride and $CdCl_2$ were used to block potassium and calcium currents in myocytes in order to focus on recording whole cell sodium currents.

4. Standard intracellular electrode solution for cardiomyocytes voltage clamp recordings

The pipette solution contained: 120 CsF, 5.0 NaCl, 2.0 $MgCl_2$, 10 Hepes and 10 EGTA. pH was adjusted to 7.3 with CsOH. The osmolarity of the solution was adjusted to 276 Osm).

5. Standard extracellular bathing solution for cardiomyocytes action potential recordings

The bath solution for the whole cell current clamp recordings on cardiomyocytes contained (mM): NaCl 126, KCl 5.4, Hepes 10, NaH_2PO_4 0.33, $MgCl_2$ 1.0, $CaCl_2$ 1.8 and glucose 10. pH was adjusted with NaOH to 7.3. The osmolarity of the solution was adjusted to 300 Osm.

6. Standard intracellular electrode solution for cardiomyocytes action potential recordings

The pipette solution used in current-clamp studies contained (mM): KCl 20, potassium aspartate 110, $MgCl_2$ 1.0, Hepes 5.0, EGTA 10 and Na_2-ATP 5.0. pH was adjusted to 7.2 with KOH. The osmolarity of the solution was adjusted to 295 Osm.

I. Whole cell voltage-clamp recordings from HEK293 cells.

The coverslip was placed in the middle of the patch-clamp recording chamber containing 300ul extracellular bath solution. All recordings were performed at room temperature. Data were acquired using HEKA EPC-10 patch-clamp amplifier and Pulse program v8.65 (HEKA Electronic, Lambrecht/Pfalz, Germany). Glass pipettes were pulled and polished with resistance between 0.9 and 2 MΩ. After the pipettes attach cell surface, Gigaohm was formed by applying slight negative pressure through the glass pipettes. Once a gigaohm or greater seal was formed between the cell of interest and the recording pipette, the whole cell configuration was obtained using gentle suction pulses. Recordings were started around 5 minutes after forming whole cell configuration to allow sufficient equilibration of the intracellular solution and the pipette solution. In the conductance-voltage relationship studies, the cells were held at -100 mV then a 100ms pulse from -100mV to +45 mV with 5mV increments was used to elicit the currents. In steady-state inactivation studies, cells were held at -100 mV and then stepped to an inactivating prepulse from -150 mV to -10 mV with 10 mV increments for 500 ms. The channels that remain available after each inactivating prepulse were evaluated by the peak current produced during a test pulse to 0 mV for 20 ms. In the recovery from inactivation protocol, 500ms depolarization pulse to +20mV was induced to fully inactivate the channel, and recovery was assessed by a test pulse from -100mV to 0mV with a varying time between pulses (0-50ms).

J. Whole cell voltage-clamp recordings from neonatal cardiomyocytes.

Whole-cell cardiac sodium currents were recorded at room temperature from neonatal cardiomyocytes within 24-72 h after cell culture. Voltage-clamp protocols used were similar as previously described in voltage-clamp recordings in HEK293 cells.

K. Whole cell current-clamp recordings from neonatal cardiomyocytes.

Action potentials were elicited by 2 ms stimulus pulses at a frequency of 1 Hz. Spontaneous action potential generation was recorded given the current input at 0 pA. Action potential recordings were started 5 min after establishing the whole cell configuration. No TTX was added to the external recording solution for action potential studies.

L. Transient transfection and preparation of stably transfected HEK293 cells

Cells were transfected using the calcium phosphate precipitation method. The transfection reagents containing 2X HEPES buffer (280 mM NaCl, 1.5mM Na_2HPO_4, 50mM Na-HEPES, pH=7), double distilled water; 2 M $CaCl_2$ was mixed with DNA and eGFP. Each tube contains 40 µl HEPES, 4.5 µl DNA (1 µg/µl), 0.5 µl eGFP (1 µg/µl), 5 µl $CaCl_2$ and 30 µl double distilled water. The mixture of DNA and calcium phosphate was kept in the cell culture hood for 30 minutes before added to the medium. After 30 minutes, the 80 µl DNA and calcium phosphate mixture was added to 2 ml Dulbecco's Modified Eagle Medium. Then the cell culture medium was replaced by the Dulbecco's Modified Eagle Medium containing DNA and calcium phosphate mixture. After three hours incubation, the culture medium was replaced again with standard culture

medium. Patch-clamp recordings were performed 24–48 h after transfection. Cells were selected based on the expression of green fluorescence protein. Stable cell lines were generated using similar procedure without adding eGFP to the DNA and calcium phosphate mixture. At 48-72 hours post transfection, cells were moved to 100 mm dishes and G418 was added to the dish at 400 μg/ml concentration. Typically, culture medium with selection antibiotic was replaced every 4 days for up to four weeks. The cell colonies were transferred and cultured for further functional assessments.

M. Preparation of cell lysate and tissue lysate.

The use of animals was in compliance with the Guide for the Care and Use of Laboratory Animals published by the US National Institutes of Health and was approved by the Indiana University School of Medicine Animal Care and Use Committee. Heart tissue (300mg) from Sprague Dawley rats was homogenized in 10 ml lysis buffer (20mM Hepes, 20mM NaCl, 5mM EDTA, 1% Triton X-100, 500 μl protease inhibitor cocktail set V). Tissues were cut into small pieces and lysed using electric homogenizer (Wheaton). The homogenate was centrifuged at 4°C at 13,200 X g, and the supernatant was collected. Aliquots of supernatant were stored at −80°C.

Cell lysate was prepared using the same lysis buffer. Cells were washed three times with ice-cold PBS (Thermo Fisher Scientific). 1.5 ml lysis buffer was added to each 10mm dish after the third wash and incubated for 5 mins on ice. Cell lysates were collected using 1.5ml eppendorf tubes and sonicated to agitate

and disrupt the cell membranes. The lysates were centrifuged at 4°C at 2,000 g, and the supernatant was collected and store at -80°C.

N. Acyl biotin exchange method

Cell lysate was treated overnight using N-ethylmaleimide (NEM) to block free cysteines while rotating at 4°C to ensure complete cysteine alkylation. Next day, the insoluble component was discarded after centrifuge at 13500 X g for 5 mins. The cell lysate was washed by chloroform-methanol precipitation to remove excess chemicals. The protein interface was washed twice using methanol. After the last centrifugation, protein was dissolved in 500ul PBS containing 1% SDS. The soluble protein was divided into two equal groups, each containing 250µl and treated with either NH_2OH (0.7M Hydroxylamine, 1mM biotin, 0.2% Triton X-100, 500µl protease inhibitor cocktail set V) or control solution (200mM Tris, 1mM biotin, 0.2% Triton X-100, 500µl protease inhibitor cocktail set V) solution. The reaction was carried out in a dark environment for 1hr. The remaining chemicals were removed using a chloroform methanol wash and resolubilized in PBS containing 1% Triton X-100 and 0.2% SDS. The biotinylated proteins were captured by streptavidin-Sepharose (GE Healthcare) beads at 4°C overnight. Beads were washed four times with PBS containing 1% Triton X-100 and 0.2% SDS the next day. Electrophoresis loading buffer (LDS containing 2% β-mercaptoethanol) was added to each sample and heated for 10 min at 80°C.

O. Metabolic labeling and detection of Nav1.5 palmitoylation

HEK293 cells with stable expression of human Nav1.5 channels were

cultured in 100mm dishes, while untransfected HEK293 cells were used as negative controls. Each dish was labeled with 120μCi/ml [3H] palmitic acid (PerkinElmer) in DMEM containing 10% FBS overnight. The medium was removed the following day and cells were rinsed 3 times with PBS. Cell lysates were collected and added to the protein G agarose bead, which was prepared by coupling Nav1.5 pan antibody overnight. After four hours' incubation, the lysate was removed, the protein-G beads were washed 3 times with lysis butter (20mM Hepes, 20mM NaCl, 5mM EDTA, 1% Triton X-100, 1×protease inhibitor cocktail set V(Millipore)), and proteins were eluted from the beads using 4X LDS sample buffer with 2% beta-mercaptoethanol. Samples were then analyzed according to the standard denaturing PAGE protocol (Novex Gel System, Life Technologies, Carlsbad, CA, USA). The gel was washed three times with hot water and stained with Coomassie Blue for 1 hour. In order to increase the sensitivity of tritium detection, protocols using EN3HANCE (PerkinElme, Waltham, MA, USA) were followed based on manufacturer's instructions. To precipitate the fluor in the gel, gel was washed with 10% PEG 800 and 1% glycerol with agitation for 30 minutes. To further prevent the gel from cracking, the gel was incubated in gel dying buffer (30% Ethanol, 10% glycerol) for 30 minutes and transferred onto Whatman filter paper for vacuum drying (ThermoSavant, Waltham, MA, USA). Dried gels were exposed to Biomax high sensitivity film (Sigma-Aldrich, St. Louis, MO) and were stored at -80°C freezer for approximately 3 weeks before developing the film.

P. Gel Electrophoresis and Western Immunoblotting

Samples were solubilized in 4×LDS sample buffer and β-mercaptoethanol. Gel electrophoresis and protein transfer was performed according to the standard protocol (Life Technologies, Carlsbad, CA, USA). 4-12% gradient precast gels (Life Technologies, Carlsbad, CA, USA) were used for protein seperation and a constant voltage of 200mV was applied. Sodium channel pan antibody (1:1000 diluted, Sigma-Aldrich, St. Louis, MO) was used as a primary antibody to detect Nav1.5 signal. In the cardiac tissue study, caveolin3 antibody (1:5000 diluted, BD Biosciences, San Jose, CA, USA) was used to detect caveolin expression in the cardiac tissues. The fluorescently-labeled secondary antibody (IRDye 800CW goat anti-mouse, 1:5000 diluted) was obtained from Li-Cor (Lincoln, Nebraska, USA).

Q. Coomassie staining and silver staining of protein gels

Coomassie staining was performed right after gel electrophoresis. The gel was transferred to a glass container filled with boiling water and washed for 15 minutes. This step was repeated three times before staining solution (Coomassie G-250 Staining) was added into the gel. After 1.5 hours, the staining solution was removed by washing with distilled water for 2 hours.

Silver staining was performed using the mass Spectrometry compatible silver staining kit (Thermo Fisher Scientific, Waltham, MA, USA). The gel was washed twice with 5 minutes each time after the gel electrophoresis. Fixing solution (30% ethanol, 10% acetic acid) was then added to the gel and incubated for 30 minutes (replace with refresh fixing solution after 15 minutes). The remaining solution was removed by washing with ethanol wash (twice, 5 minutes

each time) and ultrapure water (twice, 5 minutes each time). The gel was then incubated in sensitizer working solution (50μL sensitizer and 25 mL water) for exactly 1 minute, followed by washing in ultrapure water (twice, 1 minute each time). Next, the gel was incubated with enhancer (0.25 mL enhancer and 25 mL stain) for 5 minutes and washed with ultrapure water twice (20 seconds each). Developer working solution (0.25mL enhancer and 25mL developer) was added to the gel and incubated until the protein bands appear (about 2 minutes). As soon as the protein band appears and reaches desire intensity, the developer working solution was replaced by the stop solution (5% acetic acid), followed by a brief wash and incubation in acetic acid for 10 minutes. After a final wash with ultrapure water for 10 minutes, the protein band was excised immediately using a clean scalpel and placed in 0.5 mL microcentrifuge tubes.

R. Copper (I)-catalyzed azide-alkyne cycloaddition reaction (click chemistry).

Untransfected HEK293 cell and HEK293 cells stably expressing Nav1.5 channels were cultured in DMEM with 10% FBS. Cells were then incubated in 17-ODYA labeling media (DMEM with 10% dialyzed FBS (Gemini Bio Products, West Sacramento, CA) and 25mM 17-octadecynoic acid (Cayman Chemical, Ann Arbor, Michigan, USA) for 4 hours, washed with D-PBS (Thermo Fisher Scientific, Waltham, MA, USA), and lysed with cell lysis buffer (20mM Hepes, 20mM NaCl, 5mM EDTA, 1% Triton X-100, 1×protease inhibitor cocktail set V (Millipore)). Cleared lysates were immunoprecipitated with anti-Nav1.5 pan antibody and protein G-Sepharose for 4 h. The beads were washed 3 times in

lysis buffer and resuspended with 44µl D-PBS. Click chemistry reagents containing1mM CuSO4, 1mM tris(2-carboxyethyl)phosphine, 100 µM tris[(1-benzyl-1H-1,2,3-triazol-4-yl)methyl]amine (Sigma-Aldrich, St. Louis, MO) and 1µl IRDye® 680RD Azide (Thermo Fisher Scientific, Waltham, MA, USA) were then added to the beads. After one-hour incubation at room temperature, the beads were washed 3 times with D-PBS and treated with 1X SDS gel loading buffer. The supernatants were separated into two equal amounts of 25 µl samples. For control experiments, 1.25 µl of 50% stock of hydroxylamine (pH7.0) was added into one of the two equal amount samples in order to remove the thioester-dependent labeling. The sample mix was then incubated at room temperature for 1 hour, heated at 85°C for 10 minutes and analyzed by standard SDS-PAGE gel electrophoresis. In-gel fluorescence of probe-labeled proteins was detected by Li-Cor Odyssey CLx Imager.

S. Computational simulations of cardiac myocyte

Computer models of cardiac AP firing were employed to simulate the impact of the consequences of the changes in channel gating induced by sodium channel palmitoylation. The cardiac myocyte model was adapted from that previously implemented by Ingemar Jacobson in the NEURON simulation environment (which is available at http://senselab.med.yale.edu/ModelDB/ShowModel.asp?model=3800). The only changes made to the mathematical formulations used in the model were to the voltage-dependent sodium current (Naf in the original model). We ran simulations with 1) wild-type Nav1.5 currents, 2) Nav1.5 currents with simulated

2-Br-palmitate treatment and 3) Nav1.5 currents with simulated palmitic acid treatment. A Markov model of Nav1.5, based on the Hodgkin-Huxley formulation of Nav1.5 in the original cardiac model of AP firing, was used as it is more amenable to implementation of the palmitic acid and 2-Br-palmitate effects. This formulation also included slow inactivation states. Supplementary Fig. 6 shows a diagram for the Markov model of the simulated Nav1.5 conductance and Table 5 shows the transition rate expressions for Nav1.5 and the currents simulating the two treatment groups.

T. Data analysis

Whole cell patch clamp data were analyzed using the Pulsefit (v 8.65, HEKA Electronic, Germany), GraphPad Prism (GraphPad Software Inc. La Jolla, CA, USA) and origin pro 8 (Originlab Corp, Northampton, MA, USA). All data points are shown as mean±s.e.m., and n is presented as the number of the separate experimental cells. Steady-state activation and inactivation curves were fitted using Boltzmann equation: I(V)=Offset+{amplitude/[1+exp((V-V1/2)/Z)]}, in which V1/2 represents midpoint of activation and inactivation curve. V stands for the test potential and Z represents the slope factor. Two tailed, Student's t-tests were used to study the statistical difference of the channel functional parameters with and without channel depalmitoylation, including current density, half maximal activation/inactivation, slope factor, recovery rate. We concluded that a significant difference exists when P values were less than 0.05.

III. Results

A. Characterization of cardiac sodium channel palmitoylation

1. Characterization of Nav1.5 palmitoylation in HEK293 cells using acyl biotin exchange method

To study whether cardiac sodium channels are palmitoylated in HEK293 cells, we first use a non-radioactive acyl biotin exchange (ABE) assay to detect Nav1.5 palmitoylation. The basic principles of ABE assay is to substitute palmitoylated cysteines with biotin and to enable a rapid detection of dynamic protein palmitoylation by the measurement of thiol-biotinylated proteins(Brigidi and Bamji 2013). HEK293 cells stably expressing Nav1.5 recombinant channels were used in the experiment. HEK293 cells, which eliminates the contamination of endogenous sodium currents, serves as a simple but robust expression system for Nav1.5 studies.

Before the ABE assay, original cell lysates were collected from two 10mm dishes of Nav1.5 stable cells. An additional two dishes of untransfected HEK293 cells were used as a control. Two groups were treated with hydroxylamine(NH_2OH) and tris solution respectively in the experiment. Here hydroxylamine was applied to specifically cleave the thioester bond and a tris solution was used as control. Samples collected from both groups were further processed using gel electrophoresis and western immunoblotting. Original lysates, samples from hydroxylamine treated group and control group were loaded on the same gel.

Our results demonstrate clear evidence that Nav1.5 is S-palmitoylated in HEK293 cells (Figure 13). The western blot signal in the '+' (hydroxylamine treatment) lane indicates the thiol-biotinylated protein component captured by streptavidin, which reflects the S-palmitoylated protein before hydroxylamine cleavage. The absence of signal in the '-' (control) lane provides confidence that the signal in the '+' lane is indeed dependent on hydroxylamine activity and reflects S-palmitoylation. Therefore, the presence of biotinylated protein in hydroxylamine treatment group provides us strong evidence that Nav1.5 is palmitoylated in the HEK293 cells.

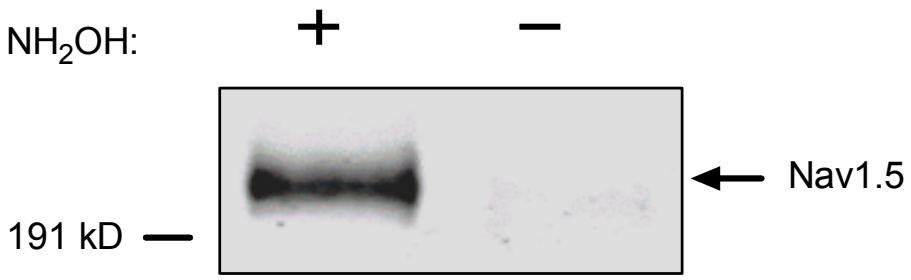

Figure 13. Nav1.5 are post-translationally modified by protein palmitoylation in HEK293 cells. "+" (hydroxylamine treated group) indicates the existence of protein palmitoylation on Nav1.5 channels and "-" is the negative control group. All the biotinylated proteins (previously palmitoylated proteins) were immunoprecipitated using a streptavidin pull down assay. A sodium channel pan antibody was used to detect sodium channel proteins.

2. Characterization of Nav1.5 palmitoylation in cardiac tissues using acyl biotin exchange method

Since Nav1.5 is predominately expressed in the cardiac cells, we wanted to further investigate whether endogenous Nav1.5 is palmitoylated in cardiac myocytes. Cardiac tissues from adult Sprague Dawley Rats were used in the experiment to identify Nav1.5 palmitoylation in cardiac tissues. As described previously, the signal in the hydroxylamine treatment lane indicates Nav1.5 palmitoylation in cardiac tissues (Figure 14A). Caveolin, which has been previously reported to be palmitoylated in cardiac tissue(Dietzen, Hastings et al. 1995, Tulloch, Howie et al. 2011), was used as a positive control (Figure 14C). Calmodulin, which does not contain any cysteine residues, was used as a negative control and shows that there is no signal for non-palmitoylated proteins (Figure 14B). These results provide evidence of Nav1.5 palmitoylation in its native expression system.

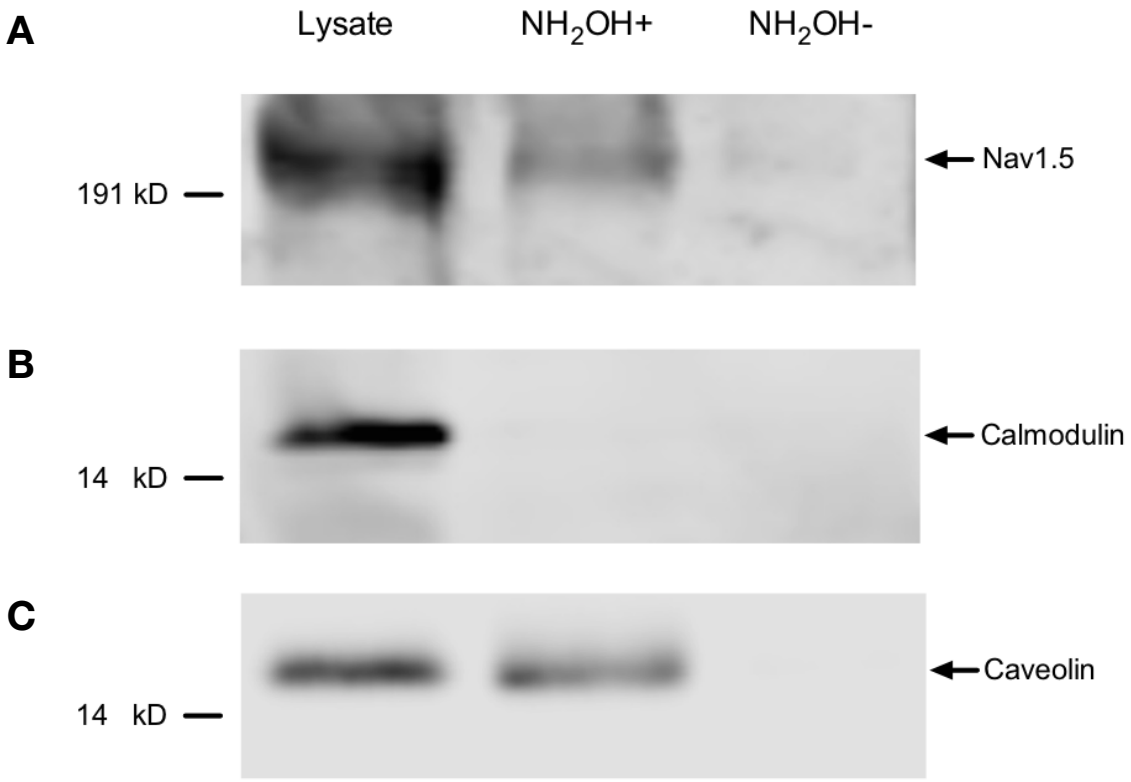

Figure 14. Identification of Nav1.5 palmitoylation using ABE assay. The results are representative of at least three independent experiments. Left lane indicates total input lysate. The middle lane (NH_2OH+) indicates palmitoylated protein. The right lane (NH_2OH-) indicates the negative control group treated with tris solution. (A) Nav1.5 is palmitoylated in cardiac tissues. (B) Calmodulin is present but not palmitoylated in cardiac tissues. (C) Caveolin is palmitoylated in cardiac tissues.

3. Characterization of Nav1.5 palmitoylation using metabolic labelling assay

Although palmitoylation is the most common acylation modification of proteins in mammalian cells, it is not the only possible modification detected by the ABE method. As a direct measure of Nav1.5 palmitoylation, we metabolically labeled HEK293 cells stably expressing Nav1.5 with tritium labeled palmitate. Nav1.5 was immunoprecipitated and palmitoylation was detected by autoradiography following SDS-PAGE. The same set of samples were loaded on another gel and used for further western immunoblotting analysis. The autoradiography film cassette was stored in -80°C freezer for exposure (up to three months). Nav1.5 palmitoylation was shown after three weeks of exposure (Figure 15A) and three months of exposure (Figure 16A). Western blot analysis further confirms palmitoylated Nav1.5 from three independent experiments (Figure 15B, 16B). These experiments demonstrated that tritium labeled palmitic acid was incorporated into Nav1.5 channels as identified by immunoprecipitation and western blot analysis.

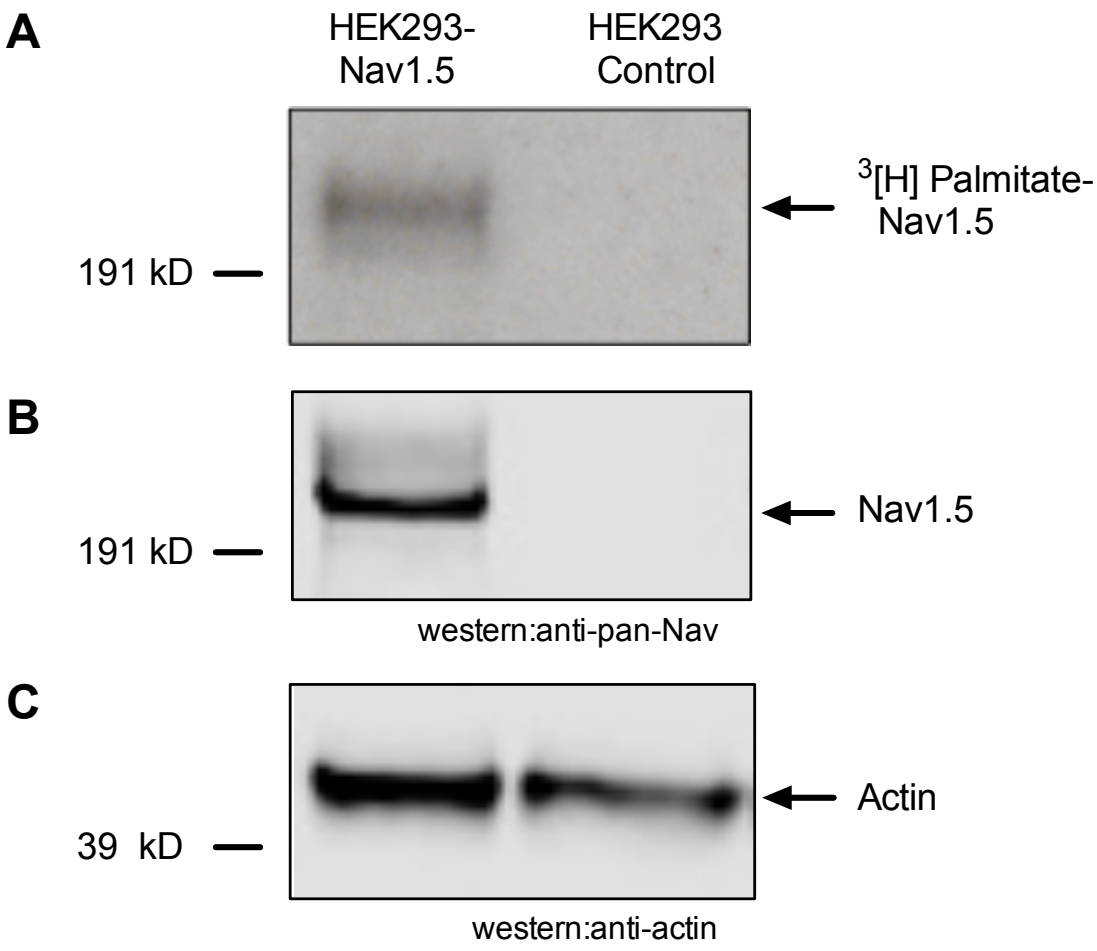

Figure 15. Identification of Nav1.5 palmitoylation in HEK293 cells using metabolic tritium labeling (short term exposure). (A)Scanned image of film developed after three weeks of exposure. Tritium labeled palmitoylated Nav1.5 was detected in HEK293 cells stably expressing Nav1.5, but not in control HEK293 cells; (B) Nav1.5 was shown in Western blot analysis using the same samples; (C) comparable amount of actin from the same samples was shown in Western blot analysis.

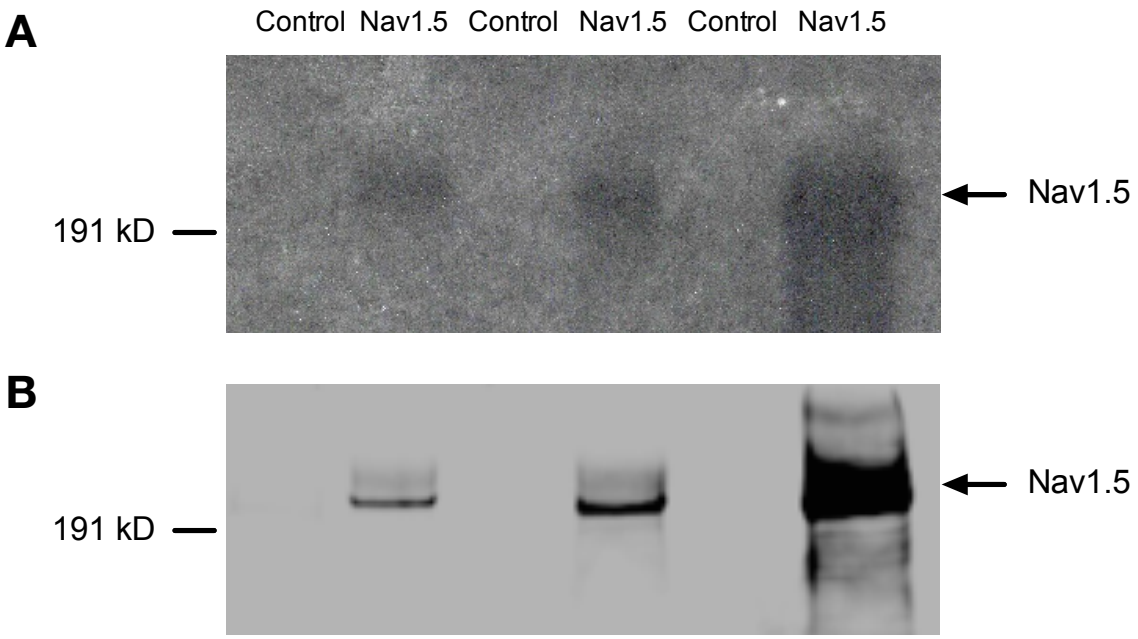

Figure 16. Identification of Nav1.5 palmitoylation in HEK293 cells using metabolic tritium labeling (long term exposure). Samples from three independent ABE experiments were used for autoradiography and western blot analysis. (A) Scanned image of film developed after three months of exposure. Tritium labeled palmitoylated Nav1.5 was present in HEK293 cells stably expressing Nav1.5. As shown in this figure, long term exposure also increased the background signal. (B) Western blot analysis of the same membrane used for film development.

4. Characterization of Nav1.5 palmitoylation using click chemistry assay

We were also able to detect Nav1.5 palmitoylation with copper-catalyzed click chemistry assay, as a third measurement of palmitoylation. This method is based on metabolic incorporation of alkynyl derivatives of palmitic acid that can be detected with direct in-gel fluorescence analysis.

In the experiment, HEK293 cells stably expressing Nav1.5 (Figure 16, two lanes on the right) were used to study Nav1.5 palmitoylation and untransfected HEK293 cells (Figure 17, two lanes on the left) were used as negative control. During the click chemistry experiment, azide-linked reporter tags will specifically label the previously palmitoylated proteins for fluorescence visualization in later steps.

Our results indicate Nav1.5 is palmitoylated in HEK293 cells. Red bands (Figure 17A) indicating palmitoylated proteins labeled by the azide-linked reporter tags after click chemistry reaction. Hydroxylamine (shown as '+' or '-' in the figure), which cleaves the thioester bond, was used at the final step to demonstrate specificity of thioester-dependent labeling and protein palmitoylation. The absence of palmitoylation signal in '+' group indicates that the azide-activated fluorescent dye which previously attached to the palmitoylated site was removed by hydroxylamine cleavage, confirming the specificity of the fluorescence signal observed in '-' group (Figure 17A) is indeed Nav1.5 palmitoylation. The same set of samples used for fluorescence visualization were loaded on an additional gel for further identification using gel electrophoresis and

western blot analysis (Figure 17B). These results demonstrate Nav1.5 palmitoylation in HEK293 cells.

Altogether, three lines of biochemical evidence provide sufficient confidence to conclude that Nav1.5 is indeed palmitoylated in both the heterologous expression system and native cardiac tissue.

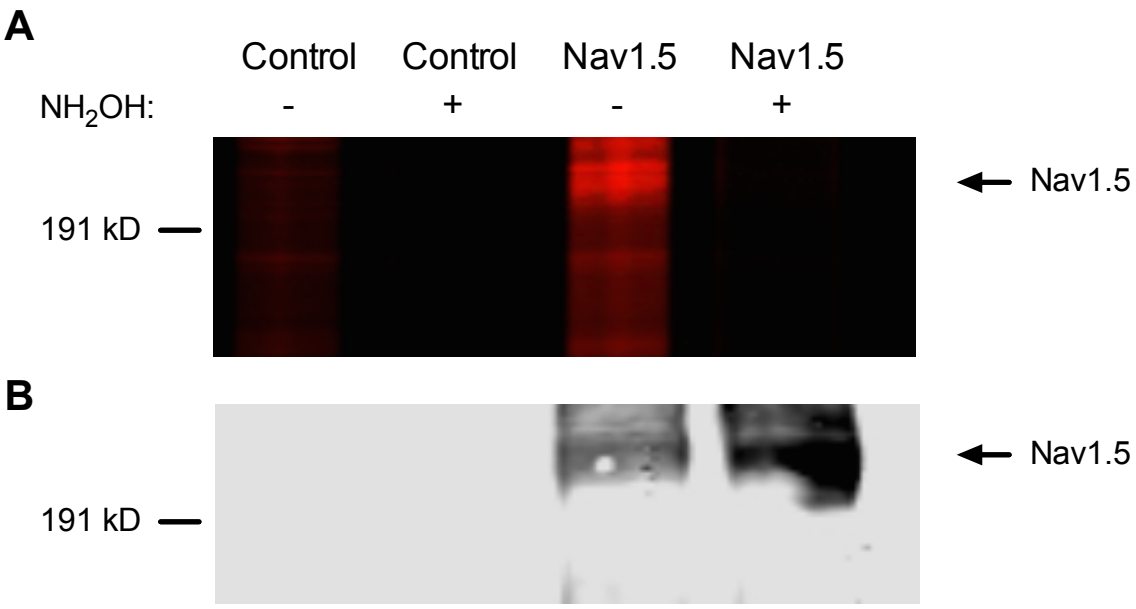

Figure 17. Identification of cardiac sodium channel palmitoylation using copper-catalyzed click chemistry. The results are representative of at least three independent experiments. The first and second lane were from untransfected HEK293 cells and the third and forth lane were from HEK293 cells with stable expression of Nav1.5. (A) In-gel fluorescence analysis of protein palmitoylation after immunoprecipitation of Nav1.5 from HEK293 cells stably expressing Nav1.5. The location of Nav1.5 protein was marked by the arrows. (B) Western blot analysis of the samples used in panel A. Nav1.5 was detected using sodium channel pan antibody in both hydroxylamine treated and untreated samples. Nav1.5 protein was not expressed in untransfected HEK293 samples.

B. Bi-directional regulation of Nav1.5 palmitoylation

To determine whether Nav1.5 palmitoylation can be regulated in living cells, we incubated the Nav1.5 stable HEK293 cells with 2-Br-palmitate, a nonmetabolizable palmitate analog that is broadly used as a inhibitor of palmitoyltransferase. 2-Br-palmitite can irreversibly inhibite palmitoylation and thus leading to protein depalmitoylation(Webb, Hermida-Matsumoto et al. 2000, Davda, El Azzouny et al. 2013). Although at least one study demonstrated that 2-Br-Palmitate may also inhibit acyl-protein thioesterase activity (Pedro, Vilcaes et al. 2013), this inhibition is not predicted to be appreciable at 25 μM.

We treated the Nav1.5 stable cells with various concentrations of 2-Br-palmitate for 24 hours and then performed the ABE assay. Results of this experiment indicate that 2-Br-palmitate can eliminate Nav1.5 palmitoylation in HEK293 cells at concentrations starting from 25 μM (Figure 18).

By introducing extra 2-Br-palmitate to the system, we increased the total amount of palmitic lipid. Therefore, we cannot rule out the possibility that the treatment effect was induced by extra palmitic lipid in the system. Thus, in another set of experiments, we pre-incubated the cells with palmitic acid, a palmitic lipid that has similar structure as 2-Br-palmitate. Palmitic acid does not inhibit palmitoyltransferase, but rather is considered as a substrate for palmitoylation. 24 hours treatment of palmitic acid was predicted to increase the substrate for palmitoylation. Our results show that the addition of palmitic acid does not inhibit palmitoylation. Moreover, it was able to substantially enhance Nav1.5 palmitoylation at concentrations as low as 10 μM (Figure 18B). Higher

concentration of palmitic acid also increased Nav1.5 palmitoylation (data not shown). Therefore, we conclude that 2-Br-palmitate can abolish protein palmitoylation by inhibiting palmitoyltransferase enzymatic activities while extra palmitic acid leads to the enhancement of palmitoylation, probably due the addition of palmitoylation substrate in the system.

Overall, these data demonstrate that the two distinct forms of palmitate exert opposite effects on regulating Nav1.5 protein palmitoylation. These data confirm that Nav1.5 palmitoylation is subject to bidirectional regulation and provided a paradigm that we took advantage of to study how site specific palmitoylation of Nav1.5 modulates the biophysical properties of the channel.

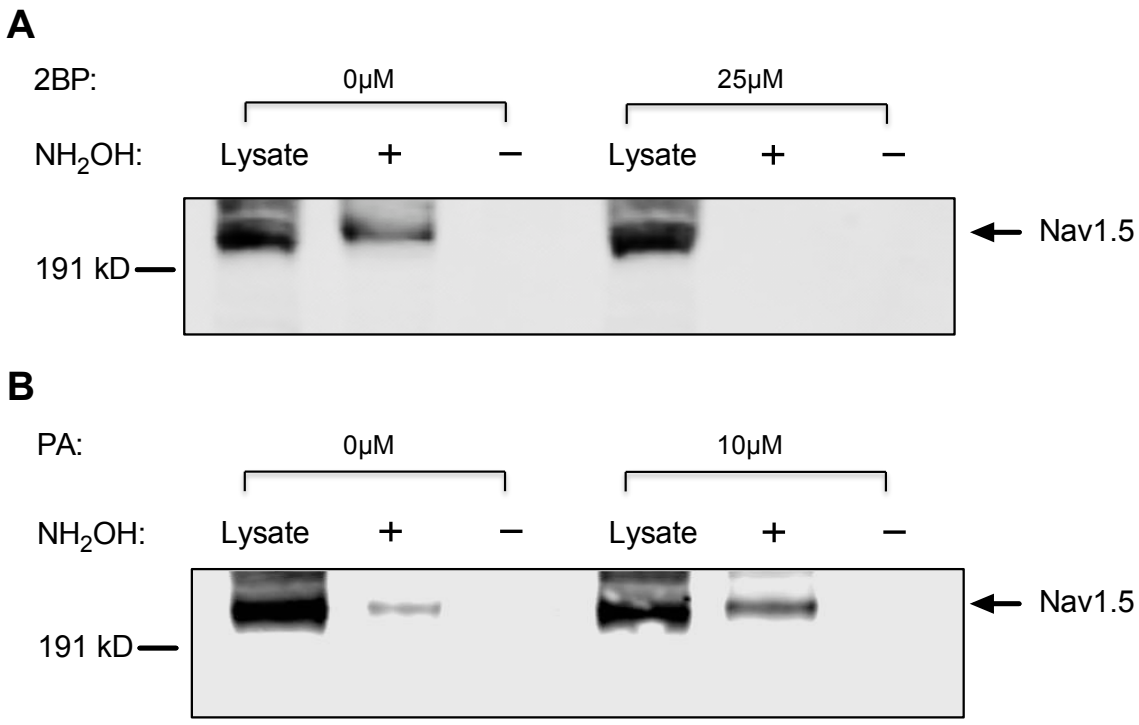

Figure 18. Palmitate lipid treatments alter Nav1.5 palmitoylation in HEK293 cells that stably express Nav1.5. The results are representative of at least three independent experiments. (A) 2-Br-palmitate(2BP) treatment inhibited Nav1.5 palmitoylation at 25μM. (B) Palmitic acid(PA) treatment increased Nav1.5 palmitoylation at 10μM.

C. Palmitoylation regulates cardiac excitability

1. Palmitoylation alters spontaneous beating activity of cardiomyocytes

Cardiac excitability and arrhythmia generation is critically dependent on the gating of multiple ion channel proteins. Recent evidence suggests that the activity of numerous proteins, including ion channels, may be modulated by the palmitoylation, one of the most common post-translational lipid modifications. As we already showed cardiac sodium channel is palmitoylated, we asked if manipulating protein palmitoylation in cardiac myocytes would alter excitability.

In control myocyte cultures we routinely observed numerous beating cells on each coverslip and around 70% of the myocytes that exhibited inward current in voltage-clamp recordings generated spontaneous action potentials in current clamp recordings (Figure 19). To decrease protein palmitoylation, we incubated the cells with 2-Br-palmitate (25μM). After 24 hours treatment with 2-Br-palmitate, spontaneously beating myocytes were rarely observed and none of the cells that exhibited inward sodium current in voltage-clamp recordings was able to generate action potentials in current clamp recordings (Figure 19). The cells were placed at resting membrane potential in our experiment settings, however, it is still possible that prolonged hypoperolarization may restore the cardiomyocyte excitability in 2-Br-palmitate treatment group. In contrast, we observed distinct effects when myocytes were cultured in the presence of additional palmitate acid (10μM), the primary substrate for palmitoylation. Our biochemistry data indicates that excess palmitic acid can enhance Nav1.5 palmitoylation (Figure 18). In contrast to 2-Br-palmitate treatment, palmitic acid did not abolish beating but

rather many cells in the palmitic acid treated group displayed spontaneous beating and action potentials were readily recorded from myocytes in this treatment group.

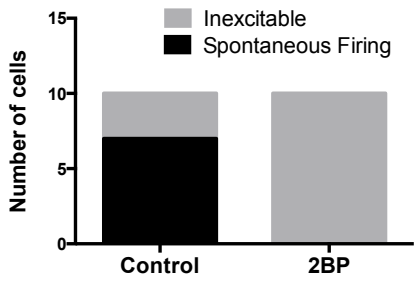

Figure 19. Palmitoylation alters cardiomyocytes beating activity. Only cells that exhibited inward sodium current were analyzed. 7 out of 10 cells (70%) in the control group fired spontaneous action potentials. None of the 10 cells in the 2-Br-palmitate (2BP) group were able to generate action potentials.

2. Palmitoylation regulates action potential duration and firing frequency

Since palmitoylation alters cardiac myocyte spontaneous beating activity, we further asked if palmitoylation could also affect action potential activities. Here we only compared non-treatment group and palmitic acid treatment group since none of the cells in 2-Br-palmitiate treatment group was able to generate an action potential in our experiments. According to our study, the recorded action potentials from the palmitic acid treatment group exhibited an increased action potential duration (Figure 20A, 20B, 20C) and a decreased firing frequency (Figure 20D) compared to the non-treatment group.

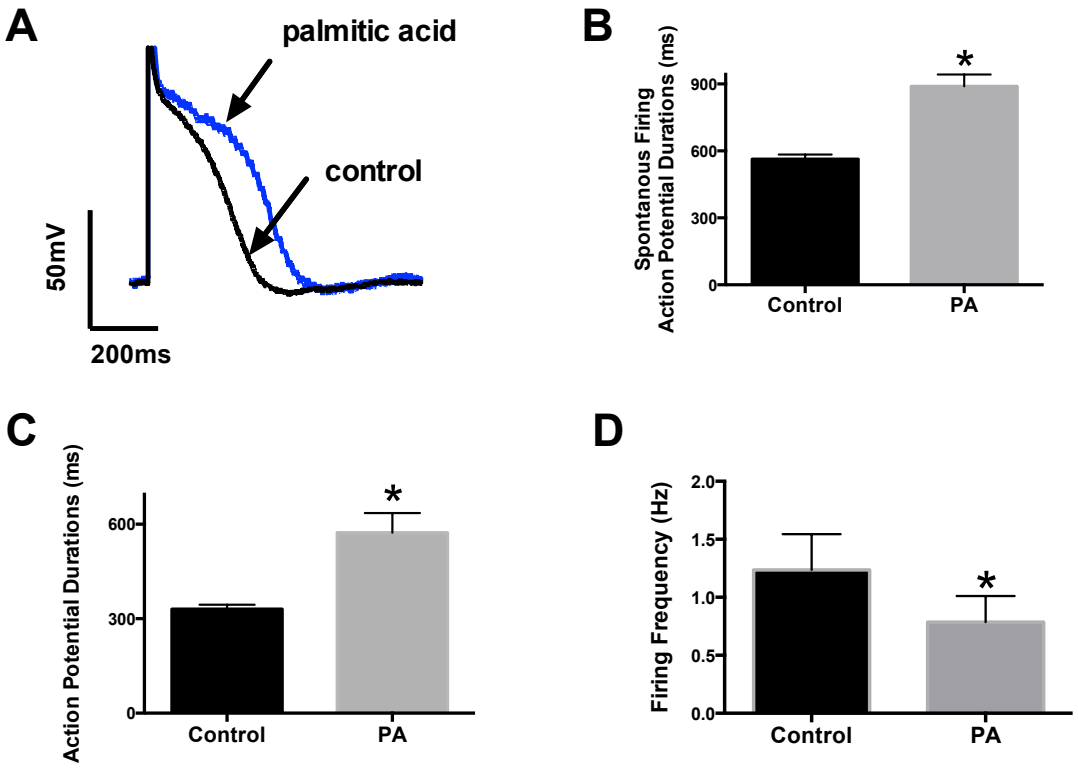

Figure 20. Palmitoylation regulates cardiac action potential duration and firing frequency. (A) Representative action potential traces of cardiomyocytes with (blue) and without (black) palmitic acid treatment. Palmitic acid(PA) treatment increases the action potential duration. (B) Averaged APD measurements (from the beginning of depolarization phase to the end of repolarization phase) from the spontaneous firing myocytes. Averaged APD is 563ms in the control group and 890ms in the palmitic acid treatment group. (C) Averaged APD measurements of single action potential waveform elicited by 2 ms stimulus pulses. APD is 330.4ms in the non-treatment group and 572.8ms in the palmitic acid treatment group. (D) Firing frequency in control group and palmitic acid treatment group. The firing frequency is 1.2±0.10 in the control group and 0.79±0.11 in the palmitic acid treatment group.

3. Palmitoylation induces early after-depolarization like phenomenon

Interestingly, when comparing the spontaneous action potential waveforms, we often observed an early after-depolarization (Meadows and Isom) like phenomenon in the palmitic acid treatment group (Figure 21B, 21C), but not under the control condition (Figure 21A). In general, EADs occur with abnormal depolarization during action potential phase 2 or phase 3, and are identified by the presence of ectopic action potentials before normal repolarization is completed (Zeng and Rudy 1995). Unusual openings of sodium channels is one of the factors that contributes to the generation of EADs. EADs can result in torsades de pointes, tachycardia, and many other arrhythmias. Our data suggest that reducing palmitoylation in cardiac myocytes attenuates excitability and enhancing palmitoylation (by increasing the availability of substrate) increases cardiomyocyte excitability and may enhance risk of cardiac arrhythmia generation.

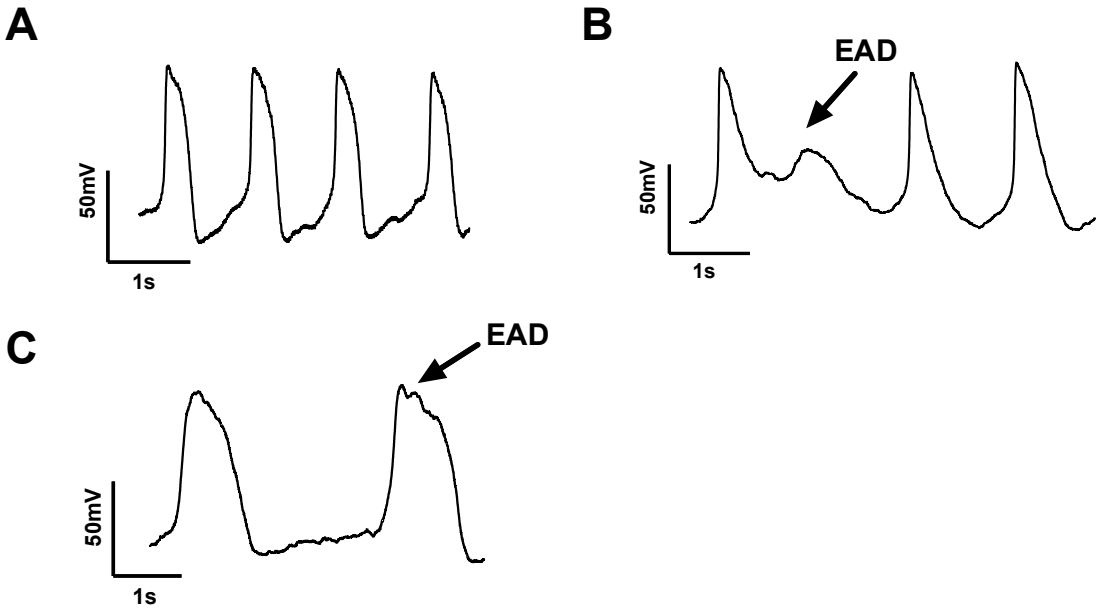

Figure 21. Spontanous action potential recorded from non-treatment and palmitic acid treatment group. (A) Cardiomyocyte spontanous action potential generated under non-treatment condition. The action potential firing occurs at a constant rate with no ectopic firing observed. (B,C) Action potential recorded from palmitic acid treatment group. EAD phenomenon is indicated with arrows. The results are representative of at least three independent experiments.

D. Palmitoylation modulates cardiac myocyte sodium currents

1. Palmitoylation does not alter Nav1.5 fast inactivation in cardiomyocytes

To investigate if bidirectional alterations in the palmitoylation of cardiac sodium channels might contribute to the observed changes in cardiomyocyte excitability, we examined voltage-gated sodium currents in the cultured cardiomyocytes from neonatal rats. In these experiments, we blocked potassium and calcium currents in order to record isolated voltage-gated sodium currents. Cells were pre-incubated with 2-Br-palmitate and palmitic acid, respectively, to study the effect of decreased and enhanced palmitoylation. Cells were held at -100mV and a depolarizing protocol from -100mV to -20mV was performed to generate the isolated sodium currents. Our results indicate that sodium current recorded from neonatal cardiomyocytes activates and decays rapidly, and that neither 2-Br-palmitate nor palmitic acid treatment significantly changed the rate of sodium current fast inactivation in myocytes (Figure 22).

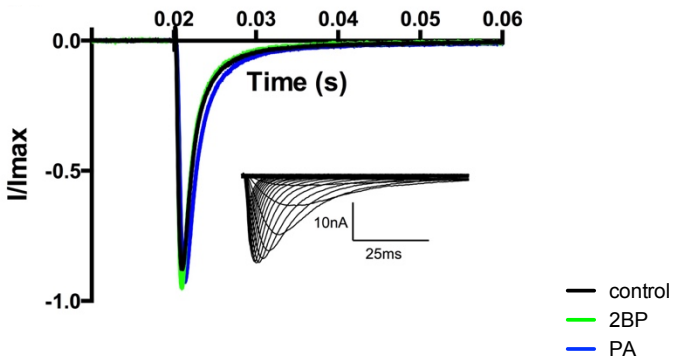

Figure 22. Normalized Nav1.5 current with and without palmitate lipid treatment. All data are shown as mean±s.e.m. Data from the 24-hour pretreatment of 2-Br-palmitate and palmitic acid are shown in green and blue, respectively. Black lines indicate data from the control condition. Cells were depolarized to −20 mV from a holding potential of −100 mV. Inset indicates representative family of traces of Nav1.5 current in cardiomyocytes evoked with depolarizations ranging from -80 to +40 mV.

2. Palmitoylation does not alter Nav1.5 current densities in cardiomyocytes

To study whether palmitoylation alters Nav1.5 protein expression at cell surface, we compared the sodium peak current in different treatment groups. Sodium currents were generated using a depolarizing protocol from -100mV to -20mV. Our results indicate there is no significant difference of cell size (Figure 24, $p>0.05$, unpaired Student's t-test) or current density among untreated cells, 2Br-palmitate treated cells and palmitic acid treated cells (Figure 23, $p>0.05$, unpaired Student's t-test), suggesting palmitoylation might not play a major role in regulating cardiac sodium channel surface expression.

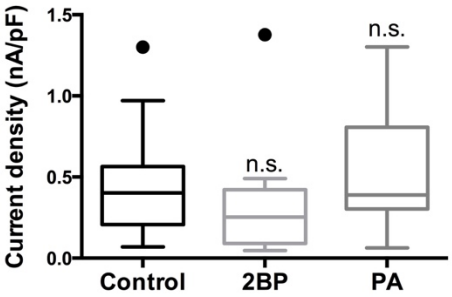

Figure 23. Comparison of normalized current density. Current density was measured as the peak current divided by cell capacitance (nA/pF). Box and Whisker plots were generated to compare the mean difference. The box was drawn from the 25th to 75th percentiles. Tukey analysis was used to determine the outliers (shown as individual points above the whiskers). In the non-treatment group, mean current density is 0.43±0.04 nA/pF,n=35; In the 2-Br-palmitate treated group, mean current density is 0.30±0.08 nA/pF,n=16. In the palmitic acid treatment group, the current density is 0.56±0.10 nA/pF,n=13. No significant statistical difference is observed in 2-Br-palmitate group (p=0.13, unpaired Student's t-test) or palmitic acid group (p=0.18, unpaired Student's t-test)

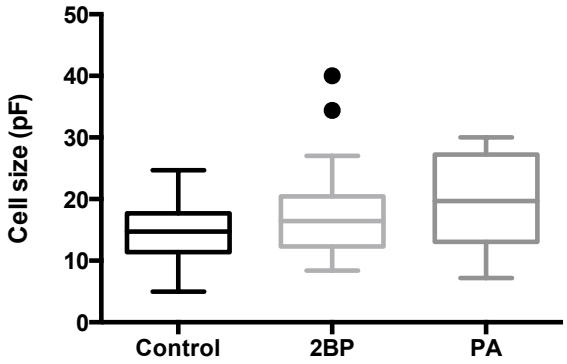

Figure 24. Comparison of cardiomyocyte size. Cell size was measured by cell capacitance (pF). Box and Whisker plots were used to compare the difference in mean. The box was drawn from the 25th to 75th percentiles. Tukey analysis was used to determine the outliers (shown as individual points above the whiskers). In the non-treatment group, mean cell size is 14.75±0.84 pF; In the 2-Br-palmitate treated group, mean cell size is 18.48±2.15 pF. In the palmitic acid treatment group, mean cell size is 19.54±2.24 pF. No significant statistical difference is observed among groups.

3. Palmitoylation alters persistent current of Nav1.5 in cardiomyocytes

In excitable cells, the transient sodium currents activate and inactivate rapidly, initiating action potentials, helping regulate the duration of the action potential waveform and modulating the frequency of action potential firing activities. However, there is a small sustained component of sodium current called persistent current(or late sodium current) that fails to inactivate rapidly(Kiss 2008). Persistent current generally consists of less than 5% of peak sodium currents. However, it has profound influence on cell excitability under both physiological and pathological conditions.

Previous studies show that persistent sodium current can contribute to repetitive firing of neuronal action potential(Harvey, Li et al. 2006, Stafstrom 2011). And enhanced persistent currents of sodium channels induced by inherited mutation or acquired channel dysfunction in the central nervous system is associated with epilepsy generation (Stafstrom 2007). In addition, Nav1.5 persistent currents can substantially contribute to sodium overloading in myocytes and potential cardiac arrhythmia generation(Saint 2008).

Since persistent current plays an important role in cellular excitability, we further investigated whether regulation of palmitoylation can mediate the persistent current component of Nav1.5. Our results demonstrate palmitic acid treatment, which enhances palmitoylation of cardiac sodium channels, induces a four-fold increase in the persistent(non-inactivating) component of the total sodium currents (Figure 25). Although the magnitude of the inward persistent current was slightly less than 1% of the peak current after palmitic acid treatment,

this increase is similar to that observed with several long-QT3 mutations(Bankston, Yue et al. 2007). An increase in these small but powerful late currents is likely to contribute to the prolonged APD and EAD like phenomenon shown in Figure 21. Therefore, the enhanced persistent current induced by Nav1.5 palmitoylation may partially account for the altered excitability in cardiomyocytes.

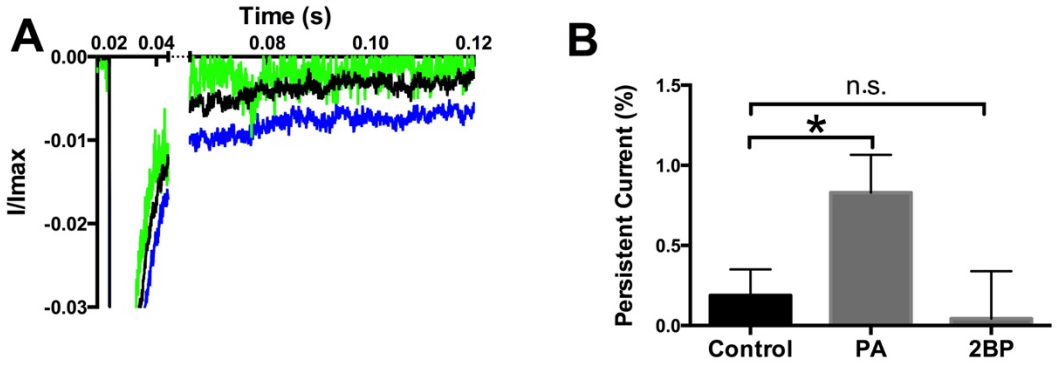

Figure 25. Persistent current (A) and statistical analysis (B) comparing the control condition and treatment groups in neonatal cardiomyocytes. The persistent current was measured as the percentage of peak current. The persistent current is 0.19± 0.16% (control, black); 0.04±0.30% (2-Br-palmitate, green); 0.83±0.24%(palmitic acid, blue). n=10. The difference between control group and palmitic acid treatment group is statistically significant (p=0.037).

4. Palmitoylation affects Nav1.5 voltage dependence of inactivation in cardiomyocytes

I also studied how palmitoylation affects Nav1.5 voltage dependence of activation and inactivation. Palmitic acid treatment substantially shifted the steady-state inactivation to more depolarized voltages (Figure 26B), which would largely increase channel availability under depolarized membrane potentials and lead to the enhanced ‘window current’. It is likely one of the factors that contributes to enhanced excitability of cardiomyocytes.

In contrast, 2-Br-palmitate induced a hyperpolarizing shift of steady-state inactivation (Figure 26A). The parameters of activation and inactivation curves, obtained from Boltzmann equation fits, are summarized in Table 7. While palmitic acid treatment induced biophysical changes in sodium current properties that would increase electrical activity in myocytes, the large negative shift (around 20mV) in the voltage-dependence of inactivation observed with 2-Br-palmitate is predicted to effectively reduce channel availability as well as cardiomyocyte excitability.

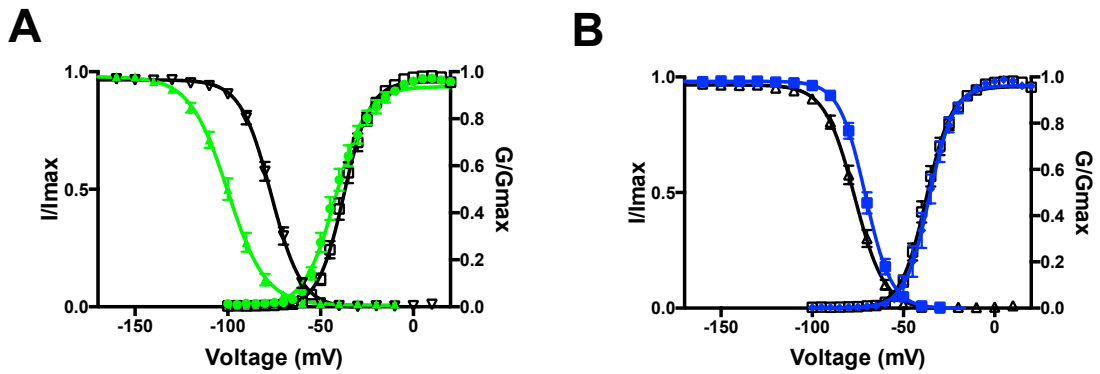

Figure 26. Comparison of sodium channel voltage dependence of activation and steady-state inactivation in neonatal cardiomyocytes. Black curve and open symbol indicates non-treatment group. Green indicates 2-Br-palmitic treatment group. Blue indicates palmitic acid treatment group.

5. Palmitoylation affects Nav1.5 recovery from inactivation in cardiomyocytes

As discussed in previous sections, sodium channels typically come to a refractory period after opening, which allows sodium channels to recover from inactivation and prevent them from repetitive opening during short time period. This mechanism is an important factor to maintain normal action potential activities. Altered recovery of Nav1.5 may disrupt cell excitability and increase the risk of cardiac arrhythmia.

To assess how palmitoylation affects Nav1.5 recovery from inactivation, we depolarized the cells to +20mV and studied the time course that sodium currents recovered from inactivation during a varying time period. Sodium channel recovery were examined under two time scales, 0-50 ms and 0-2048 ms. Our results demonstrate that palmitic acid enhanced recovery from inactivation in cardiomyocytes while 2-Br-palmitate largely slowed the recovery from inactivation (Figure 27). Therefore, the regulation of recovery rate by palmitoylation could also contribute to the altered myocyte excitability under different treatment conditions.

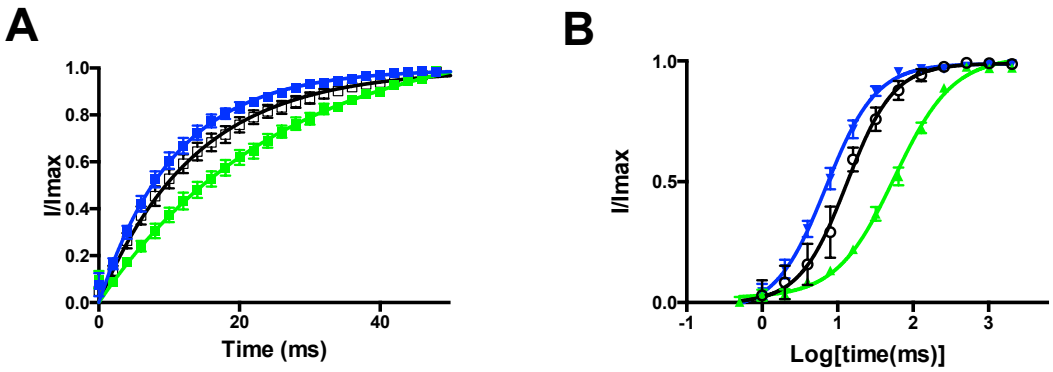

Figure 27. Comparison of sodium channel recovery from inactivation among non-treatment group (black curve and open symbol), 2-Br-palmitate (green and solid symbol) and palmitic acid treatment (blue curve and solid symbol). The recovery time duration is from 0ms to 50ms (A) and 0ms to 2048ms (B, plotted in the log form).

E. Palmitoylation alters Nav1.5 properties in HEK 293 cells

1. Palmitoylation does not alter Nav1.5 fast inactivation in HEK 293 cells

In order to explore the mechanism by which palmitoylation regulates cardiomyocyte sodium currents, we investigated whether modulation of palmitoylation alters the functional properties of Nav1.5 channels expressed in HEK293 cells. The main advantage of these cells is that they do not express significant levels of other ion channels and can be readily used to express recombinant Nav1.5 channels in isolation.

We incubated the HEK293 cells expressing Nav1.5 with 25 μM 2-Br-palmitate for 24 hours and performed whole-cell electrophysiological recordings. Sodium currents were generated by a depolarizing potential to -20mV from a holding potential of -100mV. The rate of fast inactivation was not significantly altered by 2-Br-palmitate (Figure 28A) or palmitic acid (Figure 28B) compared to the control group. Representative current traces and current-voltage plots under all three treatment conditions are shown in Figure 29.

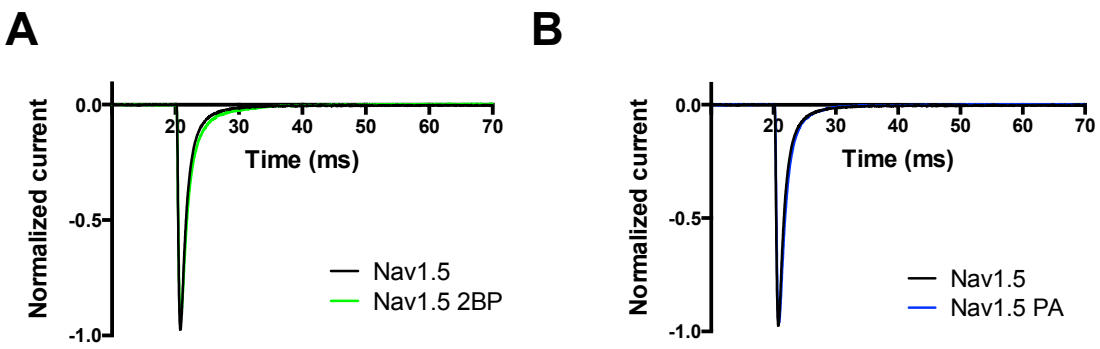

Figure 28. Normalized currents of Nav1.5 compared with 2-Br-palmitate and palmitic acid treatments. Channels were depolarized to −20 mV from a holding potential of −100 mV. 2-Br-palmitate treatment group data are shown in green and palmitic acid treatment group data are shown in blue. Control conditions are shown in black. Data were averaged from 11 sodium current measurements.

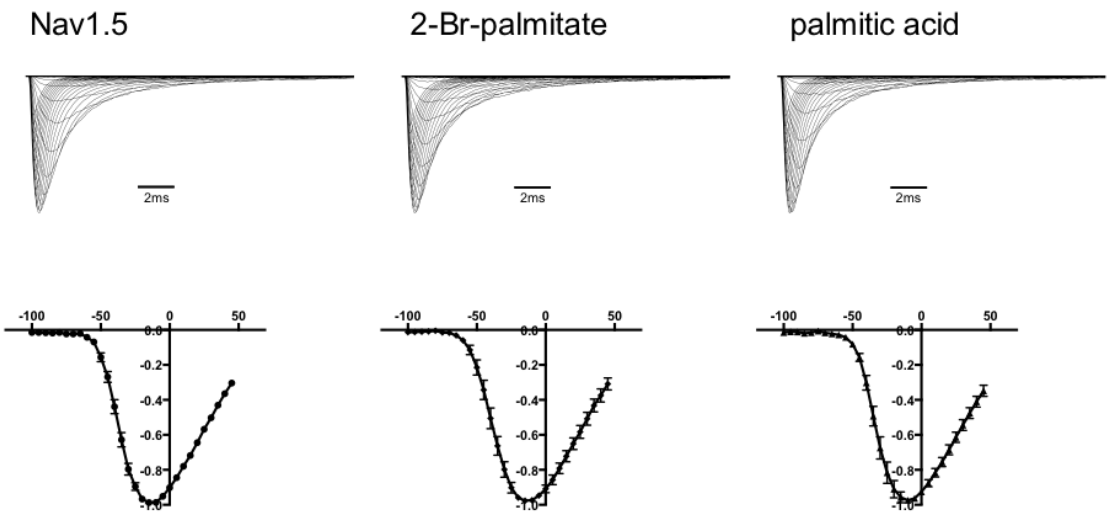

Figure 29. Representative current traces and normalized current-voltage (IV) plot. Left: control; Middle: 2-Br-palmitate treatment; Right: palmitic acid treatment. Top panel shows the representative normalized current traces and the bottom panel shows the corresponding IV curves (n=10, all data points are shown as mean±s.e.m.). Sodium currents were evoked by voltage steps from −100 to +45 mV with 5-mV increments (ΔV) from a holding potential of −100 mV.

2. Palmitoylation regulates Nav1.5 voltage-dependence of inactivation in HEK 293 cells

In addition to sodium current kinetics, we also studied how palmitoylation regulates Nav1.5 voltage dependence of activation and inactivation in HEK293 cells. Sodium currents were elicited by voltage steps from −100 to +45 mV with 5 mV increments (ΔV) from a holding potential of −100 mV. The normalized current conductance was plotted versus depolarization voltage. In order to evaluate steady-state inactivation, cells were held at -100 mV and then stepped to a 500ms inactivating prepulse from -150 mV to -10 mV with 10 mV increments. The channels that remain available after each inactivating prepulse were evaluated by the peak current produced during a 20 ms test pulse at 0 mV.

Our results revealed that 2-Br-palmitate treatment substantially shifted the steady-state inactivation of wild-type (wt) Nav1.5 to more hyperpolarized voltages (Figure 30A). By contrast palmitic acid, which enhances Nav1.5 palmitoylation in HEK293 cells, shifted the voltage-dependence of steady-state inactivation in the depolarizing direction, enhancing channel availability (Figure 30B). These effects were also observed with shorter duration (4 hr) 2-Br-palmitate treatments (Figure 31). The midpoint of the inactivation and activation curves are summarized in Table 7.

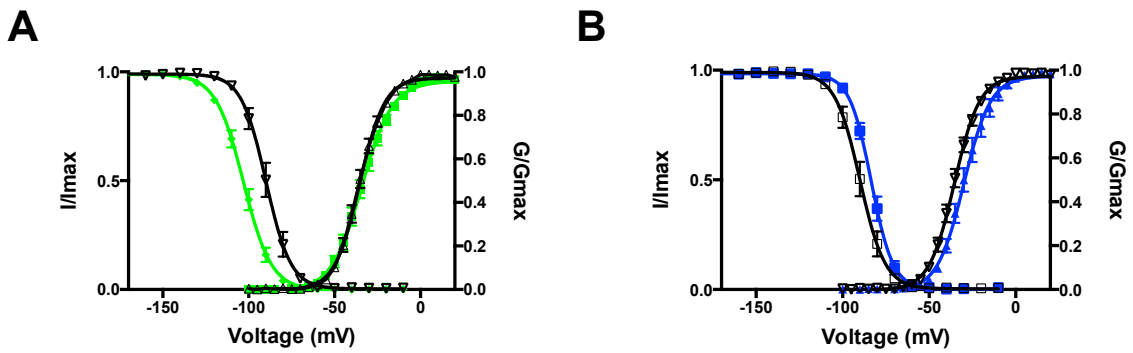

Figure 30. Palmitoylation alters voltage dependence of activation and inactivation. 2-Br-palmitate treatment group data are shown in green and palmitic acid treatment group data are shown in blue. Control conditions are shown in black lines and open symbols. All data are shown as mean±s.e.m. (A) 2-Br-palmitate treatment shifts steady-state inactivation to hyperpolarized voltages, without changing the voltage dependence of activation. (B) palmitic acid treatment shifts both voltage dependence of activation and inactivation in the depolarized direction.

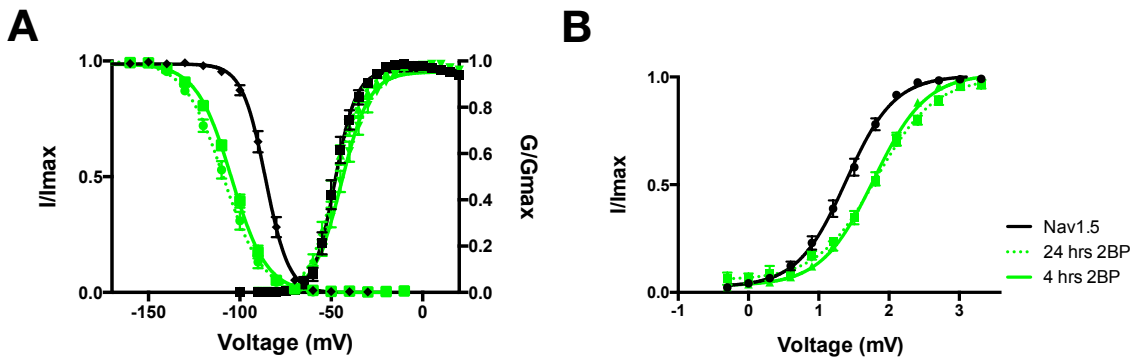

Figure 31. 2-Br-Palmitate effects on Nav1.5 biophysical properties. All data points are shown as mean±s.e.m. Green lines and symbols indicate 2-Br-Palmitate (2BP) treatment (solid lines show 4 hours treatment and dashed lines show 24 hours treatment) and black lines and symbols indicates no treatment involved. (A) Both 24 hours and 4 hours treatment significantly shift Nav1.5 steady-state inactivation. There is no significant difference between 24 hours and 4 hours treatment. (B) Both 24 hours and 4 hours treatment alter recovery from inactivation

3. Palmitoylation alters Nav1.5 recovery from inactivation in HEK 293 cells

In addition to the alteration in steady-state inactivation, 2-Br-palmitate treatment slightly slowed the rate for recovery from inactivation (Figure 32A). By contrast palmitic acid, which enhances Nav1.5 palmitoylation in HEK293 cells, increased the rate of recovery from inactivation (Figure 32B).

Overall, our data suggest that depalmitoylation induces a hyperpolarized shift on sodium channel voltage dependence of inactivation in HEK293 cells. On the other hand, enhanced palmitoylation induces a depolarized shift on voltage dependence of inactivation and speeds the rate of recovery from fast inactivation. These results are consistent with our findings from neonatal cardiomyocytes, indicating palmitoylation effects on Nav1.5 are likely conserved in different expression systems and confirming HEK293 as a valid expression system for further studies on Nav1.5 palmitoylation.

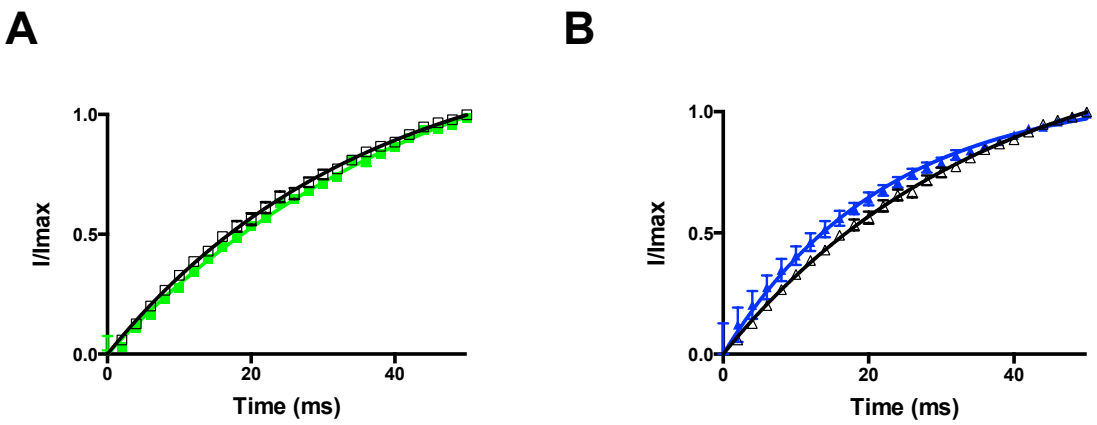

Figure 32. Palmitoylation alter Nav1.5 recovery from inactivation. (A) 2-Br-palmitate treatment (green) slightly slowed the recovery from inactivation. (B) palmitic acid treatment (blue) enhances the rate of recovery from inactivation.

4. Palmitoylation does not alter Nav1.5 slow inactivation or recovery from slow inactivation

Sodium channel inactivation is a biophysical process that prevents channel conductance in response to the membrane depolarization (Goldin 2003). The time course of sodium channel inactivation is dependent on the duration of depolarization. Inactivation that occurs within a millisecond to tens of milliseconds time frame is referred to as fast inactivation. However, longer forms of inactivation (slow inactivation) could also occur in response to prolonged depolarization, taking from hundreds of milliseconds to tens of seconds(Vilin and Ruben 2001). Slow inactivation is an important regulator of the availability of cardiac sodium channels for activation. Many mutations of Nav1.5 that associated with cardiac arrhythmia diseases exhibit altered slow inactivation (Ulbricht 2005). Therefore, we would like to explore the effects of palmitoylation on slow inactivation of Nav1.5.

The voltage clamp protocol for slow inactivation and recovery from slow inactivation is shown in Figure 31. To study the voltage dependence of slow inactivation, a 10s or 30s pre-pulse ranging from -150mV to +10mV with a 10mV interval was applied to the cells from a holding potential at -130mV. Channel availability was measured with a following depolarizing pulse at -10mV. To study the recovery from slow inactivation, cells were depolarized to 0mV to fully inactivate sodium channels and then held at -130mV for 50ms to 2000ms recovery time. Channels recovered from inactivation were measured using a 50ms depolarizing pulse at -10mV. From our results, neither 2-Br-palmitate nor

palmitic acid seems to affect the Nav1.5 voltage dependence of slow inactivation or recovery from slow inactivation (Figure 33).

The above experiment results confirm that Nav1.5 current properties are indeed regulated by modulating palmitoylation and that the HEK293 heterologous expression system serves as a model system to further explore the molecular determinants for this regulation.

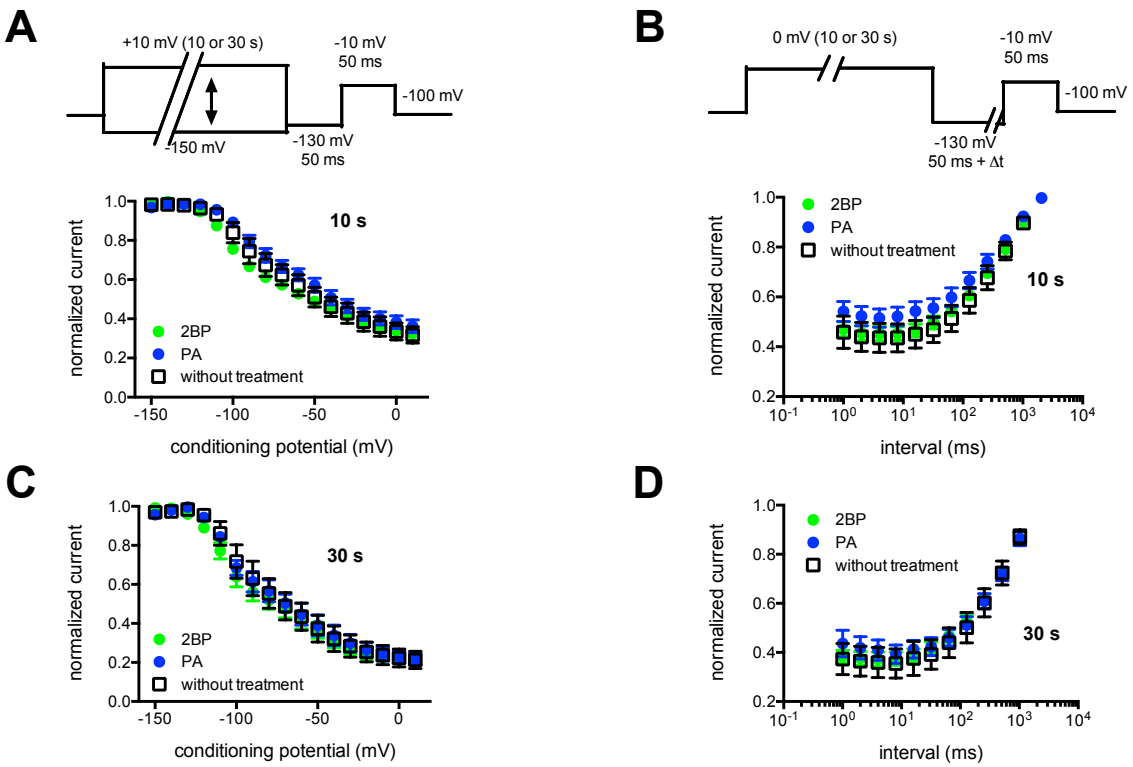

Figure 33. Palmitoylation does not affect Nav1.5 slow inactivation or recovery from slow inactivation. Black and open symbol indicates control group. Blue indicates palmitic acid treatment and green indicates 2-Br-palmitate treatment. (A,B) The duration of pre-conditioning pulse was set at 10s. (C,D) The duration of pre-conditioning pulse was set at 30s.

F. Computer simulation of Nav1.5 palmitoylation and alteration in myocyte excitability

Our previous experimental results suggest that palmitoylation of Nav1.5 in cardiac myocytes regulates cardiac excitability through manipulating Nav1.5 biophysical properties. However, we cannot rule out the possibility that palmitoylation of other proteins in cardiac myocyte could also contribute to the altered excitability.

To assess if the observed changes in sodium channel activity might indeed be sufficient to account for the changes in cardiomyocyte excitability shown in Figures 19, 20 and 21, we replicated the 2-Br-palmitate and palmitic acid induced changes in Nav1.5 in a computational model of a human myocyte and assessed the impact on action potential generation. The computational model, previously implemented in the NEURON simulation environment(Hines and Carnevale 1997), was minimally adjusted (Figure 34). The consequences of increased palmitoylation (palmitic acid treatment) were simulated by shifting the voltage-dependence of inactivation by 5 mV in the positive direction and increasing the non-inactivating component by approximately 4-fold (Figure 35B,C). The consequences of Nav1.5 depalmitoylation were simulated by shifting the voltage-dependence of inactivation 24 mV in the negative direction and slightly decreasing the non-inactivating component (Figure 35B,C). In the model myocyte, the simulated sodium currents with enhanced palmitoylation substantially increased the action potential duration (Figure 35D). On the contrary, when we simulated the effects of sodium channel depalmitoylation, the

model myocyte completely failed to generate action potentials, consistent with our finding in cultured cardiomyocytes (Figure 19). This indicates the changes in cardiac sodium channel activity due to alterations in palmitoylation are sufficient to generate the altered excitability that we observed from the treatment group in primary myocyte studies. The detailed transition rate expressions for the model are summarized in Table 5.

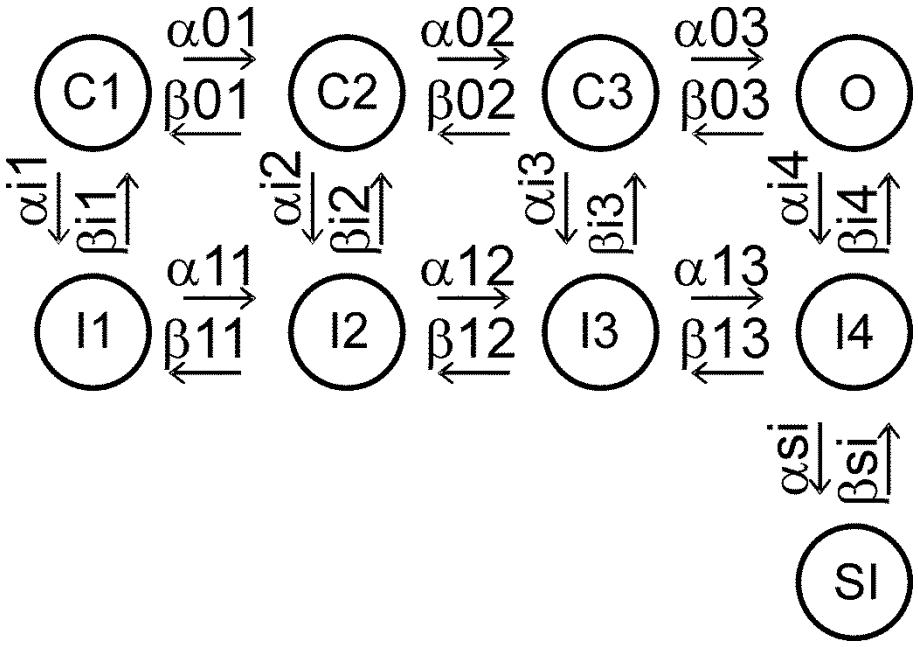

Figure 34. Diagram of Markov model (a mathematical model developed to describe the stochastic behavior of single ion channels) used for computer simulation of voltage-gated sodium channel conductances. C1-C3, closed (non-conducting) states; O, open (conducting) state; I1-I4, fast-inactivated (non-conducting) states; SI, slow-inactivated (non-conducting) state. Forward and reverse transitions are indicated and transition rate expressions are provided in table 5.

Table 5 Transition rate expressions for Nav1.5 conductance models. Values are in ms^{-1}.

Transition	Nav1.5 control conditions	PA treatment	2BP treatment
α01	-3*0.32*(v+47.13)/(exp(-0.1*(v+47.13))-1)	unchanged	unchanged
β01	0.08 * exp(-(v)/11)	unchanged	unchanged
α02	-2*0.32*(v+47.13)/(exp(-0.1*(v+47.13))-1)	unchanged	unchanged
β02	2 * (0.08 * exp(-(v)/11))	unchanged	unchanged
α03	-0.32*(v+47.13)/(exp(-0.1*(v+47.13))-1)	unchanged	unchanged
β03	3 * (0.08 * exp(-(v)/11))	unchanged	unchanged
α11	-3*0.32*(v+47.13)/(exp(-0.1*(v+47.13))-1)	unchanged	unchanged
β11	0.08 * exp(-(v)/11)	unchanged	unchanged
α12	-2*0.32*(v+47.13)/(exp(-0.1*(v+47.13))-1)	unchanged	unchanged
β12	2 * (0.08 * exp(-(v)/11))	unchanged	unchanged
α13	-0.32*(v+47.13)/(exp(-0.1*(v+47.13))-1)	unchanged	unchanged
β13	3 * (0.08 * exp(-(v)/11))	unchanged	unchanged
αi1	(1/(0.13*(1+(exp(-1*(v+10.66)/11.1)))))	(1/(0.13*(1+(exp(-1*(v-1.66)/11.1)))))	(1/(0.13*(1+(exp(-1*(v+75.66)/11.1)))))
βi1	(0.135*exp(-0.147*(v+80)))	unchanged	unchanged
αi2	(1/(0.13*(1+(exp(-1*(v+10.66)/11.1)))))	(1/(0.13*(1+(exp(-1*(v-1.66)/11.1)))))	(1/(0.13*(1+(exp(-1*(v+75.66)/11.1)))))
βi2	(0.135*exp(-0.147*(v+80)))	unchanged	unchanged
αi3	(1/(0.13*(1+(exp(-1*(v+10.66)/11.1)))))	unchanged	unchanged
βi3	(0.135*exp(-0.147*(v+80)))	unchanged	unchanged

αi4	(1/(0.13*(1+(exp(-1*(v+10.66)/11.1)))))	unchanged	unchanged
βi4	((0.135*exp(-0.147*(v+80)))+0.0022)	((0.135*exp(-0.147*(v+80)))+.01)	((0.135*exp(-0.147*(v+80)))+.0006)
αsi	0.00321	unchanged	unchanged
βsi	(.0037933*0.00001)*exp(-(v)/7.7)	unchanged	unchanged

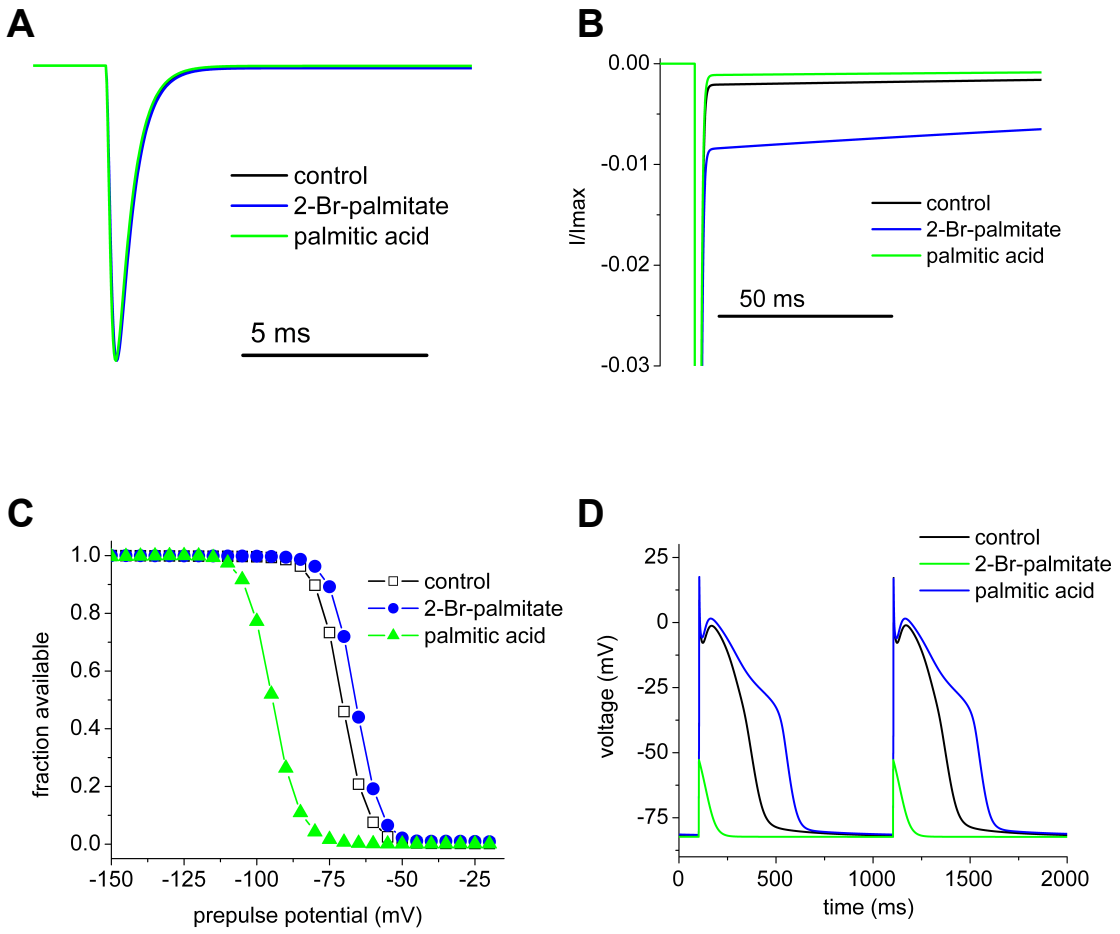

Figure 35. Computer simulations illustrate the impact of depalmitoylation versus enhanced palmitoylation on cardiomyocyte excitability. (A) Comparison of peak simulated control Nav1.5, 2-Br-palmitate and palmitic acid "treated" currents elicited by a step depolarization to -20 mV. In the simulation, the kinetics of activation and open-channel inactivation were not altered under the three conditions. The current densities were set to be equal to the peak control current density for comparison of kinetic differences. (B) Comparison of persistent (or so-called late) Nav1.5 currents for the three simulated conditions. (C) Comparison of voltage-dependence of steady-state inactivation for control Nav1.5 (black lines and open symbols), 2-Br-palmitate (green lines and symbols) and palmitic acid (blue lines and symbols) "treated" currents. (D) Simulated action potentials from modeled cardiac myocytes are shown. Action potentials were paced at 1 Hz in

these simulations and the second and third action potentials are shown. The black trace shows action potentials with the control Nav1.5 channels, the green trace with Nav1.5 channels modeled to reflect the changes induced by depalmitoylation with 2-Br-palmitate and the blue trace with Nav1.5 channels modeled to reflect the changes induced by enhanced palmitoylation with palmitic acid treatment.

G. Identification of palmitoylation sites

1. Prediction of potential palmitoylation sites using bioinformatics tools

In order to determine how Nav1.5 activities are regulated by palmitoylation, we interrogated the channel sequence for potential post-translational modification sites. Although no single conserved sequence of palmitoylation has been identified, the bioinformatics tool CSS-Palm 3.0 can predict which cysteines are potential palmitoylation sites(Zhou, Xue et al. 2006). By comparing the similarity of amino acid sequence surrounding cysteines with previously determined palmitoylation sites, the entire Nav1.5 sequence was analyzed and four endogenous intracellular cysteine residues that are highly predicted to be palmitoylated were identified (Figure 36A, Table 6). These four cysteines are located in the cytoplasmic linker between domains II and III and three out of four residues form a cysteine cluster (Figure 36B).

A

Position	Sequence	Region
981	KRTTWDFCCGLLRQR	DII-DIII
1176	TEGCVRRCPCCAVDT	DII-DIII
1178	GCVRRCPCCAVDTTQ	DII-DIII
1179	CVRRCPCCAVDTTQA	DII-DIII

B

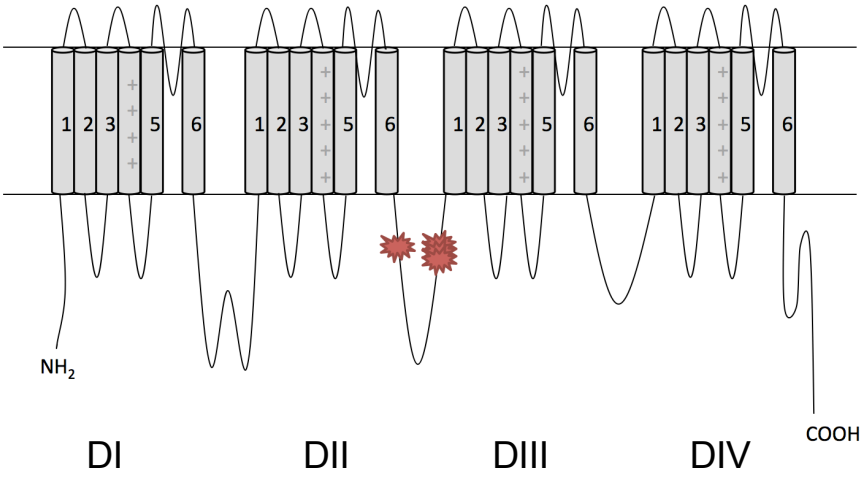

Figure 36. Identification of potential palmitoylation sites using CSS-palm 3.0. (A) Position and sequence of the potential endogenous sites that are predicted by the bioinformatics tool CSS-palm 3.0 with high threshold. (B) Schematic view of the localization of four predicted endogenous palmitoylation sites. All four mutations are located on the domain II to domain III linker area.

Table 6. The score matrix of the palmitoylation prediction results from CSS-PALM 3.0.

The predicted palmitoylation sites (C981, C1176, C1178, C1179) are indicated with red colored text. Any cysteine site with a score that is larger than the corresponding cutoff value is considered as a potential palmitoylation site. The high threshold setting of CSS-PALM was used for the prediction cutoff.

Position	Peptide	Score	Cutoff	Cluster
139	LFNMLIMCTILTNCV	0.286	0.308	Cluster A
145	MCTILTNCVFMAQHD	0.454	0.497	Cluster B
182	KILARGFCLHAFTFL	0.167	0.308	Cluster A
260	VMVLTVFCLSVFALI	0.124	0.308	Cluster A
280	MGNLRHKCVRNFTAL	0.339	1.225	Cluster C
326	GTSDVLLCGNSSDAG	0.281	0.308	Cluster A
335	NSSDAGTCPEGYRCL	0.769	1.225	Cluster C
341	TCPEGYRCLKAGENP	0.364	1.225	Cluster C
373	FRLMTQDCWERLYQQ	0.167	0.497	Cluster B
489	MSSGTEECGEDRLPK	0.167	0.308	Cluster A
597	KKNSTVDCNGVVSLL	0.934	1.225	Cluster C
649	MLTSQAPCVDGFEEP	0.119	0.308	Cluster A
683	LEESRHKCPPCWNRL	0.194	0.497	Cluster B
686	SRHKCPPCWNRLAQR	0.306	0.497	Cluster B
699	QRYLIWECCPLWMSI	0.554	1.225	Cluster C

700	RYLIWECCPLWMSIK	1.116	1.225	Cluster C
726	TDLTITMCIVLNTLF	0.727	1.225	Cluster C
896	LIIFRILCGEWIETM	0.014	0.308	Cluster A
906	WIETMWDCMEVSGQS	0.11	0.308	Cluster A
915	EVSGQSLCLLVFLLV	1.198	1.225	Cluster C
981	KRTTWDF**C**CGLLRQR	**1.083**	0.497	Cluster B
982	RTTWDFCCGLLRQRP	1.14	1.225	Cluster C
1004	AQGQLPSCIATPYSP	0.372	1.225	Cluster C
1046	PGDPEPVCVPIAVAE	0.306	1.225	Cluster C
1128	AEPQAPGCGETPEDS	0.289	1.225	Cluster C
1136	GETPEDSCSEGSTAD	0.537	1.225	Cluster C
1167	DVKDPEDCFTEGCVR	0.033	0.308	Cluster A
1172	EDCFTEGCVRRCPCC	0.12	0.497	Cluster B
1176	TEGCVRR**C**PCCAVDT	**0.806**	0.497	Cluster B
1178	GCVRRCP**C**CAVDTTQ	**0.333**	0.308	Cluster A
1179	CVRRCPC**C**AVDTTQA	**0.75**	0.497	Cluster B
1198	WWRLRKTCYHIVEHS	0.306	1.225	Cluster C
1272	KYFTNAWCWLDFLIV	0.496	1.225	Cluster C
1341	IMNVLLVCLIFWLIF	0.11	0.308	Cluster A
1363	FAGKFGRCINQTEGD	0.25	0.497	Cluster B
1384	IVNNKSQCESLNLTG	0	0.308	Cluster A
1539	VTIMFLICLNMVTMM	0.727	1.225	Cluster C

1575	VAIFTGECIVKLAAL	0.694	1.225	Cluster C
1703	TFANSMLCLFQITTS	0.09	0.308	Cluster A
1728	LNTGPPYCDPTLPNS	0.223	1.225	Cluster C
1742	SNGSRGDCGSPAVGI	0.488	1.225	Cluster C
1850	VSGDRIHCMDILFAF	0.471	1.225	Cluster C

2. Biophysical and biochemical characterization of potential palmitoylation sites

To further investigate the functional role of these four endogenous cysteines in regulating channel palmitoylation, we constructed a mutant channel with these four cysteine residues substituted to alanine residues using site-directed mutagenesis in an attempt to eliminate endogenous palmitoylation. This mutant channel construct, referred to as Nav1.5-AAAA, was used in experiments described below.

To assess the functional role of the four predicted endogenous palmitoylation sites, we transiently transfected the Nav1.5-AAAA channel into HEK293T cells and subsequently treated the cells with 2-Br-palmitate. The results demonstrate that 2-Br-palmitate does not alter Nav1.5-AAAA fast inactivation significantly (Figure 37A, right). Wild-type Nav1.5 was transiently transfected into a second set of cells as a control. Treatment with 2-Br-palmitate shifted the steady-state inactivation of transiently transfected wt Nav1.5 in the hyperpolarized direction (Figure 37B left), similar to that previously observed with the Nav1.5 stable cell line. Interestingly, although chemical inhibition of palmitoylation still shifted steady-state inactivation of Nav1.5-AAAA in the hyperpolarized direction (Figure 37B, right panel Table 7), the effect was substantially smaller (<3 mV) compared with wt Nav1.5 (~17 mV). The differential effect implies that one or more of these four cysteines are crucial in the regulation of Nav1.5 by palmitoylation. In addition, we found that the midpoint (V½) of Nav1.5-AAAA steady-state inactivation under control conditions was

quite close to that of wt Nav1.5 after 2-Br-palmitate treatment, leading us to conclude that the cysteine to alanine substitution(s) alter steady-state inactivation, probably through regulation of palmitoylation on one or more of the four predicted cysteines. To confirm that the ablation of 2-Br-palmitate's effect is due to the alteration in palmitoylation status, we used the ABE assay to assess palmitoylation of wt Nav1.5 and Nav1.5-AAAA channels. Our results indicate that the substitution of cysteine residues to alanine residues largely reduced the palmitoylation of the channel (Figure 38). These data strongly support the hypothesis that palmitoylation induced changes in Nav1.5 function is produced by specific modification of one or more of these four endogenous cysteine residues.

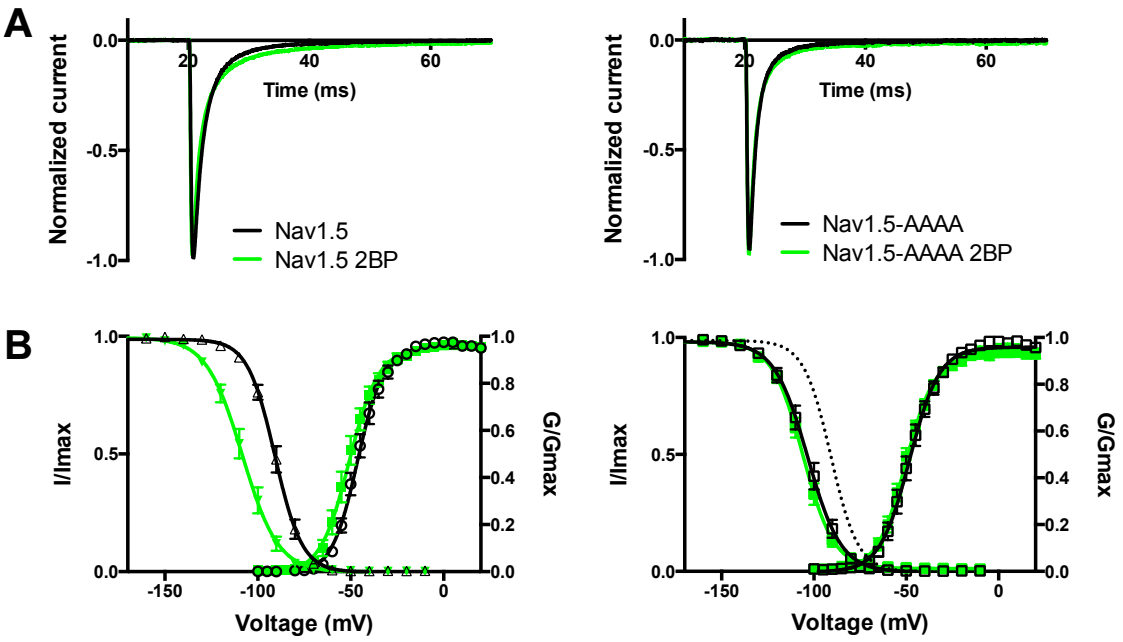

Figure 37. Effects of chemical inhibition of palmitoylation on the biophysical properties of wild-type Nav1.5 and Nav1.5-AAAA. Black lines and open symbols indicate data from control conditions and green indicates data from the 2-Br-palmitate (2BP) treatment group. (A) Normalized currents from cells transfected with Nav1.5 (left) and Nav1.5-AAAA with and without 2BP treatment. (B) Comparison of wild-type Nav1.5 (left) and Nav1.5-AAAA channel voltage-dependence of activation and steady-state inactivation before (black) and after (green) channel depalmitoylation. The dotted line indicates the wild-type Nav1.5 steady-state inactivation.

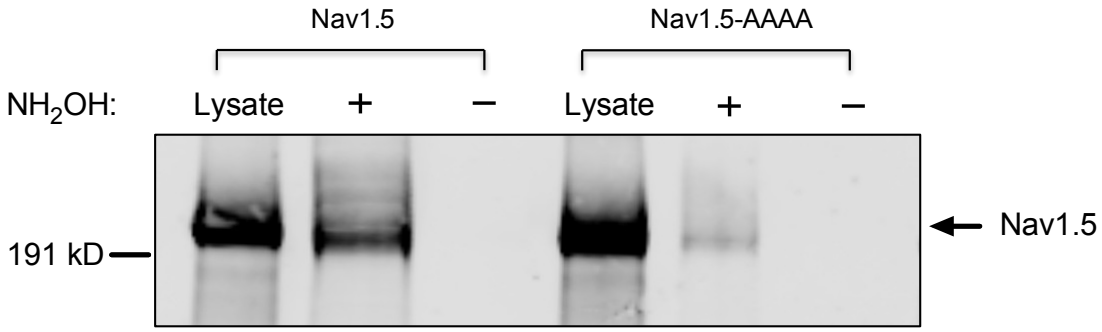

Figure 38. Characterization of Nav1.5 AAAA palmitoylation using ABE method. The reduced signal of Nav1.5 AAAA in '+' lane (hydroxylamine treated) indicates largely reduced palmitoylation of Nav1.5 AAAA. The results are representative of at least three independent experiments.

H. Palmitoylation site associated with Nav1.5 disease mutation

1. Nav1.5 mutation at C981 is associated with cardiac arrhythmia disease

Numerous missense mutations in Nav1.5 have been identified in individuals with cardiac arrhythmia. In a previously published study, the missense mutation C981F was reported in patient samples submitted for long QT syndrome genetic testing(Kapplinger, Tester et al. 2009) (Figure 39A). Because this mutation occurs at one of the four endogenous palmitoylation sites, we developed a Nav1.5 construct containing this mutation (Nav1.5-C981F) and investigated its biophysical properties in HEK293T cells. A significant shift of steady-state inactivation to more hyperpolarized voltages was observed when comparing to wt Nav1.5 (Figure 39B). No change in the rate of open channel fast inactivation was detected (Figure 39C) and the C981F mutant channel did not exhibit enhanced persistent current generation.

A

Position	Sequence	Region
981	KRTTWDFFCGLLRQR	DII-DIII

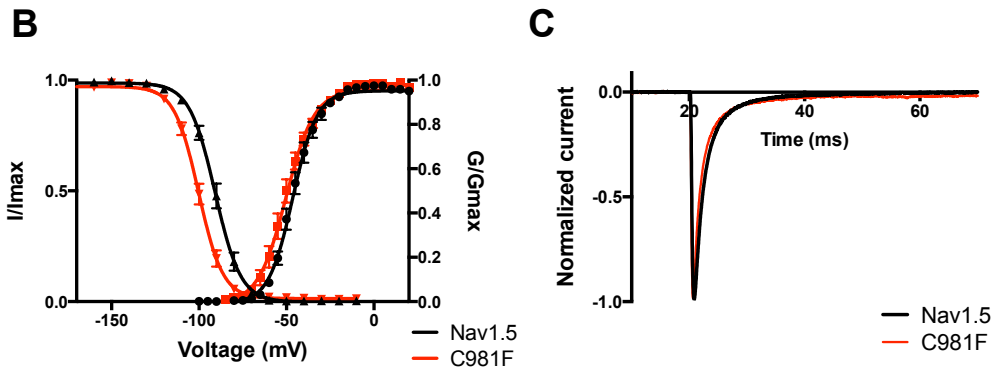

Figure 39. Loss of cysteine mutation identified from a patient with cardiac arrhythmia affects biophysical properties of Nav1.5. All data are shown as mean±s.e.m. (A) Long-QT3 mutation (C981F, red) that can potentially abolish the endogenous palmitoylation in wild-type Nav1.5. (B) Comparison of voltage dependence of activation and steady-state inactivation of wild-type Nav1.5 (black) and C981F mutant channels (red). (C) Normalized current of wild-type Nav1.5 channel (black) and Nav1.5-C981F (red).

2. Identification of C981 as a critical site for Nav1.5 palmitoylation

To understand if altered palmitoylation contributes to the shift of the inactivation curve, we treated the Nav1.5-C981F transfected cells with 2-Br-palmitate as in previous experiments. We found that 2-Br-palmitate treatment had very little effect on Nav1.5-C981F channel steady-state inactivation (Figure 40A). To confirm that the effect is specifically due to the loss of the cysteine residue and not to insertion of a bulky hydrophobic residue, we examined a cysteine to alanine mutation at the same site. Nav1.5-C981A also exhibited a hyperpolarized steady-state inactivation and revealed insensitivity to 2-Br-palmitate treatment (Figure 40B). Moreover, in our study, both C981F and C981A exhibited very similar properties to the Nav1.5-AAAA channel. This indicates that the C981 site alone accounts for the major palmitoylation effect on Nav1.5 steady-state inactivation, and is likely to be the most important site among the four predicted cysteines. To further confirm the role of the C981 site and investigate the roles of other cysteine residues, we also tested a Nav1.5 mutant with C981 intact and the other three cysteines mutated to alanines (Nav1.5-AAA). Results with this mutant channel indicate that depalmitoylation has a significant effect on Nav1.5-AAA steady-state inactivation (Figure 40C). This effect was also observed in the C1178A mutation (Figure 40D). These results further validate the critical and specific role of C981 palmitoylation in regulating channel gating properties.

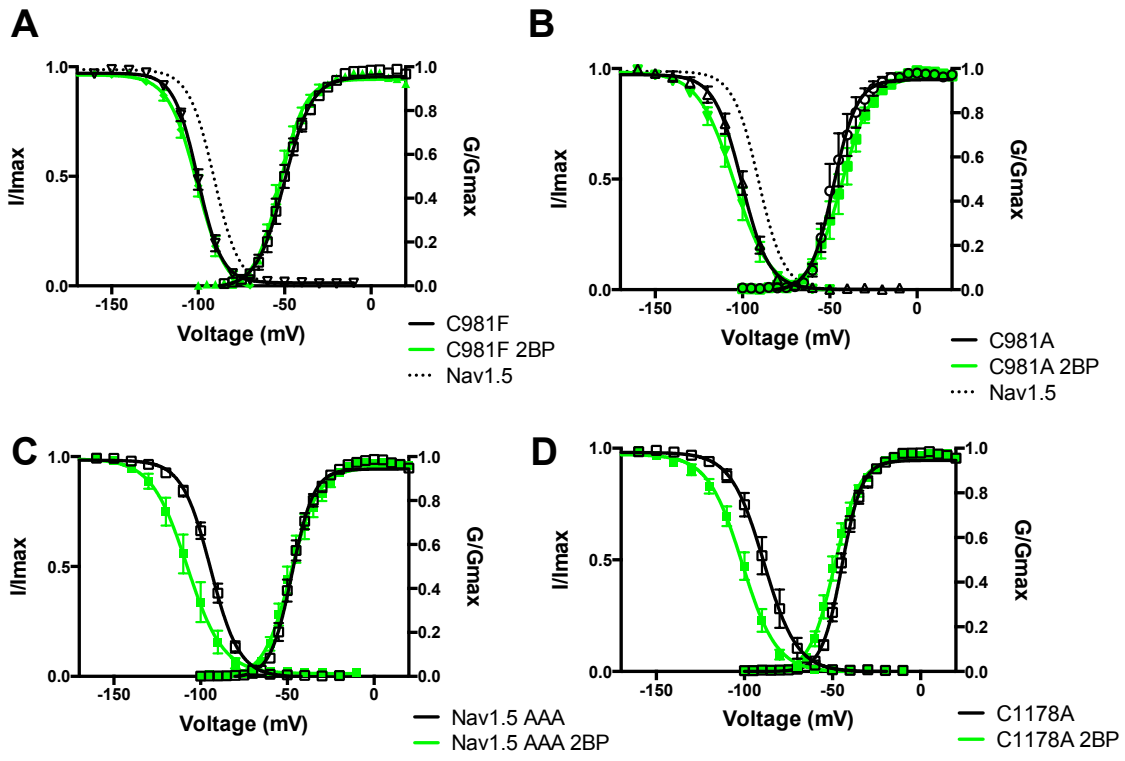

Figure 40. Identification of Nav1.5 palmitoylation at C981. (A) Nav1.5-C981F channel activation and steady-state inactivation with (green) and without (black) 2-Br-palmitate(2BP) treatment. (B) Nav1.5-C981A voltage dependence of activation and steady-state inactivation with (green) and without (black) 2-Br-palmitate treatment. The dotted line indicates the wild-type Nav1.5 steady-state inactivation. (C-D) 2-Br-palmitate treatment (green) affect Nav1.5-AAA (C) and Nav1.5-C1178A (D) voltage dependence of activation and steady-state inactivation.

Table 7. Midpoint voltage of activation and steady state inactivation with a standard Boltzmann distribution fit.

All data are shown as mean±s.e.m. # indicates $p<0.05$ compared with wild-type group. * indicates $p<0.05$ compared with the corresponding non-treatment group. The two-tailed, Student's t-test was used to study the statistical significance.

Channel construct	**Activation**		**Inactivation**	
	$V_{1/2}$ (mV)	K (mV)	$V_{1/2}$ (mV)	K (mV)
Nav1.5 stable	-33.4±0.3	7.8±0.2	-90.4±0.6	7.1±0.5
Nav1.5 stable 2BP	-34.1±0.4	8.9±0.4*	-103±0.5*	8.1±0.4*
Nav1.5 stable PA	-29.9±0.4	7.7±0.4	-83.4±0.4*	6.3±0.4
Nav1.5 transient	-46.3±0.4	6.9±0.3	-90.8±0.5	7.3±0.4
Nav1.5 transient 2BP	-50.8±0.6	7.8±0.5	-108.4±0.7*	9.7±0.6
Nav1.5-AAAA	-48.2±0.4	8.1±0.4	-103.4±0.7#	9.0±0.6
Nav1.5-AAAA 2BP	-50.4±0.5	7.7±0.4	-106.0±0.5	8.4±0.5
Nav1.5 C981F	-50.2±0.5	8.1±0.4	-100.2±0.5#	6.9±0.4
Nav1.5 C981F 2BP	-52.6±0.4	7.3±0.4	-100.7±0.7	8.3±0.6
Nav1.5 C981A	-47.8±0.7	6.7±0.6	-100.5±0.6#	7.9±0.5

Nav1.5 C981A 2BP	-43.2±0.7	8.5±0.6	-104.8±0.9	10.3±0.8
Nav1.5 cardiomyocytes	-37.3±0.3	7.1±0.3	-76.6±0.5	8.2±0.4
Nav1.5 cardiomyocytes 2BP	-42.2±0.6	8.5±0.5*	-99.4±0.6*	10.1±0.5*
Nav1.5 cardiomyocytes Palmitic acid	-36.1±0.5	6.7±0.5	-71.0±0.5*	7.3±0.5

I. Supplemental results

1. Identification of 2-Br-palmitiate as a palmitoylation inhibitor

To verify 2-Br-palmitate effect on protein palmitoylation, we use a palmitoylated fluorescent GFP protein which can indicate its palmitoylation level by fluorescence visualization. This pCAG-mGFP (Addgene plasmid 14757) is a membrane bound form of EGFP(Matsuda and Cepko 2007), containing a palmitoylation sequence of GAP43 at its N-terminus (Figure 41). This protein can be expressed on the surface when it is palmitoylated and therefore serves as a useful tool to visualize palmitoylation level change in the cell.

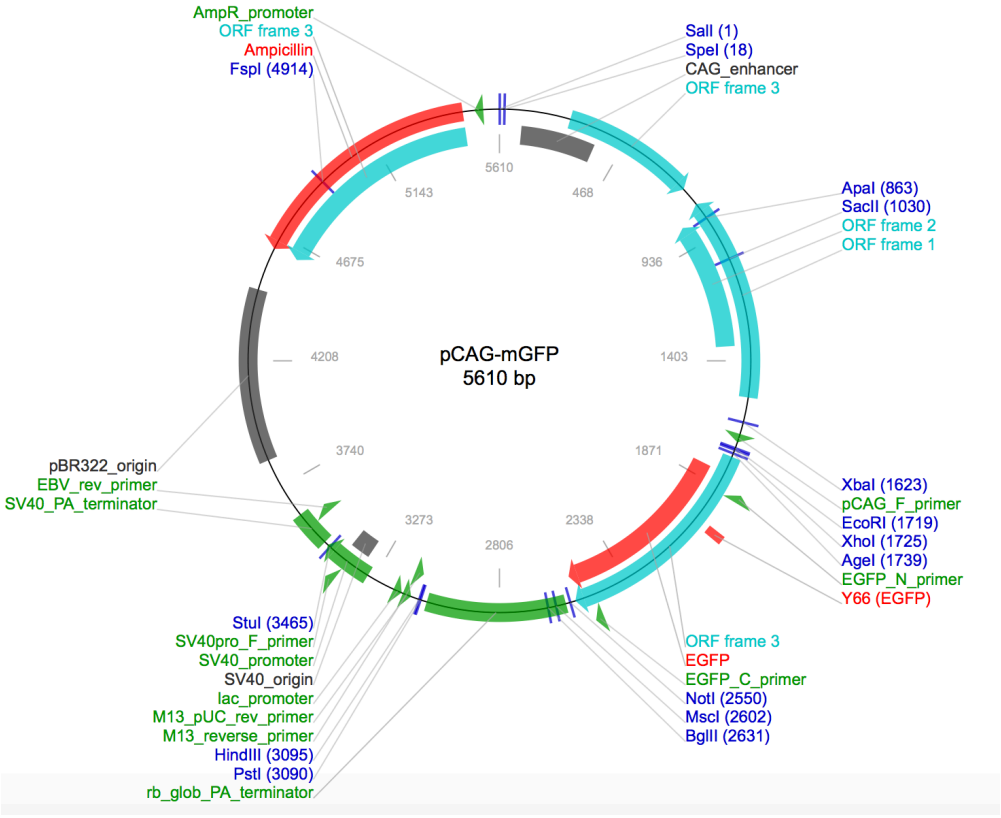

Figure 41. Plasmid map of cDNA construct of pCAG-mGFP. The copyright of this map belongs to the Addgene Inc. pCAG-mGFP encodes a membrane-bound form of fluorescent protein (GFP) with a palmitoylation sequence of GAP43 at its N-terminus. The total length of this vector is about 5610 bp.

HEK293 cells were used in the experiments and plated in a glass bottom dish. The pCAG-mGFP construct was transfected into the cell and treated with 2-Br-palmitate for 24 hours. Images of fluorescent cells were captured using epifluorescence microscope the next day. All data were analyzed using image processing software Image J.

In our result, we observed a ring like structure on the edge of each cell in control group and further analysis of representative cells indicates peak fluorescence at cell surface, which suggest the palmitoylation and surface expression of fluorescent protein in the control group (Figure 42 upper panel). However, in the 2-Br-palmitate treatment group, we were not able to observe the clear surface expression of fluorescence protein and the image analysis also indicates the consistent level of fluorescence throughout the cell (Figure 42 middle and lower panels). These data further verify 2-Br-palmitate as a valid tool to manipulate palmitoylation level in HEK293 cells.

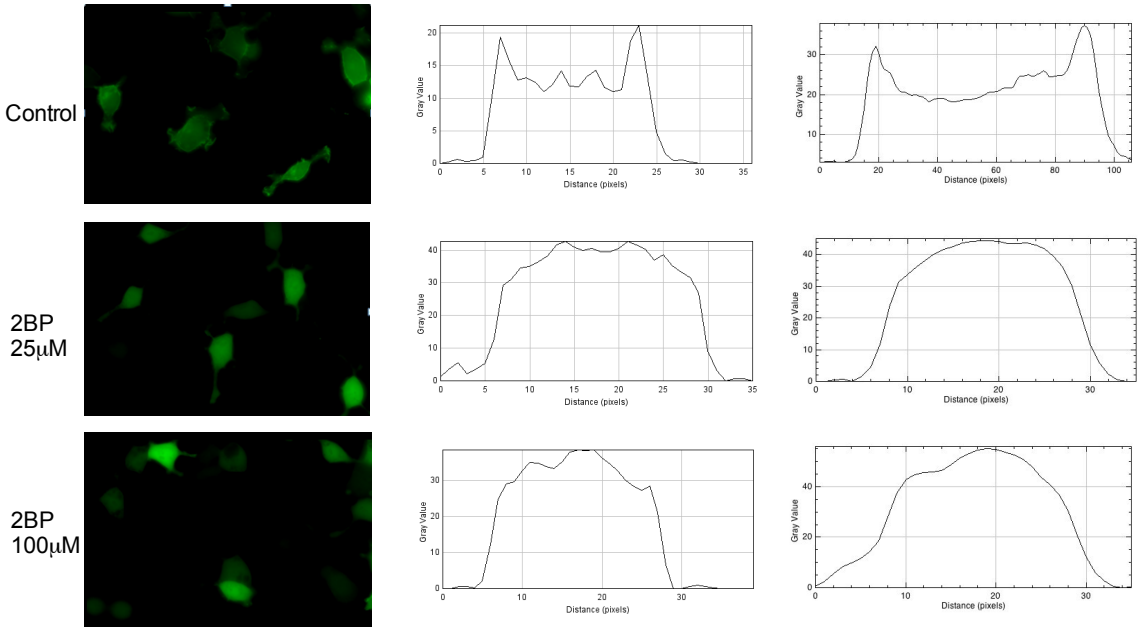

Figure 42. 2-Br-palmitate affect palmitoylation of mGFP in HEK293 cells. Left column indicates images recorded from epifluorescence microscope. Right lane shows the analysis of fluorescence of representative cells in each group. The top panel shows the data from control group. Middle and bottom panel shows the fluorescence image after 24 hours treatment of 25 μM and 100 2-Br-palmitate.

2. 2-Br-palmitiate does not affect bacterial sodium channel gating properties

Votage-gated sodium channels regulate cell electric activity by mediating sodium ion conductance. Therefore, eukaryotic sodium channels are critical components in excitable cells. Recently, a number of prokaryotic voltage-gated sodium channels were identified. Among them, NaChBac from Bacillus halodurans, is the most studied and characterized prokaryotic sodium channels (Charalambous and Wallace 2011).

Eukaryotic sodium channels contain four homologous domains, each domain has six transmembrane segments, of which S1-S4 serves as the voltage sensor and S5-S6 forms the pore subdomain. However, unlike eukaryotic sodium channels, NaChBac is one domain homo-tetramer of six transmembrane helices. NaChBac also contains a voltage-sensing component of S1-S4 and a pore-forming region by S5-S6. The positively charged amino acids on S4 of NaChBac is the key residues involved in channel activation (Chahine, Pilote et al. 2004). The current kinetics of NaChBac, including activation, inactivation and recovery, are much slower compared to eukaryotic sodium channels (Ren, Navarro et al. 2001, Koishi, Xu et al. 2004). NaChBac can be heterologous expressed in mammalian cells for functional characterization, providing a useful model for studying voltage-gated ion channels.

Protein palmitoylation is unlikely to occur on NaChBac since the amino acid sequence of NaChBac does not contain any cysteine residues (Figure 43 Lower panel). This provides us excellent opportunity to study potential non-

specific effects of 2-Br-palmitate on voltage-gated sodium channels. Here, we pretreated the cells with 2-Br-palmitate for 24 hours and compared the results from control group with treatment group. Our results indicate that 2-Br-palmitate does not affect NaChBac voltage dependence of activation and inactivation significantly (Figure 44). Therefore, we are further convinced that the 2-Br-palmitate effect on Nav1.5 is due to inhibition of palmitoylation, rather than other non-specific effects.

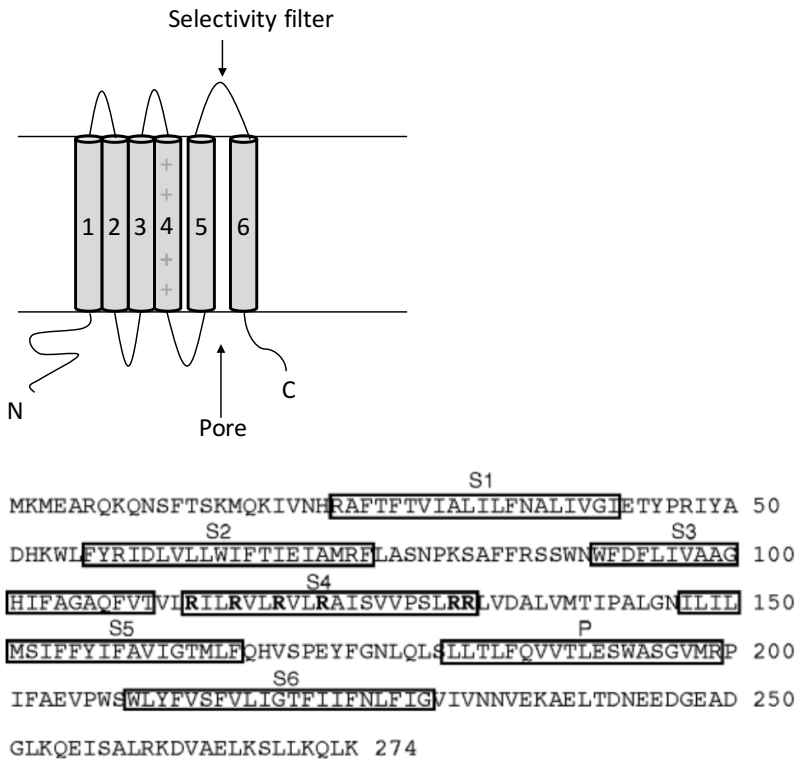

Figure 43. Schematic diagram (upper panel) and sequence (lower panel) of voltage-gated bacteria sodium channel structure. S1-S4 transmembrane helices forms the voltage sensor of NaChBac and S5-S6 comprises the central pore of the channel. Bottom panel shows the amino acid sequence of NaChBac. The six transmembrane helices S1-S6 and the central pore region are indicated. The positively charged residues in the S4 region are in bold. This sequence is from “A prokaryotic voltage-gated sodium channel.” (Ren, Navarro et al. 2001)

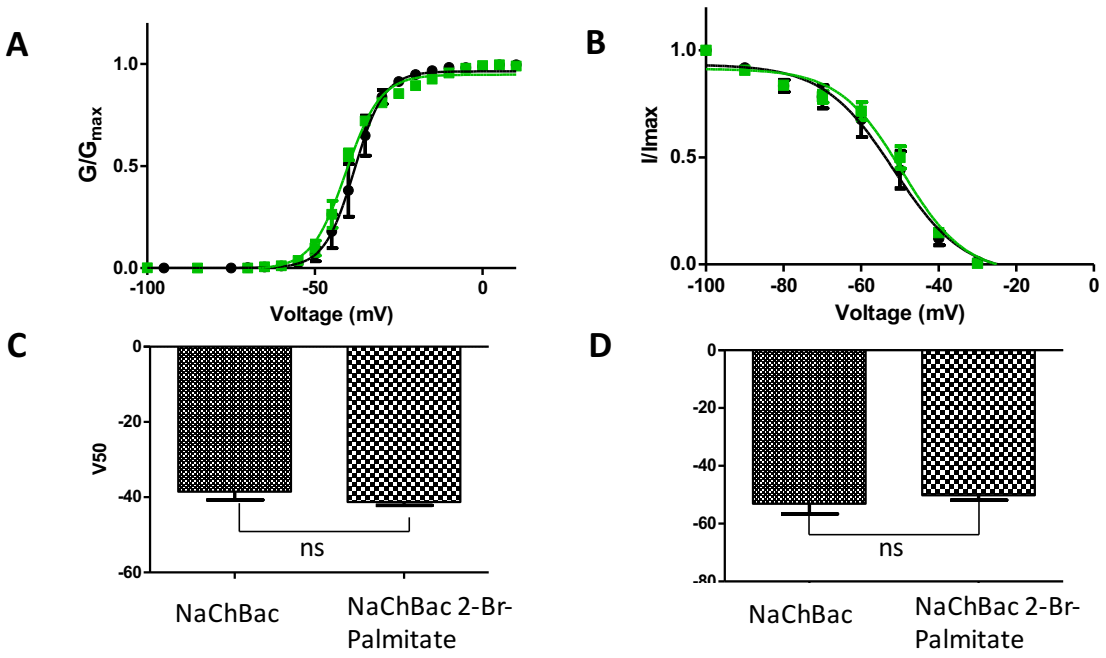

Figure 44. 2-Br-palmitate treatment does not affect Bacteria sodium channel biophysical properties. Black curve indicates NaChBac gating properties without treatment and green curve shows the NaChBac gating properties with 2-Br-palmiate treatment. Bottom panels shows the statistical analysis of V_{50} of voltage dependence of activation and inactivation. There is no statistical significance identified.

IV. Discussion

A. Overview of the dissertation research

Palmitoylation is a reversible modification that regulates various steps during protein life cycle, including trafficking, stability and membrane association. Palmitoylation regulation of membrane association plays a role for many peripheral membrane proteins(Dudler and Gelb 1996, Chamberlain, Lemonidis et al. 2013) and affects trafficking and surface expression of ion channels(Jeffries, Geiger et al. 2010, Chen, Bi et al. 2013).

Although a few studies have indicated that VGSCs in the brain are subject to palmitoylation(Schmidt and Catterall 1987, Bosmans, Milescu et al. 2011), it had not previously been determined if sodium channels from other excitable tissues are also subject to modulation by palmitoylation. More importantly, how palmitoylation would affect cellular excitability in any tissue was unclear. This study, for the first time, utilized both biochemical and electrophysiology techniques for investigation of palmitoylation in voltage-gated sodium channel modulation. Our data, in conjunction with computer simulations, indicate that palmitoylation can substantially regulate cardiac sodium currents and that alterations in Nav1.5 palmitoylation are likely to play important roles in acquired and inherited cardiac channelopathies. Table 8 summarizes key results of how palmitoylation regulates Nav1.5 activities.

Table 8. Summarization of palmitoylation regulation of Nav1.5 activities.

	2BP	PA	Nav1.5-AAAA	Nav1.5-981A
Current Density	no change	no change	no change	no change
Fast Inactivation	no change	no change	no change	no change
$V_{1/2}$ (Activation)	no change	no change	no change	no change
$V_{1/2}$ (Inactivation)	hyperpolarize shift	depolarize shift	hyperpolarize shift	hyperpolarize shift
Recovery(fast inactivation)	delay	enhance	—	—
Slow Inactivation	no change	no change	—	—
Recovery(slow inactivation)	no change	no change	—	—
Persistent Current	no change	enhance	no change	no change
AP activity	reduce	prolong AP duration	—	—
Palmitoylation	reduce	enhance	reduce	—

B. Biochemical characterization of protein palmitoylation

In recent years, the progress of ion channel palmitoylation research has been facilitated by the development of new biochemical and proteomics tools(Martin 2013, Storck, Serwa et al. 2013) and the identification of palmitoyltransferases (Greaves and Chamberlain 2011, Korycka, Lach et al. 2012). The traditional method of detecting protein palmitoylation involves metabolic labeling of cells with radioactive palmitate followed by immunoprecipitation and further identification of target proteins by autoradiography (Schmidt, Schmidt et al. 1988, Tsai, Wynne et al. 2014). This experiment provides direct evidence of protein palmitoylation(Martin and Cravatt 2008). However, it also requires extensive utilization of radioactive materials and lenthy film exposure for weeks or even months depending on the intensity of the palmitoylation signal (Yang, Di Vizio et al. 2010, Martin, Wang et al. 2011). The development of the non-radioactive ABE assay allows more rapid detection of protein palmitoylation(Brigidi and Bamji 2013). This method uses hydroxylamine to selectively cleave the thioester bond at palmitoylated sites, followed by subsequent labeling of the newly exposed cysteine thiol with cysteine-reactive biotin reagents. Biotinylated proteins can be further immunoprecipitated for palmitoylation detection or purified for mass spectrometry identification of palmitoylation sites(Drisdel and Green 2004). This method provides higher sensitivity compared to traditional metabolic labeling and allows for quantitative estimates of palmitoylation. It is ideal for measuring the dynamics of palmitoylation process. However, one caveat of this methodology is the

detection of all existing S-acylated proteins, instead of more specific identification of protein palmitoylation. This method also requires complete block of all free cysteines before thioester cleavage, or false positive result will be generated due to incomplete alkylation of endogenous hydroxylamine-sensitive thioesters. Another commonly used non-radioactive assay for palmitoylation detection is click chemistry method(Hang, Geutjes et al. 2007). This method uses the alkyne fatty acid analog 17-octadecynoic acid (17-ODYA), which can be metabolically incorporated into endogenous cellular machinery at palmitoylation sites(Martin and Cravatt 2009). 17-ODYA labeled proteins can be further linked to azide-reporter tags by copper-catalyzed click chemistry and visualized by in-gel fluorescence analysis(Speers and Cravatt 2004). This approach can also measure the rates of incorporation and dynamic turnover of palmitoylation process using the traditional pulse-chase method (Zhang, Tsou et al. 2010). One important advantage of this method is that it largely reduces the chance of false positive results compared with ABE assay.

The most convincing demonstration of palmitoylation sites will be the mass spectrometry results. However, it is often lacking in most studies due to the complexity of this lipid modification and difficulties of resolving the palmitoylated peptides in mass spectrometry (further discussed in section E). Therefore, many studies utilize mutagenesis methods combined with metabolic labeling of palmitate to screen potential palmitoylation sites. Here in our experiment, Nav1.5 palmitoylation was demonstrated by three lines of biochemistry evidence. Although we were able to detect Nav1.5 palmitoylation with tritiated palmitate, the

intensity of the palmitoylation signal in metabolic labeling experiments was relatively weak due to the low sensitivity of the method and the difficulties in enrichment of membrane proteins. Film exposure time of more than one month was required for clear visualization of palmitoylation signal. Therefore, ABE experiment was mostly used in our work.

C. Alteration of Nav1.5 gating properties by palmitoylation

In our study, palmitoylation induced a small change in current density(Figure 22). However, this difference was not statistically significant, indicating that palmitoylation has negligible impact on cell surface expression of Nav1.5. Instead, our data demonstrate that Nav1.5 palmitoylation has profound impact on channel availability by regulating the voltage-dependence of steady-state inactivation in both HEK293 cells (Figure 30) and cardiomyocytes (Figure 26). Nav1.5 inactivation was largely enhanced in 2-Br-palmiate treatment group, narrowing the membrane potential range of window currents. On the contrary, Nav1.5 inactivation was significantly delayed with palmitic acid treatment, increasing the voltage range of window currents. We also observed an elevated persistent sodium current with palmitic acid treatment, which, together with the alteration in Nav1.5 inactivation, could potentially lead to the reactivation of Nav1.5 and enhancement of sodium conductance during action potential phase 3. The opposite direction of changes in sodium channel gating properties between these two treatment groups suggests that palmitoylation level can dynamically regulate Nav1.5 functions by mediating channel inactivation. Based on the relative magnitude of the shifts induced by palmitic acid (+6 mV) and 2-Br-palmitate (-20 mV) compared to control experiments, these data could be an indication that as many as two-thirds of the channels are palmitoylated under our control conditions. However, several studies have identified crosstalk between palmitoylation and other post-translational modifications in ion channel proteins(Pickering, Taverna et al. 1995, Tian, Jeffries et al. 2008, Hayashi,

Thomas et al. 2009, Zhou, Wulfsen et al. 2012) and it is therefore unclear if all Nav1.5 channels were palmitoylated in our experiments. On the other hand, if a substantial fraction of channels remained un-palmitoylated after treatment with excess palmitate, one would expect to see either a biphasic voltage-dependence of inactivation curve, result in a large variance or a curve with a shallower slope. These would be consistent with a mixed population of channels, but neither was observed. In addition, the hyperpolarized shift of inactivation curve of Nav1.5-AAAA is similar to that obtained with 2-Br-palmitate treatment, indicating that we are able to obtain near complete removal of palmitoylation. Regardless, our data show that palmitoylation can modify the voltage-dependence of Nav1.5 inactivation by 20 to 25 mV, suggesting a remarkable effect on bi-directional regulation of palmitoylation.

D. Alteration of cardiomyocyte excitability by palmitoylation

Our data indicate that palmitoylation of Nav1.5 has a pronounced impact on cardiomyocyte excitability. Specifically, in our experiment, inhibiting palmitoylation greatly reduced myocyte excitability. The treatment of 2-Br-palmiate abolished beating cells and no action potential (spontaneously or stimulated) was generated. Even though myocytes from 2-Br-palmiate group remained ‘inexcitable’ in our experiment settings, it is still possible that prolonged hypoperolarization by injecting negative current may restore the cardiomyocyte excitability in 2-Br-palmitate treatment group. In contrast, enhancing palmitoylation increased APD and induced aberrant action potential firing. Though our experimental results illustrate the changes in cardiomyocyte excitability, we are not able to rule out the possibility that other electrophysiologic properties, for example, automaticity was changed as well. Due to the shift of voltage-dependence of activation and inactivation, it is likely that the alteration in window currents might also change the automaticity. In addition to that, due to the lack of information of the substrate specificity of palmitoytransferase in cardiaomyocytes, we cannot rule out the possibility that palmitoylation modulation could also affect many proteins other than sodium channels. While multiple cardiac proteins involved in the cardiac action potential might be palmitoylated, our computer simulations indicate that changes in Nav1.5 gating due to palmitoylation are sufficient to cause the excitability changes that we observed in myocytes. Furthermore, the C981F mutation provides additional evidence that alteration of Nav1.5 palmitoylation is likely to impact cardiac action

potentials and contribute to arrhythmogenesis. This mutation was identified in the genomic DNA sample of a patient referred for long-QT syndrome clinical genetic testing(Kapplinger, Tester et al. 2009). In a patient cohort of 2500 unrelated cases, 110 distinct mutations were identified in *SCN5A* that were absent in the >2,600 control alleles. Although most of the patients were believed to have been referred due to a long-QT phenotype, some were referred because they had Brugada syndrome phenotypes (Kapplinger, Tester et al. 2009). Based on the biophysical analysis of C981F mutation, we predict that the patient with the C981F mutation more likely had a Brugada or overlapping syndrome phenotype, although unfortunately definitive phenotypic data was not available in the study that reported the C981F mutation(Kapplinger, Tester et al. 2009).

Interestingly, we also identified four long-QT3 mutations in the literature (R34C, R1175C, F1473C, R1644C) that our analysis predicts could add an additional palmitoylation site on Nav1.5, suggesting that enhanced palmitoylation may contribute to the biophysical alterations induced by some long-QT mutations. In contrast to C981F effects, Bankston and colleagues reported that the F1473C Nav1.5 mutation, a long-QT mutation associated with a severe clinical phenotype, had similar biophysical consequences as those we observed with palmitic acid treatment(Bankston, Yue et al. 2007). The F1473C mutation shifted the midpoint of Nav1.5 inactivation in the depolarizing direction by 9 mV and increased persistent (late) currents to ~0.6% of the peak current. Furthermore, they used a computer model of a ventricular myocyte to show that the combined

shift in steady-state inactivation and increase in persistent current amplitude is sufficient to double the duration of the ventricular action potential.

All together these data suggest that while depalmitoylation of a key Nav1.5 cysteine can result in reduced cardiac excitability similar to that observed with Brugada syndrome, excessive palmitoylation of Nav1.5 can lead to enhanced cardiac activity similar to that observed with long QT-syndrome mutations.

E. Potential endogenous palmitoylation sites

Palmitoylation has been identified on various types of proteins, however, there is no clear consensus sequence of palmitoylation among substrate proteins. Previous studies show that cysteines that are close to transmembrane domains are preferred sites for protein palmitoylation, probably because the accessibility to membrane associated palmitoyltransferase (Bijlmakers and Marsh 2003). Apart from their distance to transmembrane domains, palmitoylation sites are often close to myristoylation and prenylation sites and/or surrounded by hydrophobic residues (Salaun, Greaves et al. 2010).

The lack of a precise consensus sequence and the diverse features of the amino acids found to influence palmitoylation makes it challenging to predict the potential palmitoylation site. The bioinformatics tool CSS-Palm 3.0 utilizes a clustering and scoring algorithm by comparing the surrounding amino acid sequence similarity with experimentally determined palmitoylation sites. Four endogenous palmitoylation sites that were likely to regulate Nav1.5 palmitoylation were identified using this prediction algorithm. Moreover, we also examined the location of these four residues and they are all found in the second major cytoplasmic loop where palmitoylation is likely to happen (Figure 36). Mutation of these four cysteines to alanines had essentially the same effect on steady-state inactivation as 2-Br-palmitate treatment did on wt Nav1.5, and the Nav1.5-AAAA channels were insensitive to modulation by 2-Br-palmitate treatment (Figure 37), indicating that one or more of these cysteines are responsible for the change in inactivation observed with wild type Nav1.5

depalmitoylation. The Nav1.5 C981F and C981A channels had almost the same inactivation properties as the Nav1.5-AAAA channel (Figure 40), indicating that C981 is likely to be the crucial site at which palmitoylation modulates inactivation of Nav1.5. However, the detailed mechanism of how palmitoylation of C981 impacts the voltage-dependence of steady-state inactivation is still unknown. We noticed that all of the sites that are implicated in Nav1.5, as well as the endogenous palmitoylation sites predicted in Nav1.2 to modulate steady-state inactivation, are located in the cytoplasmic linker between domains II and III. One possibility is that by increasing association of this linker to the membrane, palmitoylation may alter the movement of the domain III voltage-sensor, which is important for channel inactivation(Cha, Ruben et al. 1999). Although our data clearly indicate that C981 palmitoylation is crucial to the gating changes that we observed, we were unable to generate a stable cell line containing only a C981 mutant channel for further biochemical analysis. Therefore, we cannot rule out the possibility that one or more of the other three predicted sites are palmitoylated and that this might modulate other properties of Nav1.5 in cardiac myocytes.

Furthermore, the mass spectrometry(MS) experiments were attempted to better identify endogenous palmitoylation sites. Unfortunately, due to the relative large size of sodium channel protein and the instability of palmitoylation sites under reducing conditions, we were not able to achieve high coverage of the sodium channel and identify protein palmitoylation at any cysteine sites (Figure 45). The standard protocol involves reducing disulfides and alkylating free-

cysteine side chains with iodoacetamide. The reducing agent (DTT) may remove some of the palmitoylation and leave the sites alkylated with iodoacetamide. Also, palmitoylated peptides are generally very challenging to resolve in Liquid chromatography (LC) and LC-MS due to the dramatic difference in hydrophobicity after lipid modification (Ji, Leymarie et al. 2013). On account of the above mentioned difficulties, further identification of precise location of palmitoylation sites with mass spectrometry could not be accomplished in this project.

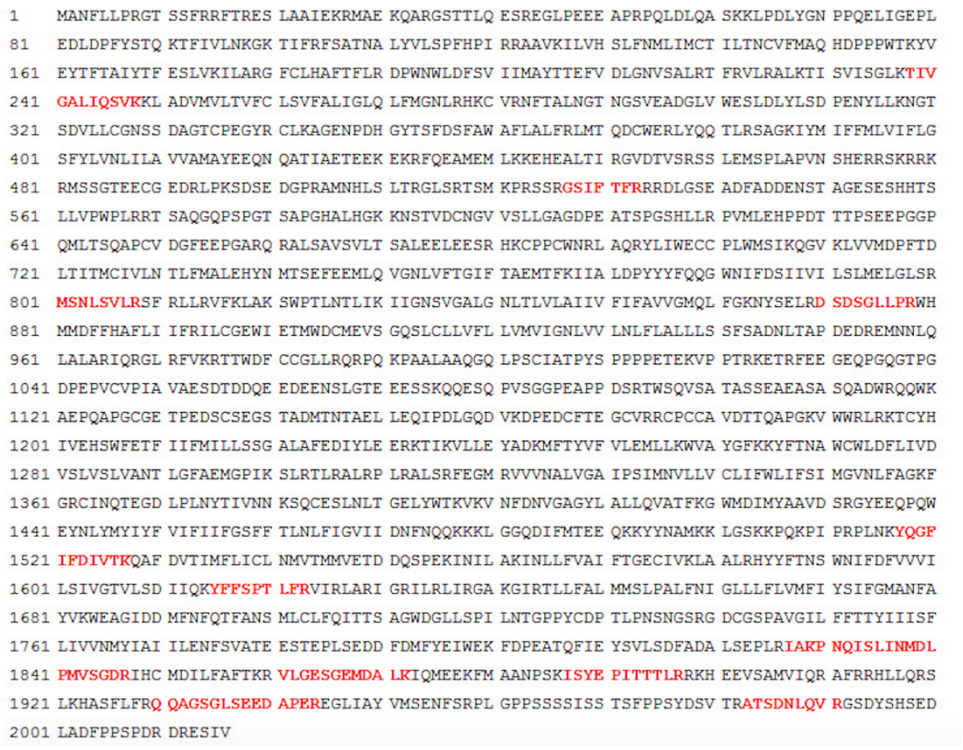

Figure 45. Identified peptides with Mass Spectrometry experiment. The red color indicates identified peptides, which covers 6% of the total sequence.

F. Future directions

Our study demonstrates that palmitoylation changes have profound impact on cardiac myocyte excitability. However, we do not yet understand the molecular mechanism behind this process and how that may alter therapeutic treatment of arrhythmia diseases. To further explore how palmitoylation alters pharmacological response to antiarrhythmic drugs, we performed a series of preliminary studies with Lidocaine, a class Ib sodium channel blocker that reduces sodium current and shortens action potential duration(Bean, Cohen et al. 1983). Our data demonstrates that the inhibition effect of lidocaine on sodium current was significantly enhanced after 2-Br-palmitate treatment. Since lidocaine preferentially binds open and inactivated sodium channels(Matsubara, Clarkson et al. 1987), one possible explanation is that enhanced inactivation of Nav1.5 after 2-Br-palmitate treatment could facilitate lidocaine binding, thus lead to increased sodium channel blockage. On the contrary, lidocaine blockage of sodium current was significantly reduced with palmitic acid treatment, probably at a result of delayed sodium channel inactivation after palmitic acid treatment. Since different types of antiarrhythmic drugs affect distinct aspects of sodium channel gating, they may respond differently upon altered palmitoylation level. Therefore, more experiments comparing different classes of antiarrhythmic drugs need to be done to further explore the differential regulation on channel pharmacological effects by palmitoylation. Overall, our preliminary data supports the idea that palmitoylation may have substantial impact on pharmacological

response to antiarrhythmic drugs and may provide guidance on the therapeutic management of cardiac arrhythmia diseases.

G. Summary and conclusion

This dissertation research provides important insights into how palmitoylation regulates cardiac sodium channel function and myocyte excitability. In this study, we demonstrate that Nav1.5 is palmitoylated in both a heterologous expression system and in native cardiac tissue, using both biochemical and electrophysiological assays. Our data show that palmitoylation of Nav1.5 can substantially modulate the inactivation properties of cardiac sodium currents and lead to bidirectional alterations in cardiac excitability. We also identify potential palmitoylation sites regulating this process(Pei, Xiao et al. 2016).

The existence of disease related mutations that alter potential palmitoylation sites illustrates how the potential loss of palmitoylation at this crucial residue alters channel inactivation and dysregulates myocyte excitability to contribute to cardiac disease. Thus the modulation of cardiac sodium channel palmitoylation is likely to be an unrevealed mechanism of cardiac arrhythmia generation. A previous study indicates that palmitoylation of cardiac proteins increases during reoxygenation of anoxic cardiac tissue(Lin, Fine et al. 2013), and thus enhanced palmitoylation of cardiac sodium channels could contribute to reperfusion induced arrhythmias. Evidence indicates that palmitoylation can also be altered by diet, stress and redox signaling(Burgoyne, Haeussler et al. 2012). Although the vast majority of long-QT3 and Brugada syndrome mutations may not directly alter Nav1.5 palmitoylation, increased palmitoylation of Nav1.5 is predicted to enhance EADs and arrhythmias in patients with long-QT3 and

reduced palmitoylation of Nav1.5 is expected to exacerbate symptoms in patients with Brugada syndrome; thus regulation of Nav1.5 activity by palmitoylation could be important in multiple cardiac pathophysiological conditions. Brain sodium channel activity is also likely to be regulated by palmitoylation(Kang, Wan et al. 2008) and altered palmitoylation has been implicated in a number of neurological disorders(Young, Butland et al. 2012). Overall, alterations in palmitoylation of voltage-gated sodium channels are likely to have profound effects on cellular excitability in a variety of tissues and pathophysiological conditions.

Reference list

Agnew, W. S. (1984). "Voltage-regulated sodium channel molecules." Annu Rev Physiol **46**: 517-530.

Aiba, T., G. G. Hesketh, T. Liu, R. Carlisle, M. C. Villa-Abrille, B. O'Rourke, F. G. Akar and G. F. Tomaselli (2010). "Na+ channel regulation by Ca2+/calmodulin and Ca2+/calmodulin-dependent protein kinase II in guinea-pig ventricular myocytes." Cardiovasc Res **85**(3): 454-463.

Alexander, J. K., A. P. Govind, R. C. Drisdel, M. P. Blanton, Y. Vallejo, T. T. Lam and W. N. Green (2010). "Palmitoylation of nicotinic acetylcholine receptors." J Mol Neurosci **40**(1-2): 12-20.

Ashpole, N. M., A. W. Herren, K. S. Ginsburg, J. D. Brogan, D. E. Johnson, T. R. Cummins, D. M. Bers and A. Hudmon (2012). "Ca2+/calmodulin-dependent protein kinase II (CaMKII) regulates cardiac sodium channel NaV1.5 gating by multiple phosphorylation sites." J Biol Chem **287**(24): 19856-19869.

Bankston, J. R., M. Yue, W. Chung, M. Spyres, R. H. Pass, E. Silver, K. J. Sampson and R. S. Kass (2007). "A novel and lethal de novo LQT-3 mutation in a newborn with distinct molecular pharmacology and therapeutic response." PLoS One **2**(12): e1258.

Bean, B. P., C. J. Cohen and R. W. Tsien (1983). "Lidocaine block of cardiac sodium channels." J Gen Physiol **81**(5): 613-642.

Beltran-Alvarez, P., A. Espejo, R. Schmauder, C. Beltran, R. Mrowka, T. Linke, M. Batlle, F. Perez-Villa, G. J. Perez, F. S. Scornik, K. Benndorf, S. Pagans, T. Zimmer and R. Brugada (2013). "Protein arginine methyl transferases-3 and -5 increase cell surface expression of cardiac sodium channel." FEBS Lett **587**(19): 3159-3165.

Beltran-Alvarez, P., S. Pagans and R. Brugada (2011). "The cardiac sodium channel is post-translationally modified by arginine methylation." J Proteome Res **10**(8): 3712-3719.

Beltran-Alvarez, P., A. Tarradas, C. Chiva, A. Perez-Serra, M. Batlle, F. Perez-Villa, U. Schulte, E. Sabido, R. Brugada and S. Pagans (2014). "Identification of N-terminal protein acetylation and arginine methylation of the voltage-gated sodium channel in end-stage heart failure human heart." J Mol Cell Cardiol **76**: 126-129.

Bennett, E. S. (2002). "Isoform-specific effects of sialic acid on voltage-dependent Na+ channel gating: functional sialic acids are localized to the S5-S6 loop of domain I." J Physiol **538**(Pt 3): 675-690.

Bennett, P. B., K. Yazawa, N. Makita and A. L. George, Jr. (1995). "Molecular mechanism for an inherited cardiac arrhythmia." Nature **376**(6542): 683-685.

Bezzina, C., M. W. Veldkamp, M. P. van Den Berg, A. V. Postma, M. B. Rook, J. W. Viersma, I. M. van Langen, G. Tan-Sindhunata, M. T. Bink-Boelkens, A. H. van Der Hout, M. M. Mannens and A. A. Wilde (1999). "A single Na(+) channel mutation causing both long-QT and Brugada syndromes." Circ Res **85**(12): 1206-1213.

Bijlmakers, M. J. and M. Marsh (2003). "The on-off story of protein palmitoylation." Trends Cell Biol **13**(1): 32-42.

Bosmans, F., M. Milescu and K. J. Swartz (2011). "Palmitoylation influences the function and pharmacology of sodium channels." Proc Natl Acad Sci U S A **108**(50): 20213-20218.

Brigidi, G. S. and S. X. Bamji (2013). "Detection of protein palmitoylation in cultured hippocampal neurons by immunoprecipitation and acyl-biotin exchange (ABE)." J Vis Exp(72).

Burgoyne, J. R., D. J. Haeussler, V. Kumar, Y. Ji, D. R. Pimental, R. S. Zee, C. E. Costello, C. Lin, M. E. McComb, R. A. Cohen and M. M. Bachschmid (2012). "Oxidation of HRas cysteine thiols by metabolic stress prevents palmitoylation in vivo and contributes to endothelial cell apoptosis." FASEB J **26**(2): 832-841.

Carmeliet, E. V., J. (2002). Basic Science for the Cardiologist, Springer Science+Business Media. .

Catterall, W. A. (2000). "From ionic currents to molecular mechanisms: the structure and function of voltage-gated sodium channels." Neuron **26**(1): 13-25.

Catterall, W. A., A. L. Goldin and S. G. Waxman (2005). "International Union of Pharmacology. XLVII. Nomenclature and structure-function relationships of voltage-gated sodium channels." Pharmacol Rev **57**(4): 397-409.

Cha, A., P. C. Ruben, A. L. George, Jr., E. Fujimoto and F. Bezanilla (1999). "Voltage sensors in domains III and IV, but not I and II, are immobilized by Na+ channel fast inactivation." Neuron **22**(1): 73-87.

Chahine, M., S. Pilote, V. Pouliot, H. Takami and C. Sato (2004). "Role of arginine residues on the S4 segment of the Bacillus halodurans Na+ channel in voltage-sensing." J Membr Biol **201**(1): 9-24.

Chamberlain, L. H., K. Lemonidis, M. Sanchez-Perez, M. W. Werno, O. A. Gorleku and J. Greaves (2013). "Palmitoylation and the trafficking of peripheral membrane proteins." Biochem Soc Trans **41**(1): 62-66.

Charalambous, K. and B. A. Wallace (2011). "NaChBac: the long lost sodium channel ancestor." Biochemistry **50**(32): 6742-6752.

Chen, L., D. Bi, L. Tian, H. McClafferty, F. Steeb, P. Ruth, H. G. Knaus and M. J. Shipston (2013). "Palmitoylation of the beta4-subunit regulates surface expression of large conductance calcium-activated potassium channel splice variants." J Biol Chem **288**(18): 13136-13144.

Clancy, C. E., M. Tateyama, H. Liu, X. H. Wehrens and R. S. Kass (2003). "Non-equilibrium gating in cardiac Na+ channels: an original mechanism of arrhythmia." Circulation **107**(17): 2233-2237.

Cohen, S. A. and L. K. Levitt (1993). "Partial characterization of the rH1 sodium channel protein from rat heart using subtype-specific antibodies." Circ Res **73**(4): 735-742.

Cummins, T. R. and S. G. Waxman (1997). "Downregulation of tetrodotoxin-resistant sodium currents and upregulation of a rapidly repriming tetrodotoxin-sensitive sodium current in small spinal sensory neurons after nerve injury." J Neurosci **17**(10): 3503-3514.

Davda, D., M. A. El Azzouny, C. T. Tom, J. L. Hernandez, J. D. Majmudar, R. T. Kennedy and B. R. Martin (2013). "Profiling targets of the irreversible palmitoylation inhibitor 2-bromopalmitate." ACS Chem Biol **8**(9): 1912-1917.

Dietzen, D. J., W. R. Hastings and D. M. Lublin (1995). "Caveolin is palmitoylated on multiple cysteine residues. Palmitoylation is not necessary for localization of caveolin to caveolae." J Biol Chem **270**(12): 6838-6842.

Drisdel, R. C. and W. N. Green (2004). "Labeling and quantifying sites of protein palmitoylation." Biotechniques **36**(2): 276-285.

Drisdel, R. C., E. Manzana and W. N. Green (2004). "The role of palmitoylation in functional expression of nicotinic alpha7 receptors." J Neurosci **24**(46): 10502-10510.

Dudler, T. and M. H. Gelb (1996). "Palmitoylation of Ha-Ras facilitates membrane binding, activation of downstream effectors, and meiotic maturation in Xenopus oocytes." J Biol Chem **271**(19): 11541-11547.

Dumaine, R., J. A. Towbin, P. Brugada, M. Vatta, D. V. Nesterenko, V. V. Nesterenko, J. Brugada, R. Brugada and C. Antzelevitch (1999). "Ionic mechanisms responsible for the electrocardiographic phenotype of the Brugada syndrome are temperature dependent." Circ Res **85**(9): 803-809.

Ednie, A. R., K. K. Horton, J. Wu and E. S. Bennett (2013). "Expression of the sialyltransferase, ST3Gal4, impacts cardiac voltage-gated sodium channel activity, refractory period and ventricular conduction." J Mol Cell Cardiol **59**: 117-127.

Fukata, M., Y. Fukata, H. Adesnik, R. A. Nicoll and D. S. Bredt (2004). "Identification of PSD-95 palmitoylating enzymes." Neuron **44**(6): 987-996.

Funck-Brentano, C. and P. Jaillon (1993). "Rate-corrected QT interval: techniques and limitations." Am J Cardiol **72**(6): 17B-22B.

Goldin, A. L. (2001). "Resurgence of sodium channel research." Annu Rev Physiol **63**: 871-894.

Goldin, A. L. (2003). "Mechanisms of sodium channel inactivation." Curr Opin Neurobiol **13**(3): 284-290.

Grant, A. O. (2009). "Cardiac ion channels." Circ Arrhythm Electrophysiol **2**(2): 185-194.

Greaves, J. and L. H. Chamberlain (2011). "DHHC palmitoyl transferases: substrate interactions and (patho)physiology." Trends Biochem Sci **36**(5): 245-253.

Gubitosi-Klug, R. A., D. J. Mancuso and R. W. Gross (2005). "The human Kv1.1 channel is palmitoylated, modulating voltage sensing: Identification of a palmitoylation consensus sequence." Proc Natl Acad Sci U S A **102**(17): 5964-5968.

Hallaq, H., D. W. Wang, J. D. Kunic, A. L. George, Jr., K. S. Wells and K. T. Murray (2012). "Activation of protein kinase C alters the intracellular distribution and mobility of cardiac Na+ channels." Am J Physiol Heart Circ Physiol **302**(3): H782-789.

Hang, H. C., E. J. Geutjes, G. Grotenbreg, A. M. Pollington, M. J. Bijlmakers and H. L. Ploegh (2007). "Chemical probes for the rapid detection of Fatty-acylated proteins in Mammalian cells." J Am Chem Soc **129**(10): 2744-2745.

Harvey, P. J., Y. Li, X. Li and D. J. Bennett (2006). "Persistent sodium currents and repetitive firing in motoneurons of the sacrocaudal spinal cord of adult rats." J Neurophysiol **96**(3): 1141-1157.

Hayashi, T., G. Rumbaugh and R. L. Huganir (2005). "Differential regulation of AMPA receptor subunit trafficking by palmitoylation of two distinct sites." Neuron **47**(5): 709-723.

Hayashi, T., G. M. Thomas and R. L. Huganir (2009). "Dual palmitoylation of NR2 subunits regulates NMDA receptor trafficking." Neuron **64**(2): 213-226.

Hille, B. (1968). "Pharmacological modifications of the sodium channels of frog nerve." J Gen Physiol **51**(2): 199-219.

Hille, B. (1971). "The permeability of the sodium channel to organic cations in myelinated nerve." J Gen Physiol **58**(6): 599-619.

Hines, M. L. and N. T. Carnevale (1997). "The NEURON simulation environment." Neural Comput **9**(6): 1179-1209.

Hodgkin, A. L. and A. F. Huxley (1952). "A quantitative description of membrane current and its application to conduction and excitation in nerve." J Physiol **117**(4): 500-544.

Issa, Z. F., J. M. Miller and D. P. Zipes Clinical arrhythmology and electrophysiology : a companion to Braunwald's heart disease**:** 1 online resource (xiii, 726 pages).

Jackman, W. M., K. J. Friday, J. L. Anderson, E. M. Aliot, M. Clark and R. Lazzara (1988). "The long QT syndromes: a critical review, new clinical observations and a unifying hypothesis." Prog Cardiovasc Dis **31**(2): 115-172.

Jeffries, O., N. Geiger, I. C. Rowe, L. Tian, H. McClafferty, L. Chen, D. Bi, H. G. Knaus, P. Ruth and M. J. Shipston (2010). "Palmitoylation of the S0-S1 linker regulates cell surface expression of voltage- and calcium-activated potassium (BK) channels." J Biol Chem **285**(43): 33307-33314.

Ji, Y., N. Leymarie, D. J. Haeussler, M. M. Bachschmid, C. E. Costello and C. Lin (2013). "Direct detection of S-palmitoylation by mass spectrometry." Anal Chem **85**(24): 11952-11959.

Johnson, D., M. L. Montpetit, P. J. Stocker and E. S. Bennett (2004). "The sialic acid component of the beta1 subunit modulates voltage-gated sodium channel function." J Biol Chem **279**(43): 44303-44310.

Kang, L., M. Q. Zheng, M. Morishima, Y. Wang, T. Kaku and K. Ono (2009). "Bepridil up-regulates cardiac Na+ channels as a long-term effect by blunting proteasome signals through inhibition of calmodulin activity." Br J Pharmacol **157**(3): 404-414.

Kang, R., J. Wan, P. Arstikaitis, H. Takahashi, K. Huang, A. O. Bailey, J. X. Thompson, A. F. Roth, R. C. Drisdel, R. Mastro, W. N. Green, J. R. Yates, 3rd, N. G. Davis and A. El-Husseini (2008). "Neural palmitoyl-proteomics reveals dynamic synaptic palmitoylation." Nature **456**(7224): 904-909.

Kapplinger, J. D., D. J. Tester, B. A. Salisbury, J. L. Carr, C. Harris-Kerr, G. D. Pollevick, A. A. Wilde and M. J. Ackerman (2009). "Spectrum and prevalence of mutations from the first 2,500 consecutive unrelated patients referred for the FAMILION long QT syndrome genetic test." Heart Rhythm **6**(9): 1297-1303.

Kenyon, J. L. and J. L. Sutko (1987). "Calcium- and voltage-activated plateau currents of cardiac Purkinje fibers." J Gen Physiol **89**(6): 921-958.

Kiss, T. (2008). "Persistent Na-channels: origin and function. A review." Acta Biol Hung **59 Suppl**: 1-12.

Kligfield, P., L. S. Gettes, J. J. Bailey, R. Childers, B. J. Deal, E. W. Hancock, G. van Herpen, J. A. Kors, P. Macfarlane, D. M. Mirvis, O. Pahlm, P. Rautaharju, G. S. Wagner, E. American Heart Association, C. o. C. C. Arrhythmias Committee, F. American College of Cardiology, S. Heart Rhythm, M. Josephson, J. W. Mason, P. Okin, B. Surawicz and H. Wellens (2007). "Recommendations for the standardization and interpretation of the electrocardiogram: part I: The electrocardiogram and its technology: a scientific statement from the American Heart Association Electrocardiography and Arrhythmias Committee, Council on Clinical Cardiology; the American College of Cardiology Foundation; and the Heart Rhythm Society: endorsed by the International Society for Computerized Electrocardiology." Circulation **115**(10): 1306-1324.

Koishi, R., H. Xu, D. Ren, B. Navarro, B. W. Spiller, Q. Shi and D. E. Clapham (2004). "A superfamily of voltage-gated sodium channels in bacteria." J Biol Chem **279**(10): 9532-9538.

Korycka, J., A. Lach, E. Heger, D. M. Boguslawska, M. Wolny, M. Toporkiewicz, K. Augoff, J. Korzeniewski and A. F. Sikorski (2012). "Human DHHC proteins: a spotlight on the hidden player of palmitoylation." Eur J Cell Biol **91**(2): 107-117.

Koval, O. M., J. S. Snyder, R. M. Wolf, R. E. Pavlovicz, P. Glynn, J. Curran, N. D. Leymaster, W. Dun, P. J. Wright, N. Cardona, L. Qian, C. C. Mitchell, P. A. Boyden, P. F. Binkley, C. Li, M. E. Anderson, P. J. Mohler and T. J. Hund (2012). "Ca2+/calmodulin-dependent protein kinase II-based regulation of voltage-gated Na+ channel in cardiac disease." Circulation **126**(17): 2084-2094.

Laedermann, C. J., M. Cachemaille, G. Kirschmann, M. Pertin, R. D. Gosselin, I. Chang, M. Albesa, C. Towne, B. L. Schneider, S. Kellenberger, H. Abriel and I. Decosterd (2013). "Dysregulation of voltage-gated sodium channels by ubiquitin ligase NEDD4-2 in neuropathic pain." J Clin Invest **123**(7): 3002-3013.

Laedermann, C. J., I. Decosterd and H. Abriel (2014). "Ubiquitylation of voltage-gated sodium channels." Handb Exp Pharmacol **221**: 231-250.

Levine, E., S. Z. Rosero, A. S. Budzikowski, A. J. Moss, W. Zareba and J. P. Daubert (2008). "Congenital long QT syndrome: considerations for primary care physicians." Cleve Clin J Med **75**(8): 591-600.

Levinson, S. R. and J. C. Ellory (1973). "Molecular size of the tetrodotoxin binding site estimated by irradiation inactivation." Nat New Biol **245**(143): 122-123.

Light, P. E., C. H. Wallace and J. R. Dyck (2003). "Constitutively active adenosine monophosphate-activated protein kinase regulates voltage-gated sodium channels in ventricular myocytes." Circulation **107**(15): 1962-1965.

Lin, M. J., M. Fine, J. Y. Lu, S. L. Hofmann, G. Frazier and D. W. Hilgemann (2013). "Massive palmitoylation-dependent endocytosis during reoxygenation of anoxic cardiac muscle." Elife **2**: e01295.

Lobo, S., W. K. Greentree, M. E. Linder and R. J. Deschenes (2002). "Identification of a Ras palmitoyltransferase in Saccharomyces cerevisiae." J Biol Chem **277**(43): 41268-41273.

Loussouarn, G., D. Sternberg, S. Nicole, C. Marionneau, F. Le Bouffant, G. Toumaniantz, J. Barc, O. A. Malak, V. Fressart, Y. Pereon, I. Baro and F. Charpentier (2015). "Physiological and Pathophysiological Insights of Nav1.4 and Nav1.5 Comparison." Front Pharmacol **6**: 314.

Lu, Z., Y. P. Jiang, C. Y. Wu, L. M. Ballou, S. Liu, E. S. Carpenter, M. R. Rosen, I. S. Cohen and R. Z. Lin (2013). "Increased persistent sodium current due to decreased PI3K signaling contributes to QT prolongation in the diabetic heart." Diabetes **62**(12): 4257-4265.

Lu, Z., C. Y. Wu, Y. P. Jiang, L. M. Ballou, C. Clausen, I. S. Cohen and R. Z. Lin (2012). "Suppression of phosphoinositide 3-kinase signaling and alteration of multiple ion currents in drug-induced long QT syndrome." Sci Transl Med **4**(131): 131ra150.

Marionneau, C. and H. Abriel (2015). "Regulation of the cardiac Na+ channel NaV1.5 by post-translational modifications." J Mol Cell Cardiol **82**: 36-47.

Marionneau, C., C. F. Lichti, P. Lindenbaum, F. Charpentier, J. M. Nerbonne, R. R. Townsend and J. Merot (2012). "Mass spectrometry-based identification of native cardiac Nav1.5 channel alpha subunit phosphorylation sites." J Proteome Res **11**(12): 5994-6007.

Martin, B. R. (2013). "Chemical approaches for profiling dynamic palmitoylation." Biochem Soc Trans **41**(1): 43-49.

Martin, B. R. and B. F. Cravatt (2008). "Proteomic Profiling of Dynamic Palmitoylation."

Martin, B. R. and B. F. Cravatt (2009). "Large-scale profiling of protein palmitoylation in mammalian cells." Nat Methods **6**(2): 135-138.

Martin, B. R., C. Wang, A. Adibekian, S. E. Tully and B. F. Cravatt (2011). "Global profiling of dynamic protein palmitoylation." Nat Methods **9**(1): 84-89.

Matsubara, T., C. Clarkson and L. Hondeghem (1987). "Lidocaine blocks open and inactivated cardiac sodium channels." Naunyn Schmiedebergs Arch Pharmacol **336**(2): 224-231.

Matsuda, T. and C. L. Cepko (2007). "Controlled expression of transgenes introduced by in vivo electroporation." Proc Natl Acad Sci U S A **104**(3): 1027-1032.

Meadows, L. S. and L. L. Isom (2005). "Sodium channels as macromolecular complexes: implications for inherited arrhythmia syndromes." Cardiovasc Res **67**(3): 448-458.

Mohler, P. J., I. Rivolta, C. Napolitano, G. LeMaillet, S. Lambert, S. G. Priori and V. Bennett (2004). "Nav1.5 E1053K mutation causing Brugada syndrome blocks binding to ankyrin-G and expression of Nav1.5 on the surface of cardiomyocytes." Proc Natl Acad Sci U S A **101**(50): 17533-17538.

Mollner, S., P. Ferreira, K. Beck and T. Pfeuffer (1998). "Nonenzymatic palmitoylation at Cys 3 causes extra-activation of the alpha-subunit of the stimulatory GTP-binding protein Gs." Eur J Biochem **257**(1): 236-241.

Moric, E., E. Herbert, M. Trusz-Gluza, A. Filipecki, U. Mazurek and T. Wilczok (2003). "The implications of genetic mutations in the sodium channel gene (SCN5A)." Europace **5**(4): 325-334.

Morita, H., J. Wu and D. P. Zipes (2008). "The QT syndromes: long and short." Lancet **372**(9640): 750-763.

Mosher, H. S., F. A. Fuhrman, H. D. Buchwald and H. G. Fischer (1964). "Tarichatoxin--Tetrodotoxin: A Potent Neurotoxin." Science **144**(3622): 1100-1110.

Murray, K. T., N. N. Hu, J. R. Daw, H. G. Shin, M. T. Watson, A. B. Mashburn and A. L. George, Jr. (1997). "Functional effects of protein kinase C activation on the human cardiac Na+ channel." Circ Res **80**(3): 370-376.

Narahashi, T., J. W. Moore and W. R. Scott (1964). "Tetrodotoxin Blockage of Sodium Conductance Increase in Lobster Giant Axons." J Gen Physiol **47**: 965-974.

Nielsen, M. W., A. G. Holst, S. P. Olesen and M. S. Olesen (2013). "The genetic component of Brugada syndrome." Front Physiol **4**: 179.

O'Brien, P. J., R. S. St Jules, T. S. Reddy, N. G. Bazan and M. Zatz (1987). "Acylation of disc membrane rhodopsin may be nonenzymatic." J Biol Chem **262**(11): 5210-5215.

Park, J., M. L. Leong, P. Buse, A. C. Maiyar, G. L. Firestone and B. A. Hemmings (1999). "Serum and glucocorticoid-inducible kinase (SGK) is a target of the PI 3-kinase-stimulated signaling pathway." EMBO J **18**(11): 3024-3033.

Payandeh, J., T. Scheuer, N. Zheng and W. A. Catterall (2011). "The crystal structure of a voltage-gated sodium channel." Nature **475**(7356): 353-358.

Pedro, M. P., A. A. Vilcaes, V. M. Tomatis, R. G. Oliveira, G. A. Gomez and J. L. Daniotti (2013). "2-Bromopalmitate reduces protein deacylation by inhibition of acyl-protein thioesterase enzymatic activities." PLoS One **8**(10): e75232.

Pei, Z., Y. Xiao, J. Meng, A. Hudmon and T. R. Cummins (2016). "Cardiac sodium channel palmitoylation regulates channel availability and myocyte excitability with implications for arrhythmia generation." Nat Commun **7**: 12035.

Pickering, D. S., F. A. Taverna, M. W. Salter and D. R. Hampson (1995). "Palmitoylation of the GluR6 kainate receptor." Proc Natl Acad Sci U S A **92**(26): 12090-12094.

Qu, Y., J. Rogers, T. Tanada, T. Scheuer and W. A. Catterall (1994). "Modulation of cardiac Na+ channels expressed in a mammalian cell line and in ventricular myocytes by protein kinase C." Proc Natl Acad Sci U S A **91**(8): 3289-3293.

Rautaharju, P. M., B. Surawicz, L. S. Gettes, J. J. Bailey, R. Childers, B. J. Deal, A. Gorgels, E. W. Hancock, M. Josephson, P. Kligfield, J. A. Kors, P. Macfarlane, J. W. Mason, D. M. Mirvis, P. Okin, O. Pahlm, G. van Herpen, G. S. Wagner, H. Wellens, E. American Heart Association, C. o. C. C. Arrhythmias Committee, F. American College of Cardiology and S. Heart Rhythm (2009). "AHA/ACCF/HRS recommendations for the standardization and interpretation of the electrocardiogram: part IV: the ST segment, T and U waves, and the QT interval: a scientific statement from the American Heart Association Electrocardiography and Arrhythmias Committee, Council on Clinical Cardiology; the American College of Cardiology Foundation; and the Heart Rhythm Society. Endorsed by the International Society for Computerized Electrocardiology." J Am Coll Cardiol **53**(11): 982-991.

Ren, D., B. Navarro, H. Xu, L. Yue, Q. Shi and D. E. Clapham (2001). "A prokaryotic voltage-gated sodium channel." Science **294**(5550): 2372-2375.

Richmond, J. E., D. VanDeCarr, D. E. Featherstone, A. L. George, Jr. and P. C. Ruben (1997). "Defective fast inactivation recovery and deactivation account for sodium channel myotonia in the I1160V mutant." Biophys J **73**(4): 1896-1903.

Rivolta, I., H. Abriel, M. Tateyama, H. Liu, M. Memmi, P. Vardas, C. Napolitano, S. G. Priori and R. S. Kass (2001). "Inherited Brugada and long QT-3 syndrome mutations of a single residue of the cardiac sodium channel confer distinct channel and clinical phenotypes." J Biol Chem **276**(33): 30623-30630.

Rogart, R. B., L. L. Cribbs, L. K. Muglia, D. D. Kephart and M. W. Kaiser (1989). "Molecular cloning of a putative tetrodotoxin-resistant rat heart Na+ channel isoform." Proc Natl Acad Sci U S A **86**(20): 8170-8174.

Ross, N. W. and P. E. Braun (1988). "Acylation in vitro of the myelin proteolipid protein and comparison with acylation in vivo: acylation of a cysteine occurs nonenzymatically." J Neurosci Res **21**(1): 35-44.

Roth, A. F., Y. Feng, L. Chen and N. G. Davis (2002). "The yeast DHHC cysteine-rich domain protein Akr1p is a palmitoyl transferase." J Cell Biol **159**(1): 23-28.

Rougier, J. S., M. Albesa and H. Abriel (2010). "Ubiquitylation and SUMOylation of cardiac ion channels." J Cardiovasc Pharmacol **56**(1): 22-28.

Rougier, J. S., B. Gavillet and H. Abriel (2013). "Proteasome inhibitor (MG132) rescues Nav1.5 protein content and the cardiac sodium current in dystrophin-deficient mdx (5cv) mice." Front Physiol **4**: 51.

Ruan, Y., N. Liu, R. Bloise, C. Napolitano and S. G. Priori (2007). "Gating properties of SCN5A mutations and the response to mexiletine in long-QT syndrome type 3 patients." Circulation **116**(10): 1137-1144.

Ruan, Y., N. Liu and S. G. Priori (2009). "Sodium channel mutations and arrhythmias." Nat Rev Cardiol **6**(5): 337-348.

Saint, D. A. (2008). "The cardiac persistent sodium current: an appealing therapeutic target?" Br J Pharmacol **153**(6): 1133-1142.

Salaun, C., J. Greaves and L. H. Chamberlain (2010). "The intracellular dynamic of protein palmitoylation." J Cell Biol **191**(7): 1229-1238.

Scheuer, P. J. (1970). "Toxins from fish and other marine organisms." Adv Food Res **18**: 141-161.

Schmidt, J. W. and W. A. Catterall (1987). "Palmitylation, Sulfation, and Glycosylation of the a Subunit of the sodium channel.pdf." J Biol Chem **262**(28): 13713-13723.

Schmidt, M., M. F. Schmidt and R. Rott (1988). "Chemical identification of cysteine as palmitoylation site in a transmembrane protein (Semliki Forest virus E1)." J Biol Chem **263**(35): 18635-18639.

Schmidt, M. F. and M. J. Schlesinger (1979). "Fatty acid binding to vesicular stomatitis virus glycoprotein: a new type of post-translational modification of the viral glycoprotein." Cell **17**(4): 813-819.

Schwartz, P. J. (1985). "Idiopathic long QT syndrome: progress and questions." Am Heart J **109**(2): 399-411.

Schwartz, P. J. (2012). "Introduction to the arrhythmogenic disorders of genetic origin series." Circ Arrhythm Electrophysiol **5**(3): 604-605.

Shin, H. G. and K. T. Murray (2001). "Conventional protein kinase C isoforms and cross-activation of protein kinase A regulate cardiac Na+ current." FEBS Lett **495**(3): 154-158.

Shipston, M. J. (2011). "Ion channel regulation by protein palmitoylation." J Biol Chem **286**(11): 8709-8716.

Shipston, M. J. (2014). "Ion channel regulation by protein S-acylation." J Gen Physiol **143**(6): 659-678.

Silva, J. (2014). "Slow inactivation of Na(+) channels." Handb Exp Pharmacol **221**: 33-49.

Simpson, P., A. McGrath and S. Savion (1982). "Myocyte hypertrophy in neonatal rat heart cultures and its regulation by serum and by catecholamines." Circ Res **51**(6): 787-801.

Smits, J. P., T. T. Koopmann, R. Wilders, M. W. Veldkamp, T. Opthof, Z. A. Bhuiyan, M. M. Mannens, J. R. Balser, H. L. Tan, C. R. Bezzina and A. A. Wilde (2005). "A mutation in the human cardiac sodium channel (E161K) contributes to sick sinus syndrome, conduction disease and Brugada syndrome in two families." J Mol Cell Cardiol **38**(6): 969-981.

Song, W. and W. Shou (2012). "Cardiac sodium channel Nav1.5 mutations and cardiac arrhythmia." Pediatr Cardiol **33**(6): 943-949.

Speers, A. E. and B. F. Cravatt (2004). "Profiling enzyme activities in vivo using click chemistry methods." Chem Biol **11**(4): 535-546.

Stafstrom, C. E. (2007). "Persistent sodium current and its role in epilepsy." Epilepsy Curr **7**(1): 15-22.

Stafstrom, C. E. (2011). "A persistent little current with a big impact on epileptic firing." Epilepsy Curr **11**(2): 64-65.

Storck, E. M., R. A. Serwa and E. W. Tate (2013). "Chemical proteomics: a powerful tool for exploring protein lipidation." Biochem Soc Trans **41**(1): 56-61.

Stuhmer, W., F. Conti, H. Suzuki, X. D. Wang, M. Noda, N. Yahagi, H. Kubo and S. Numa (1989). "Structural parts involved in activation and inactivation of the sodium channel." Nature **339**(6226): 597-603.

Suzuki, H., K. Nishikawa, Y. Hiroaki and Y. Fujiyoshi (2008). "Formation of aquaporin-4 arrays is inhibited by palmitoylation of N-terminal cysteine residues." Biochim Biophys Acta **1778**(4): 1181-1189.

Tian, L., O. Jeffries, H. McClafferty, A. Molyvdas, I. C. Rowe, F. Saleem, L. Chen, J. Greaves, L. H. Chamberlain, H. G. Knaus, P. Ruth and M. J. Shipston (2008). "Palmitoylation gates phosphorylation-dependent regulation of BK potassium channels." Proc Natl Acad Sci U S A **105**(52): 21006-21011.

Tsai, F. D., J. P. Wynne, I. M. Ahearn and M. R. Philips (2014). "Metabolic labeling of Ras with tritiated palmitate to monitor palmitoylation and depalmitoylation." Methods Mol Biol **1120**: 33-41.

Tulloch, L. B., J. Howie, K. J. Wypijewski, C. R. Wilson, W. G. Bernard, M. J. Shattock and W. Fuller (2011). "The inhibitory effect of phospholemman on the sodium pump requires its palmitoylation." J Biol Chem **286**(41): 36020-36031.

Ulbricht, W. (2005). "Sodium channel inactivation: molecular determinants and modulation." Physiol Rev **85**(4): 1271-1301.

Valdivia, C. R., D. J. Tester, B. A. Rok, C. B. Porter, T. M. Munger, A. Jahangir, J. C. Makielski and M. J. Ackerman (2004). "A trafficking defective, Brugada syndrome-causing SCN5A mutation rescued by drugs." Cardiovasc Res **62**(1): 53-62.

van Bemmelen, M. X., J. S. Rougier, B. Gavillet, F. Apotheloz, D. Daidie, M. Tateyama, I. Rivolta, M. A. Thomas, R. S. Kass, O. Staub and H. Abriel (2004). "Cardiac voltage-gated sodium channel Nav1.5 is regulated by Nedd4-2 mediated ubiquitination." Circ Res **95**(3): 284-291.

Vilin, Y. Y. and P. C. Ruben (2001). "Slow inactivation in voltage-gated sodium channels: molecular substrates and contributions to channelopathies." Cell Biochem Biophys **35**(2): 171-190.

Wang, D. W., K. Yazawa, A. L. George, Jr. and P. B. Bennett (1996). "Characterization of human cardiac Na+ channel mutations in the congenital long QT syndrome." Proc Natl Acad Sci U S A **93**(23): 13200-13205.

Wang, Q., J. Shen, I. Splawski, D. Atkinson, Z. Li, J. L. Robinson, A. J. Moss, J. A. Towbin and M. T. Keating (1995). "SCN5A mutations associated with an inherited cardiac arrhythmia, long QT syndrome." Cell **80**(5): 805-811.

Webb, Y., L. Hermida-Matsumoto and M. D. Resh (2000). "Inhibition of protein palmitoylation, raft localization, and T cell signaling by 2-bromopalmitate and polyunsaturated fatty acids." J Biol Chem **275**(1): 261-270.

Wedekind, H., J. P. Smits, E. Schulze-Bahr, R. Arnold, M. W. Veldkamp, T. Bajanowski, M. Borggrefe, B. Brinkmann, I. Warnecke, H. Funke, Z. A. Bhuiyan, A. A. Wilde, G. Breithardt and W. Haverkamp (2001). "De novo mutation in the SCN5A gene associated with early onset of sudden infant death." Circulation **104**(10): 1158-1164.

West, J. W., D. E. Patton, T. Scheuer, Y. Wang, A. L. Goldin and W. A. Catterall (1992). "A cluster of hydrophobic amino acid residues required for fast Na(+)-channel inactivation." Proc Natl Acad Sci U S A **89**(22): 10910-10914.

Yang, W., D. Di Vizio, M. Kirchner, H. Steen and M. R. Freeman (2010). "Proteome scale characterization of human S-acylated proteins in lipid raft-enriched and non-raft membranes." Mol Cell Proteomics **9**(1): 54-70.

Yellen, G. (1998). "The moving parts of voltage-gated ion channels." Q Rev Biophys **31**(3): 239-295.

Young, F. B., S. L. Butland, S. S. Sanders, L. M. Sutton and M. R. Hayden (2012). "Putting proteins in their place: palmitoylation in Huntington disease and other neuropsychiatric diseases." Prog Neurobiol **97**(2): 220-238.

Yu, F. H. and W. A. Catterall (2003). "Overview of the voltage-gated sodium channel family." Genome Biol **4**(3): 207.

Zeidman, R., C. S. Jackson and A. I. Magee (2009). "Protein acyl thioesterases (Review)." Mol Membr Biol **26**(1): 32-41.

Zeng, J. and Y. Rudy (1995). "Early afterdepolarizations in cardiac myocytes: mechanism and rate dependence." Biophys J **68**(3): 949-964.

Zhang, L., K. Foster, Qiuju Li and J. R. Martens (2007). "S-acylation regulates Kv1.5 channel surface expression." Am J Physiol Cell Physiol **293**: C152–C161.

Zhang, M. M., L. K. Tsou, G. Charron, A. S. Raghavan and H. C. Hang (2010). "Tandem fluorescence imaging of dynamic S-acylation and protein turnover." Proc Natl Acad Sci U S A **107**(19): 8627-8632.

Zhou, F., Y. Xue, X. Yao and Y. Xu (2006). "CSS-Palm: palmitoylation site prediction with a clustering and scoring strategy (CSS)." Bioinformatics **22**(7): 894-896.

Zhou, X., I. Wulfsen, M. Korth, H. McClafferty, R. Lukowski, M. J. Shipston, P. Ruth, D. Dobrev and T. Wieland (2012). "Palmitoylation and membrane association of the stress axis regulated insert (STREX) controls BK channel regulation by protein kinase C." J Biol Chem **287**(38): 32161-32171.

Curriculum Vitae

Zifan Pei

EDUCATION

Ph.D. in Pharmacology, Indiana University, 2010-2017
B.S. in Chinese Pharmacy, Nanjing University of Chinese Medicine, 2006-2010

HONORS AND AWARDS

Paradise travel award (2014): Indiana University Pharmacology & Toxicology department
Trainee travel award (2013): FASEB Ion channel regulation conference

PUBLICATIONS AND POSTER PRESENTATIONS

Publications:

- **Pei, Z.**, Xiao, Y., Meng, J., Hudmon, A., Cummins, TR.. Cardiac sodium channel palmitoylation regulates channel availability and myocyte excitability with implications for arrhythmia generation. Nature Communications. 2016; June; 23;7:12035.
- Xiao, Y., Barbosa, C., **Pei Z.**, Cummins, TR.. Increased resurgent sodium currents in Nav1.8 contribute to nociceptive sensory neuron hyperexcitability in small fiber neuropathy. (In preparation)
- **Pei, Z.**, Hudmon, A., Cummins, TR.. Modulation of cardiac sodium channel by palmitoylation and its association with cardiac disease mutations. Circulation. 2014;130:A20627
- Lu, W.J., Xu, C., **Pei Z.**, Mayhoub, AS., Cushman, M., Flockhart, DA.. The tamoxifen metabolite norendoxifen is a potent and selective inhibitor of aromatase (CYP19) and a potential lead compound for novel therapeutic agents. Breast Cancer Res Treat.2012; May;133(1):99-109.

Poster presentations:

- American Heart Association Annual Scientific Sessions, Chicago, 2014
- World Pharma Congress, Boston, 2014
- FASEB Ion Channel Regulation Conference, Nassau, 2013

EXPERIMENTAL SKILLS

Molecular Biology: PCR; DNA extraction and purification; site-directed mutagenesis; sub cloning; transfection;
Ion Channel Electrophysiology: whole cell patch clamp; cardiomyocytes recording;

Biochemistry: western blot; immunoprecipitation; acyl-biotin exchange assay; click chemistry assay;
Cell Assay: cell culture; cell lysis and protein extraction; wound healing assay; trans-well assay;
Clinical Pharmacology: enzyme assay; HPLC; LC-MS; UV-Vis;
Animal Models: rat brain ischemia model; cancer model; primary cell culture (cardiaomyocyte, DRG neuron);

RESEARCH EXPERIENCE

Indiana University School of Medicine (2010 – 2016): Ph.D. Candidate
Post-translational modification of sodium channel and its association with cardiac diseases.
Novel cardiac sodium channel post-translational lipid modification, palmitoylation, was identified and validated using acyl-biotin exchange assay (ABE) and electrophysiology method. The palmitoylation sites were studied using bioinformatics prediction tool and site-directed mutagenesis. Biophysical properties change caused by channel palmitoylation was examined using voltage clamp and current clamp on both HEK293 cells and cultured cardiomyocytes. Anti-arrhythmia drugs were applied to study how palmitoylation can change the pharmacological properties of the cardiac sodium channel.

Selective modulation of gating charge mutations on cardiac sodium channel and contribution of gating pore currents to cardiac arrhythmia disease.
Characterization of gating pore currents generated by gating charge mutations located in the voltage sensor domain. Study the LQT3 mutations that neutralize gating charges and the association of generated gating pore currents with cardiac arrhythmia disease.

Indiana University School of Medicine (2011): Research Assistant/rotation student
Tamoxifen and its metabolite as potent and selective inhibitors of aromatase (CYP19) and their potential use as a therapeutic drug.
Characterization the inhibition effect of tamoxifen and its metabolites on CYP450 enzymes using microsomal incubations. High throughput characterization of the activity of recombinant human CYP isoform using enzyme activity assay. Quantification of the testosterone conversion to estradiol and of methadone conversion to EDDP using HPLC